STOCHASTIC PROGRAMMING MODELS FOR PLANNING WIND-BASED DISTRIBUTED GENERATION IN PROSUMERS OF ENERGY MODE

by

Temitope Runsewe, B.S.

A thesis submitted to the Graduate Council of
Texas State University in partial fulfillment
of the requirements for the degree of
Master of Science
with a Major in Engineering
May 2020

Committee Members:

Clara Novoa, Chair

Tongdan Jin

Tahir Ekin

FAIR USE AND AUTHOR'S PERMISSION STATEMENT

Fair Use

Duplication Permission

DEDICATION

This project is dedicated to my late father who lived an exemplary life and made it possible for me to pursue my graduate degree in industrial engineering and to my mum who remained strong and supported me throughout my graduate studies.

Finally, I would like to dedicate this project to God for granting me wisdom, knowledge and understanding to complete this work

ACKNOWLEDGEMENTS

I would like to first and foremost thank my thesis advisor Dr. Clara Novoa for providing me the opportunity to pursue a master's degree, for her continuous guidance and endless support during my studies.

Thanks to Dr. Tongdan Jin for his ideas, time and other inputs into the project. Also, thanks to other faculty and staff members of the Department of Industrial Engineering and the College of Engineering for their direct and indirect support and for creating an excellent learning and research environment through outstanding teaching, learning, and research facilities. I am especially grateful for the research/teaching assistantship provided to me during my master's program by the Industrial Engineering program.

I wish to appreciate my colleagues in the renewable energy research team who have also contributed ideas, their time and expertise into this work.

Sincere appreciation to my mother, Mrs. Olayinka Runsewe; my siblings, Oluwadamilola and Oluwayemisi Runsewe and my loved ones for their constant love and support throughout my years of study and through the process of writing this thesis. This accomplishment would not have been possible without them. Thank you all

TABLE OF CONTENTS

Page

LIST OF TABLES

Table **Page**

LIST OF FIGURES

Figure **Page**

LIST OF ABBREVIATIONS

Abbreviation	Description
ABC	Artificial Bee Colony
ACOPT	AC Optimal Power Flow
AMPL	Advanced Mathematical Programing Language
ASP	Analytic Solver Platform
BSOA	Backtracking Search Optimization Algorithm
B&BC	Branch-and-Benders-cut
CABC	Chaotic Artificial Bee Colony
CES	Community Energy Storage
CLT	Central Limit Theorem
CNSM	Cost of not using the Stochastic Model
DER	Distributed Energy Resources
DG	Distributed Generation
DL	Distribution Line
ESS	Energy Storage Systems
GA	Genetic Algorithm
HES	Household Energy Storage
IEEE	Institute of Electrical and Electronic Engineers
LCOE	Levelized Cost of Energy
MIP	Mixed Integer Programming

NSP	Non-linear non-smooth problems
OPF	Optimal Power Flow
O&M	Operating and Maintenance
PV	Photovoltaic(s)
SAA	Sample Average Approximation
SDDP	Stochastic Dual Dynamic Programming
SMIP	Stochastic Mixed Integer Programming
SoC	State of Charge
THDv	Total Harmonic Distortion Voltage
WT	Wind Turbines

ABSTRACT

This thesis formulates, solves and contrasts several stochastic programming models that a decision maker may use to determine the siting and sizing of distributed energy resources (DER) in a distributed generation (DG) system. This thesis focuses on two major approaches: strategical and operational. In the strategical one, four models are designed to minimize the lifecycle cost of DG systems powered with wind energy and a substation considering the loss of load probability and thermal constraints. The models are solved in three cities with high -medium -low wind speed profiles. Extensive data analysis is performed on the 9-year hourly wind speed data collected which permits to estimate the probability distribution for the power generation. Results from the strategical models show that the system designed using stochastic programming is highly reliable as it considers uncertainties in the wind speed. In the operational approach, two new models are proposed with the objective of minimizing the lifecycle cost of DG systems powered with wind energy and a substation using system nodes as prosumers. The first model considers the loss of load probability and thermal constraints. The second one adds energy storage system (ESS) into the first model while considering just the thermal constraints and including 365 days across a year. The second model is solved for three distinct cases: a fixed battery capacity of 100MW, a fixed battery capacity of 250MW and a variable battery capacity. This thesis demonstrates that the operational models are tractable and can be solved using commercial solvers. It also assesses the benefit of considering system nodes as prosumers using ESS

1. INTRODUCTION

The need to consider renewable sources of energy has been rising recently because human population is increasing rapidly and consequently energy consumption is growing along with carbon pollution. World human population reached 7.5 billion in 2018 (Our World in Data, 2019). Eventually, conventional sources of energy like fossil fuel will be depleted completely and moreover they currently cause a lot of environmental pollution. Energy accounts for about 60% of greenhouse gases emissions (UNPD, 2016). Several industries such as Intel, Kohl's, Walmart and Apple are now investing in renewable energy integration which contributes to solve the energy challenge faced by mankind.

The use of renewable sources of energy is expanding rapidly to potentially reduce the carbon dioxide emission and dependence on fossil fuels (Kwon et al., 2017). Wind energy is one of the fastest ubiquitous (Karki et al., 2006). However, the use of this energy type brings variability to the energy portfolio due to the intermittency of wind and such variability increases the difficulty to match demand with supply. In order to design realistic and efficient renewable energy systems it is necessary to incorporate the wind variability in the planning models to mitigate the generation intermittency.

Distributed Generation (DG) is an approach to provide electric power at the customer or at a site closer to the customer, eliminating unnecessary transmission and distribution costs (Begović et al., 2001). DG systems have emerged as promising alternatives to meet growing electricity needs because they reduce the environmental impact, improve voltage profile and reduce line losses. Presently, DG is considered

within the broader concept of Distributed Energy Resources (DER), microgrid, responsive loads and energy storage devices (Lopes et al., 2007).

DER include small scale (1ess than one kW to tens of a MW), modular, energy generation and storage technologies that provide electric capacity where the customer needs. DER systems may be either connected to the local electric power grid or isolated from the grid in stand-alone applications, known as island microgrids. DER technologies include wind turbines (WT), photovoltaics (PV), fuel cells, micro turbines, combustion turbines, and energy storage systems, among others (Alarcon-Rodriguez et al., 2010). The integration of DER can reduce energy loss and decrease the number of transmission lines needed for long distance hauls (Omu et al., 2013). DG systems integrated with wind power can be attractive for the so-called social and financial benefits. However, a major obstacle for interconnected DG systems is the relatively high lifecycle cost. Also, the integration of DER units may complicate the system design and operations (Ren and Gao, 2010) as the non-optimal siting and sizing of various DG units can cause power losses, system instability and increased operational cost. Therefore, there is need for proper siting, sizing and optimization of the DER systems to ensure that they are cost effective (El-Fergany 2015; Nguyen et al. 2017; Karki et al. 2017).

This research focuses on finding the optimal siting and sizing of WT operating in a DG system connected to the main grid through a substation considering the wind speed uncertainty. The research has two objectives. Firstly, the study determines the optimal WT capacity and their placement so that the sum of the annualized capital, operational and environmental costs is minimized. Secondly, it assesses the benefits of using different stochastic programming models for the design of the DG system and contrast

them to deterministic models. Particularly, this work provides extensive comparisons between probabilistic, chance constrained and stochastic models considering system nodes as consumers only. In the last two chapters of this thesis, comparisons are also made between the two-stage stochastic models and the deterministic models considering nodes as just prosumers and nodes as prosumers coupled with storage systems, respectively.

The major contributions of this thesis are summarized as follows. This thesis models and optimizes a DG system through the solution of multiple stochastic models considering a crucial stochastic factor which is the variability on the power supply of the WT. It also considers multiple realistic aspects of DG system design such as the loss-of-load probability, the thermal constraints, the emergence of prosumer nodes in the DG system and the use of energy storage systems. This thesis also illustrates the benefits of using the stochastic models in real settings where extensive climate data analytics were performed on large samples of wind speed. About 9,000 observations per year are collected in hourly basis over 9 years (2006-2014) for three cities (Wellington, Rio Gallegos, and New York). Thus, the proposed stochastic models are contrasted in three different settings that are considered as independent case studies. These cases do not rely on the wind generation of a few selected days or on not entirely well fitted probability distributions. This is a novel work that at the best of our knowledge no other studies have presented in the literature in the way it is covered it in this research.

2. SITING AND SIZING OF WIND TURBINES - STRATEGIG PLANNING MODELS

This chapter is divided into 10 subsections. Section 2.1 presents the DG system design problem to be modeled and solved in this chapter. Section 2.2 summarizes previous contributions on the topic of siting and sizing of WT and highlights the differences between our research and the ones in previous literature. Section 2.3 describes how previous studies have modeled wind speed and mentions the approach followed in this thesis. Section 2.4 discusses the WT power curve and explains how it is used in this thesis. Section 2.5 presents the methodology used to solve the problem. Section 2.6 presents the mathematical models proposed for the optimal siting and sizing of the DG system. Section 2.7 shows the experimental setting used in solving the models. Section 2.8 presents the values assumed for the parameters used in solving the models. Section 2.9 presents the results and sensitivity analysis carried out on the model. Section 2.10 concludes the chapter by summarizing the practical aspects related to the design of wind-based DG systems

2.1 Problem statement

The problem studied in this chapter is defined as finding the placement and capacity for a DG system that may install wind powered DER units of different types, according to their capacities (i.e. 1MW, 2MW, 3MW) and connect to a substation whose size is also to be determined (i.e. 40 or 50 MW) (see Figure 1). The problem objective is to find the system design with minimum cost. The DG system is comprised of interconnected nodes. In Figure 1, the central node (node 1) is reserved for the placement of the substation. The remaining eight nodes in the network can be small cities,

companies, department stores, or farms. The arrows in Figure 1 correspond to the distribution lines. They are treated as distribution lines because the voltage running on them is at the most 33KV.

The challenging factor on finding the optimal siting and sizing for this DG system is that the wind speed varies hourly and it affects the power output of the WT and consequently the total system reliability. The power generated by the DG system must satisfy the total load (i.e. demand) for electricity for a high percentage of the time. For instance, the DG system should have very small shortages every year, such as, one day every 365 days (i.e. a loss-of-load probability equal to 0.003). The substation provides marginal or extra supply sent from the central generation plant to mitigate the potential power shortage due to wind uncertainty. However, the use of the substation is not recommended for long periods of time due to that fact that most central generating units burn fossil fuels.

The optimal design for the DG system in Figure 1 will determine the capacity of the WT to install at each node of the network and the size of the substation to allocate at the central node to satisfy the electricity loads, at the nodes, denoted as L_2, L_3 …,L_9, considering thermal constraints at the distribution lines and the loss-of-load probability constraint. Thus, in finding the optimal design there is a trade-off between the system net costs (equipment installation and maintenance minus incentives for the use of renewable energy) and the risk of energy losses.

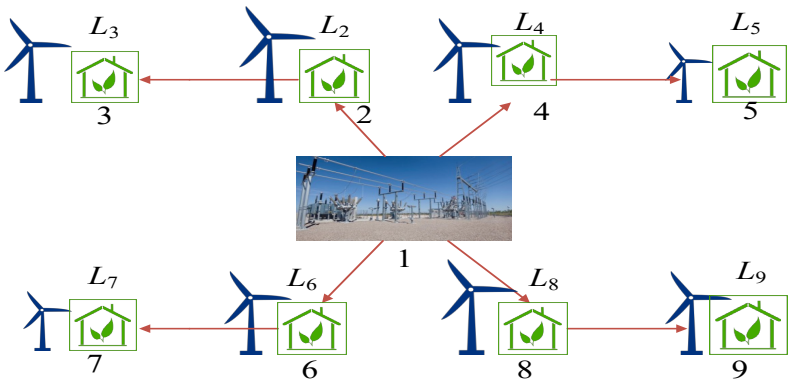

Figure 1. The DG system studied in Chapter 2

2.2 Literature review on siting and sizing of DER units

Various techniques have been considered to find the optimal placement of WT. Cetinay et al. (2017) proposed a deterministic linear programming model to determine the geographical locations and the installed capacities of wind farms to be integrated into a transmission grid, in order to maximize the expected annual wind power generation. Their model considers that new wind power plants to be integrated into the electrical grid do not violate the transmission system constraints. This requirement comes from the grid operator (i.e. transmission system operator) who is responsible for controlling the transmission grid, its topology and the bus voltage (see Appendix 6. Glossary under the item Lines for a definition of Bus and Lines). Thus, their model assures that the final power flows over each network link must be smaller than the maximum flow limit and that the total size of wind farms at each site and in each region should not exceed the limits set by the transmission system operator. The model constraints satisfy the linearized power flow equation for each network link and the power balance equation for each network node and permit the use of power at selected reserve power plants between given minimum and maximum values. The authors solved the model exactly and multiple

times by varying a parameter that they called the diversity factor. Such parameter was defined as the ratio of the power output of a wind turbine and its total installed capacity.

Abdul-Kadir et al. (2013) argued that the installation of DG units into the distribution system at nonoptimal places with nonoptimal sizing can cause high power losses, power quality violations, instability of the system (i.e. harmonic distortions), and escalating operational costs. The authors then formulated a deterministic multi-objective constrained nonlinear integer optimization program to minimize the total losses and average total harmonic distortion voltage (THD_v) of the distribution system. The model included constraints such as keeping the bus voltages between predefined limits and the THD_v below a desired threshold. Sensitivity analysis and evolutionary programming were used to determine the optimal placement and sizing of DG units. The solution methodology was tested with a 69-bus radial distribution system assuming that 2 DG units with sizes ranging between 400kW and 2000kW were to be installed. The proposed optimal placement and sizing of the DG units was found to be robust. It provided higher efficiency for the improvement of the voltage profile and the minimization of the power losses and the THDv, if compared to other method in previous literature.

Nguyen et al. (2017) studied the optimal placement and size of energy storage systems (ESS) in a high wind penetration grid to maximize the generation of ESS and wind power units and minimize total investment and total generation costs. They formulated a deterministic non-linear model named AC Optimal Power Flow (AC OPF). The model included as constraints the power balance equations, limits on voltage magnitude, bounds on real and reactive generation powers, branch thermal limits, ESS energy balance equation, ESS charging and discharging power bounds, ESS energy limits

and the budgeted maximum allowable power and energy capacity to be installed. The ESSs were used so that the time-shifting wind power match the system demand and hence improve overall system revenue. The authors presented a heuristic solution methodology to solve the resulting probabilistic AC OPF model, which considers uncertain input parameters (such as the wind and load) and their effect on the sizing of ESSs. The methodology comprised inputting and calculating cumulants of the uncertain wind and load data, solving the Genetic Algorithm (GA) and the embedded AC OPF model and constructing probability distributions for the size of the outputs (i.e. the optimal power and energy capacities of the ESS's). The GA was applied to search for the optimal siting while the OPF was used for sizing the ESSs under wind and load uncertainties. The proposed approach was tested on the IEEE 57-bus system and on an equivalent model of the Sicilian system in Italy.

El-Fergany (2015) proposed a swarm optimization technique named backtracking search optimization algorithm (BSOA) which is a new meta-heuristic algorithm developed in 2013. The BSOA has a unique mechanism for generating a trial individual and it enables to solve numerical optimization problems successfully and quickly with less effort on tuning the algorithm parameters. In this work, the BSOA solves a DG allocation problem (i.e. determine bus number and size) that has as objective to minimize the system real loss and the cumulative voltage deviation at each bus The types of DG units considered to introduce are: (1) photovoltaic arrays and fuel cells and (2) diesel synchronous generators and WT. The problem constraints are the active and reactive power balance, bus voltage limits, DG sizing limits, thermal capacities, maximum level of DG penetration, network active power loss and network short circuit level. The BSOA

was applied to the solution of 33 and 94-node radial distribution systems, respectively. The authors found that the combined power output of the network was considerably improved when introducing diesel synchronous generators and WT.

Mohandas et al. (2015) proposed a deterministic multi objective performance index model to find the optimal location of real power DG units and their capacities. The indexes quantified various outputs of the DG such as real and reactive power loss, voltage stability, line flow limit, and voltage profile and they were combined using weighted coefficients. The problem constraints were power conservation and real power generation, voltage profile and line thermal limits. The multi objective problem was solved using a Chaotic Artificial Bee Colony (CABC) algorithm for various types of load models. The Artificial Bee Colony (ABC) algorithm, which was developed based on the foraging behavior of honeybees, was combined with chaotic local search theory. The proposed CABC improves the searching behavior and avoids the solutions get trapped in local optima. The CABC is such that the exploitation capability of the ABC algorithm is increased to avoid slow convergence while obtaining the best-known result. The proposed approach was implemented on 38-node and 69-node radial distribution systems. It was concluded that the presence of DGs in the optimal locations reduced the real and reactive power losses and improved the voltage profile of the system while abiding the specified limits for the power flows on the lines. The results also showed that the presence of DG enhanced the voltage stability of the system.

Novoa et al. (2011) presented a stochastic planning model to minimize life cycle cost of DG systems considering the energy reliability criterion and loss of load probability. The optimization model was formulated to determine the optimal capacity

and placement of DG systems, the probabilistic model is then solved using genetic algorithm combined with heuristic search to find the optimal siting and sizing of DG units. The authors used statistical moments including mean and variance to model the wind power volatility and load uncertainty and stated that moment method is effective in characterizing stochastic behavior of wind power and load volatility.

Based on the literature review presented in this section, the author of this thesis found that none of the previous works solves a stochastic programming model that considers uncertainty in the wind speed and includes both a loss of load chance constraint and thermal constraints as it is done in this thesis. In sections 2.3 and 2.4 it is presented how the wind speed and the power output of a WT can be computed.

2.3 Wind speed

Annual production of wind power is determined by the wind speed at the geographical region and the capacity of the WT being deployed. Haghifam et al. (2006) studied the 20-year wind speed data collected from a meteorology station in Iran and discovered that it can be approximated by the Normal or Gaussian distribution for the first half year. Karki et al. (2006) used the normal distribution to model wind speed in three Canadian regions based on the hourly mean and standard deviation of wind speeds from a 15-year meteorological database. Furthermore, the two-parameter Weibull distribution is also used to model wind speeds. Spahić et al. (2009) analyzed the data obtained from the North Sea in Europe between 2003 and 2005, and they concluded that the annual wind speed can be approximated by the Weibull distribution with scale parameter c = 11.1 m/s and shape parameter k = 2.17.

In this thesis, hourly data for the ground wind speed notated here as, y_g, and measured in meters per second (m/s), is collected from Weather Underground (2016) and used to compute the wind speed at any given height h above the ground which is notated in this thesis as y_h . Equation (1) permits to estimate the wind speed at any given height h above the ground, y_h , as a function of the ground wind speed, y_g, the height of the ground, h_g, typically 10m, and the Hellman exponent, k. This equation was originally proposed by Spera and Richards, (1979) and is presented below.

$$y_h = y_g \left(\frac{h}{h_g} \right)^k \tag{1}$$

The value of the exponent depends on the costal location, the shape of the terrain, and the stability of the air. A value of 0.27-0.34 is often assumed for k in the human inhabited areas (Blackadar and Tennekes, 1968; Heier, 2005). The Hellman exponent adjusts the data reasonably well in the range of heights from 10 up to 100-150 meters (Bañuelos-ruedas and Camacho, 2011). Equation 1 indicates that a taller WT encounters stronger wind profile and it matches the experience of human beings.

2.4 Wind turbine power curve

The power output of a WT can be determined from its power curve using equation (2) (Novoa et al., 2011; Goudarzi et al., 2014). The power curve plots the generated WT power, P, against the wind speed, y, across the turbine blades. The power curve has four operating phases: standby ($0 < y < v_c$) in which no power is produced; nonlinear power production ($v_c \leq y \leq v_r$) in which the power output, P, is proportional to the cubic wind speed; rated power region ($v_r \leq y \leq v_s$) in which the maximum power output is produced; and cut-off phase ($y > v_s$) in which the generator is shut down for protection.

$$P(y)=\begin{cases}0 & 0<y<v_c, y>v_s \\ 0.5\eta_{\max}\rho A h^3 & v_c \le y \le v_r \\ P_m & v_r \le y \le v_s\end{cases} \quad (2)$$

The power curve described in equation (2) is grounded on the kinetic theory of the air flow dynamics. The parameter η_{max} is used to describe the conversion rate from wind power to electrical power, ρ is the air density, A is the area covered by the turbine blades and P_m represents the rated power or WT capacity. Equation (2) shows that the power of a WT is directly proportional to air density, blade area, and the cube of wind velocity when $v_c \le y \le v_r$.

Figure 2 shows a typical WT power curve. In this thesis, once equation (1) is used to estimate the wind speed y_h (m/s), equation (2) lets to find the power output of a WT operating at height h, $P(y_h)$. To simplify the notation, in the future sections of this thesis, the power output of a WT operating at height h will be notated just as P dropping the function argument.

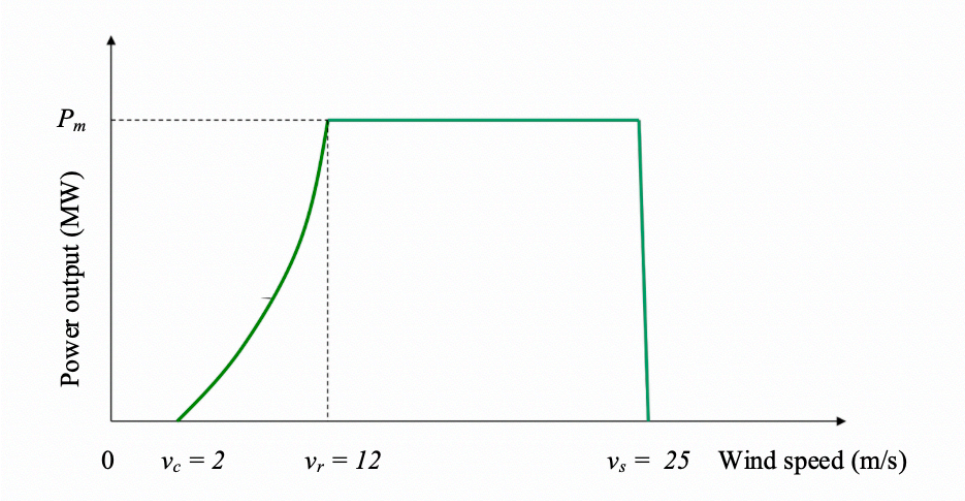

Figure 2. A typical wind power curve

2.5 Methodology

The problem of finding the siting and sizing of WT in the DG system described in section 2.1 is approached with the formulation and solution of four mathematical programming models named probabilistic or chance constrained (Model 1), deterministic (Model 2), stochastic programming (Model 3) and simulation-optimization (Model 4). The reasons for using multiple mathematical programming models are to approach the stochastic behavior of the wind under different perspectives, contrast the difficulty of the models and validate the solution quality. All models are explained in the next section.

2.6 Mathematical models for the optimal design of a DG system powered by wind turbines and a substation

As mentioned in Section 2.1, Problem Statement, the DG planning problem that a system planner confronts aims to search a trade-off between the system cost and the risk of energy losses. Such problem can be formulated as an optimization model that looks to minimize the expected system cost subject to the reliability constraint on the energy losses and also considering the thermal constraints. The following subsections present the four different optimization models proposed to solve the wind-based DG planning problem.

2.6.1 Model 1 - Chance constrained model:

Model 1 is a chance constrained model that includes a probabilistic constraint to assure that the probability that the total power generated by the system exceeds the total load (i.e. total demand) be a high value (i.e. 99% or similar). The model also assumes that the power and the load (i.e. demand) at each node of the DG system are characterized by

their mean and standard deviation. Tables 1-5 present the notation for Model 1. The optimization model is presented and discussed immediately in the tables below.

Table 1. Sets for Models in Section 2.6

Notation	Definition
I	Types of DER (i.e. WT and substations) possible to install
J	Nodes in the DG system
F	Upper nodes in the DG network. Upper nodes have distribution lines that link them with other nodes different to the substation and thus they can provide power to other nodes.
E	Lower or terminal nodes in the DG network
E_f	Lower or terminal nodes originating from a particular upper node f
K	Capacity types feasible to adopt for the substation located at the central node

Table 2. Decision Variables for Models in Section 2.6

Notation	Definition
x_{ij}	Binary decision variable. It becomes equal to 1 if a DER type i is installed in node j and 0 otherwise

Table 3. Power Parameters for Models in Section 2.6

Notation	Definition
P_{ij}	Power generated by DER type i installed at node j. P_{ij} is a random variable and a function of y_h. Function argument y_h is dropped to simplify notation
$E[P_{ij}]$	Expected value (i.e. mean) of the power generated by DER type i installed at node j.
$\sigma^2(P_{ij})$	Variance of the power output for DER i at node j
P	Total power generated in the DG system. P is a random variable. Using the central limit theorem, $P \sim N\left(\sum_{i\in I}\sum_{j\in J} E\left[P_{ij}\right]x_{ij}, \sum_{i\in I}\sum_{j\in J}\sigma^2\left(P_{ij}\right)x_{ij}^2\right)$ Here P is a function of P_{ij}, x_{ij} and the wind speed y_h Again the function argument y_h is dropped to simplify the notation
$E[P]$	Expected value (i.e. mean) of the total power generated in the DG network and computed as: $E\left[P\right]=\sum_{i\in I}\sum_{j\in J} E[P_{ij}]x_{ij}$
$P_i^{(c)}$	Capacity of DER type i

Table 4. Probability Functions for Models in Section 2.6

Notation	Definition
f_P	Probability density function for the system total power generated, P
f_L	Probability density function for the system total required load (i.e. demand), L

Table 5. Additional Parameters for Models in Section 2.6

Notation	Definition
a_i	Present cost per MW for installing DER type i
ϕ	Factor to convert a present worth to annuity given by: $\phi = \left(\frac{r(1+r)^h}{(1+r)^h - 1} \right)$ Where r *is* the annual interest rate and h is the number of years during which the equipment installation cost is paid off.
b_i	Annual operation and maintenance cost per MW for DER type i
c_i	Tax incentive or subsidy per MW for installing DER type i (a penalty cost per MW if using a substation)
$E[L_f]$	Mean load (i.e. demand) at an upper node f
$E[L_e]$	Mean load (i.e. demand) at lower node e
L	System total load (i.e. demand). L is a random variable. Using the central limit theorem, $L \sim N\left(\sum_{i \in I} E\left[L_i\right], \sum_{j \in J} \sigma^2\left(L_i\right) \right)$ where $E[L_i]$ and $\sigma^2[L_i]$ represent the mean load and its variance at node i
E[L]	Expected value (i.e. mean) of the total system load (i.e. demand) and computed as: $E\left[L\right] = \sum_{j \in J} E\left[L_J\right]$
I_f	Maximum current flow at upper node f
I_e	Maximum current flow at lower node e
V_{DG}	Voltage at any distribution line of the DG network
α	loss-of-load probability

Model 1

Minimize

$$g(x) = \sum_{i \in I} \sum_{j \in J} a_i \phi P_i^{(c)} x_{ij} + \sum_{i \in I} \sum_{j \in J} E[P_{ij}](b_i + c_i) x_{ij} \tag{3}$$

Subject to

$$\int_0^{\infty}\left(\int_y^{\infty} f_p(z)\,dz\right) f_L(y)\,dy \geq 1-\alpha \tag{4}$$

$$\sum_{e\in E_f}\left(E[L_e]-\sum_{i\in I} x_{ie}E[P_{ie}]\right)+E[L_f]-\sum_{i\in I} x_{if}E[P_{if}] \leq V_{DG}I_f \qquad \forall f \in F \tag{5}$$

$$E[L_e]-\sum_{i\in I} x_{ie}E[P_{ie}] \leq V_{DG}I_e \qquad \forall e \in E \tag{6}$$

$$\sum_{i\in I} x_{ij} \leq 1 \qquad \forall j \in J \tag{7}$$

$$\sum_{k\in K} x_{k1} = 1 \tag{8}$$

$$x_{ij} \in [0,1] \tag{9}$$

As listed in Table 2, the model has binary decision variables, $x_{ij,}$ that become equal to 1 if DER type i is installed in node j, and 0 otherwise. The objective function (3) minimizes $g(x)$, the annual cost of the DG system based on the assumption that the power generated at the nodes does not vary and is equal to the expected value. In the objective function, three cost components are considered: (a) the annualized installation cost per MW of DER type i ($\emptyset a_i$), (b) the annual operating and maintenance cost per MW of DER type i (b_i) and (c) the annual penalty due to the emission of greenhouse gases of DER type i (c_i). The penalty cost due to emission of greenhouse gases, is primarily associated with generation equipment using fossil fuels, instead of renewable energy. Power plants operating with gas turbines that use fossil fuels have negative impact on the environment due to the emission of greenhouse gases, while there is an incentive or subsidy if a WT is installed. The term c_i in the objective function represents a penalty if a substation is placed into a node and a tax incentive or subsidy if a WT is installed. It is assumed that

the annual operating and maintenance costs per MW of DER equipment of the same type do not vary according to the location where the equipment ends installed.

Constraint (4) ensures that the power quality of service is guaranteed for a high percentage of the time. Constraint (4) can be re-written as $\Pr\{P > L\} \geq 1 - \alpha$ and thus it computes the probability that the total power, P, in the network exceeds the total load L. As mentioned in Section 2.1, Problem Statement, the smaller the value of α the more reliable the power supplied by the system. For example, if the distribution system is allowed for one day power shortage every year, then α should be less than 0.003 (i.e., 1/365). Uncertainty of the wind reduces the reliability of single WT and therefore the total system reliability. In practice, when this happen it could be necessary to use marginal or extra capacities from substations to haul additional electricity from the central generation plants and mitigate the power shortage resulting from wind uncertainty.

Given a model solution (i.e. a siting and sizing for the WT and the substation), x_{ij}, the left-side of constraint (4) can be computed exactly by an optimization solver as shown in detail in Appendix A assuming the total power (P) and the total load (L) are normally distributed according to the central limit theorem (CLT). The CLT states that the distribution of the sum of a sufficiently large number of independent random variables with finite mean and variance has a limiting cumulative distribution which approaches the normal distribution. The CLT is still valid when individual variables are weakly correlated as it may be the case in this problem where the nodes may be in the same geographic location. Parameters for the distributions of P and L are given in Tables 3 and 5, respectively. Constraint (4) makes Model 1 a chance constrained, non-linear integer

program which is a non-smooth one. Non-linear non-smooth problems (NSP) are often difficult type of optimization problems to solve since derivative information is not meaningful for them. An algorithm looking for a solution to an NSP may find an "improved" solution which is not necessarily a global or even a local optimal solution (Frontline systems, 2006). However, there are currently in the market non-linear solvers that can find local optimal solutions to NSP.

Thermal constraint (5) is for those network nodes that may provide power to other nodes (i.e. upper nodes) excluding the central node. The constraint ensures that the total mean load (i.e. demand) on the distribution line (DL) serving an upper node and all its lower nodes does not exceed the maximal power such DL can bear after considering that the DER equipment installed on the nodes will mitigate some of the load. Thermal constraint (6) has a similar purpose but it is for the terminal nodes in the network (i.e. lower nodes).

Equation (7) specifies that at most one DER is installed in each node of the DG network. This condition can be easily relaxed if needed in real applications. Equation (8) requires that the substation be installed at the central node (i.e. Node 1). According to El-Khattam et al. (2004), this constraint is quite reasonable because the substation is responsible for delivering bulk electricity, and the central node facilitates the distribution of power to local nodes.

2.6.2 Model 2 – Deterministic model

In order to simplify the complexity on solving Model 1, the probabilistic loss-of-load constraint (4) in Model 1 (i.e. $P(P > L) \geq 1-\alpha \rightarrow P(P-L>0) \geq 1-\alpha$ can be relaxed by assuming that the power generation and the load (i.e. demand) are

independent. Using CLT, constraint (4) is transformed into its deterministic counterpart as given by constraint (10) by using the well-known theory about the distribution of the difference of two random normal variables (Mathworld, 1999). In this new constraint, z corresponds to the z-score of the normal standard distribution and μ and σ^2 represent the mean and variance for the probability distributions of the total power (notated as $P(x)$ to indicate that is a function of the problem decision variables, x) and the total load (L).

Model 2 is then given by equations (3), (10), and (5-9). Model 2 turns into a deterministic linear program in which the system variability is captured by including in the model the standard deviations for the total power and the total load.

$$\mu_P \geq \mu_L + z_{1-\alpha}\left(\sigma^2_{P(x)} + \sigma^2_L\right)^{1/2} \tag{10}$$

2.6.3 Model 3 - Stochastic programming model

Modeling the output power of the WT by its mean value as done in Models 1 and 2 may have unfavorable consequences (Birge and Louveaux, 1997). Thus, in this section a stochastic programming model that optimizes considering simultaneously multiple scenarios for the output power of the WT is formulated. This model is expected to be more robust than the models discussed in the previous sections.

Model 3 is a stochastic program that results from enlarging the thermal constraints in the chance constrained model (Model 1) to consider simultaneously eleven different scenarios in characterizing all possible power outputs of the WT. The extensive form (Rardin, 2017; Birge and Louveaux, 1997) of Model 3 is a non-linear chance-constrained model.

Decision variables for the proposed stochastic programming model, Model 3, are given in Table 6. The reader can refer to the notation introduced in Tables 1-5 in

subsection 2.6.1 since most of it applies to Model 3. Additional notation for sets and parameters used in Model 3 is in Tables 7 and 8. The extensive form of the model is presented and discussed immediately below the tables.

Table 6. Decision Variables for Model 3 Stochastic Program

Notation	Definition
x_{ij}	Binary decision variable. It becomes equal to 1 if DER type i is installed in node j and 0 otherwise

Table 7. Additional Sets for Model 3 Stochastic Program

Notation	Definition
S	Wind speed scenarios. Each scenario corresponds to a vector of realizations for wind speeds at each one of the nodes in the network

Table 8. Additional Parameters for Model 3 Stochastic Program

Notation	Definition
p_{sj}	Wind speed probability for scenario s at node j
P_{ijs}	Power generated if DER unit type i is installed at node j and wind speed scenario is s

Model 3:

Minimize

$$g(x) = \sum_{i\in I}\sum_{j\in J} a_i \phi P_i^{(c)} x_{ij} + \sum_{i\in I}\sum_{j\in J}\sum_{s\in S} p_{sj} P_{ijs} (b_i + c_i) x_{ij} \tag{11}$$

Subject to

$$\int_0^{\infty} \left(\int_y^{\infty} f_p(z)\, dz \right) f_L(y)\, dy \geq 1 - \alpha \tag{12}$$

$$\sum_{e\in E_f} (E[L_e] - \sum_{i\in I} P_{ies} x_{ie}) + E[L_f] - \sum_{i\in I} P_{ifs} x_{if} \leq V_{DG} I_f \qquad \forall f \in F, s \in S \tag{13}$$

$$E[L_e] - \sum_{i \in I} P_{ies} x_{ie} \leq V_{DG} I_e \qquad \forall e \in E, s \in S \qquad (14)$$

$$\sum_{i \in I} x_{ij} \leq 1 \qquad \forall j \in J \qquad (15)$$

$$\sum_{k \in K} x_{k1} = 1 \qquad (16)$$

$$x_{ij} \in [0,1] \qquad (17)$$

Since P_{ij}, the power generated by DER type i at node j, is considered as a random variable in Model 3, the objective function $g(x)$ in (11) represents the expected annual cost of the DG system. The model presented here is conceived to be used at a strategic decision level. Besides being connected to a substation, this stochastic model does not assess the value of additional recourse actions to hedge against the various wind speed scenarios. Such assessment is considered in the next chapter of this thesis where t a new model that involves strategic and operational decisions is presented.

The original loss-of-load probabilistic constraint (constraint 12) is kept in this model. The thermal constraints at the nodes are specified in constraints (13-14) for each wind speed scenario s. These constraints have a meaning like the one mentioned in the chance constrained model (Model 1). If a WT is installed on a node, the energy supplied by the WT helps to satisfy the node load (i.e. demand). The model also requires that at most one DER unit be installed at each node (constraint 15) and that the substation be located at the central node (constraint 16). Constraint (17) is a sign constraint that specify that the decision variables x_{ij} are binary.

The objective function in this stochastic model is more complicated to compute since it considers simultaneously multiple scenarios instead of just the mean case. Also,

the number of thermal constraints grows since they need to be satisfied for each of the considered scenarios.

2.6.4 Model 4 - Simulation optimization model

The simulation-optimization model (Model 4) is based on the simulation optimization concepts presented in Frontline Solvers (2019), Jian and Henderson (2015) and Fu (2001). The idea behind simulation optimization or optimization via simulation is to compare different alternative decisions while keeping the stochasticity in the model.

Model 4 keeps the chance constraint for the loss of load probability introduced in Model 1 and thus is still a non-linear model. However, instead of assuming the power generated by a DER at each node is equal to its expected value as in Models 1 and 2, or enlarging the model by incorporating explicitly a fixed number of scenarios as in Model 3, Model 4 uses simulation to generate a single matrix of realizations for the power generated at by each DER type at each node. The model is evaluated with such matrix of realizations on a given solution for the siting and sizing of the WT and the substation (i.e. a feasible solution that is not necessarily optimal). The process of generating a matrix of realizations for the power is repeated for a large number of trials (or scenarios) and then the expected objective function cost at the given solution is computed. This simulation steps are repeated for a given pool of feasible solutions. Through a heuristic method another pool of feasible solutions is generated. The evaluation of those new solutions is done again with the described simulation method until a prescribed number of iterations for the heuristic method is reached. The solution with the best expected cost is output.

The decision variables for the simulation optimization model, Model 4, are the same as the ones given in Table 6 for Model 3. The reader can refer to Tables 1-5,7 and

8 in the previous sections to learn about the notation for sets, parameters, and probability functions used in Model 4. The simulation optimization model is given by equations (18)-(24). Model 4 is a chance-constrained non-linear integer program as Models 1 and 3.

Model 4

Minimize

$$g(x,s') = \sum_{i\in I}\sum_{j\in J} a_i \phi P_i^{(c)} x_{ij} + \sum_{i\in I}\sum_{j\in J} P_{ijs'}(b_i + c_i)x_{ij} \tag{18}$$

Subject to

$$\int_0^{\infty}\left(\int_y^{\infty} f_p(z)dz\right) f_L(y)dy \geq 1-\alpha \tag{19}$$

$$\sum_{e\in E_f}(E[L_e] - \sum_{i\in I} P_{ies'}x_{ie}) + E[L_f] - \sum_{i\in I} P_{ifs'}x_{if} \leq V_{DG}I_f \qquad \forall f \in F \tag{20}$$

$$E[L_e] - \sum_{i\in I} P_{ies'}x_{ie} \leq V_{DG}I_e \qquad \forall e \in E \tag{21}$$

$$\sum_{i\in I} x_{ij} \leq 1 \qquad \forall j \in J \tag{22}$$

$$\sum_{k\in K} x_{k1} = 1 \tag{23}$$

$$x_{ij} \in [0,1] \tag{24}$$

In the objective function (18) the subscript s' in $P_{ijs'}$ represents a single realization of the WT power output at each network node. Similarly, in constraints (20-21) $P_{ies'}$ and $P_{ifs'}$ correspond to a realization of the WT power at the lower and upper nodes, respectively. These realizations can be easily computed by generating a random sample

of the wind speeds at the nodes of the network and computing the associated power as will be detailed in Figure 6 on Section 2.8.2. The objective function $g(x,s')$ in (18) represents the cost of the DG system under scenario or realization s'. The simulation-optimization model given by (18)-(24) is evaluated repeatedly a very large number of trials or scenarios, NT, to compute the expected DG system annual cost, $E(g(x,s))$, as shown in Equation (25).

$$E(g(x,s')) = \frac{1}{NT}\sum g(x,s') = \frac{1}{NT}\left[\sum_{i\in I}\sum_{j\in J} a_i \phi P_i^{(c)} x_{ij} + \sum_{i\in I}\sum_{j\in J} P_{ijs'}(b_i + c_i)x_{ij}\right] \qquad (25)$$

2.7 Experimental setting

2.7.1 Network topology

The four optimization models presented in the previous section are tested on the 9-node network DG system shown in Figure 3. This network topology is originally given in (El-Khattam et al., 2004; Hadian et al., 2009). It is a typical DG network to be served with WT and a substation which is the primary electric power supplier. The eight power distribution lines are represented by the long arrows. In the figure, L_2, …, L_9 represent the loads (i.e. power demands) at the nodes. DER units can be placed in any of the nodes enumerated from 2 to 9. The only node allowing for a substation is the central node.

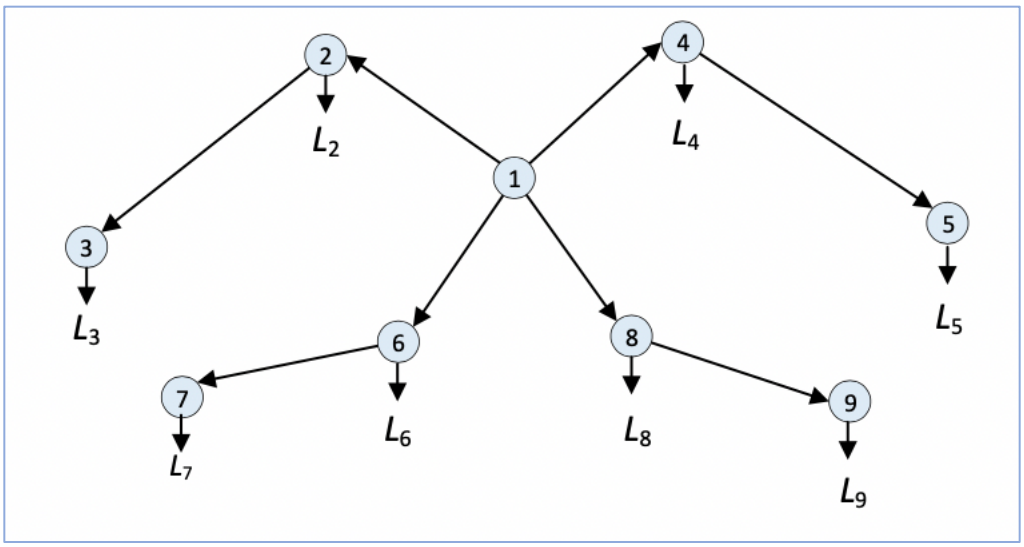

Figure 3. The DG system used for the numerical study in Chapter 2

2.8 Values for the parameters in the models

2.8.1 DG system costs

Table 9 presents all the DER costs and capacities. A substation of 40MW or 50MW capacity can be located only at the central node. A WT with capacity 1MW, 2MW or 3MW may be installed at each of the remaining nodes. The DER equipment installation costs and the operating and maintenance (O&M) costs decrease as the DER capacity is larger because of economies of scale. There are only penalty costs associated with the substation and there are no tax incentives associated with the WT.

Table 9. Costs for the DER units

i	DER Unit	DER Capacity (MW) $P_i^{(c)}$	Equipment Installation Cost ($/MW) a_i	Annual Operating and Maintenance (O&M) Cost ($/MW) b_i	Annual Penalty Cost ($/MW) c_i
1	WT 1	1	1,400,000	15,000	0
2	WT 2	2	1,250,000	12,750	0
3	WT 3	3	1,100,000	10,500	0
4	Substation	40	273,000	22,500	5,000
5	Substation	50	227,500	18,750	7,500

The values assumed for the annual interest rate, *r*, and the number of years to pay the equipment installation cost, *h,* are 4% and 20 years, respectively. These values are used to compute the factor ϕ that convert the present installation cost a_i to annuity. The formula to compute ϕ was defined in Table 5 in Section 2.6.

2.8.2 Probability distribution for the power output by DER type i at node j (P_{ij})

The models are tested in three cities: Wellington (W), New Zealand, Rio Gallegos (RG), Argentina and New York (NY), USA. Large samples (about 9,000 observations in each) of wind speed data at ground level (y_g) were collected hourly from Weather Underground (2016) for each of these 3 cities for 9 years (2006-2014). This data was used to compute the wind speed at the WT blades (y_h) and the probability distribution for the power output of each type of WT at each node. The height of the WT is assumed 80 m (i.e. h=80 m).

None of the sampled years and cities let to conclude that y_h adjusted to a theoretical probability distribution. However, in most of the cases the normal distribution was the one providing the lowest fitting error but still the *p*-value was less than 0.05 indicating that such distribution was not a good fit. Appendix B summarizes the distributions that were found as the "best fits" for each sample.

Figure 4 shows a histogram that permits to compare the wind speed (m/s) at the WT blades (y_h) and its mean, standard deviation and sample size for the 3 cities studied for the year 2010.The figure reveals also that the normal distribution is not a good fit for these data. Figure 5 has a boxplot for the data collected for wind speed (m/s) at the WT blades (y_h) for all years and cities studied. Figure 5 shows that the data for Rio Gallegos had some strong outliers but not for years 2009, 2010 and 2014. Figures 4 and 5

corroborate that Wellington is a city with high winds as well as Rio Gallegos. On the other hand, New York has less winds. Appendix C contains tables with the most relevant statistics for y_h for each city and year.

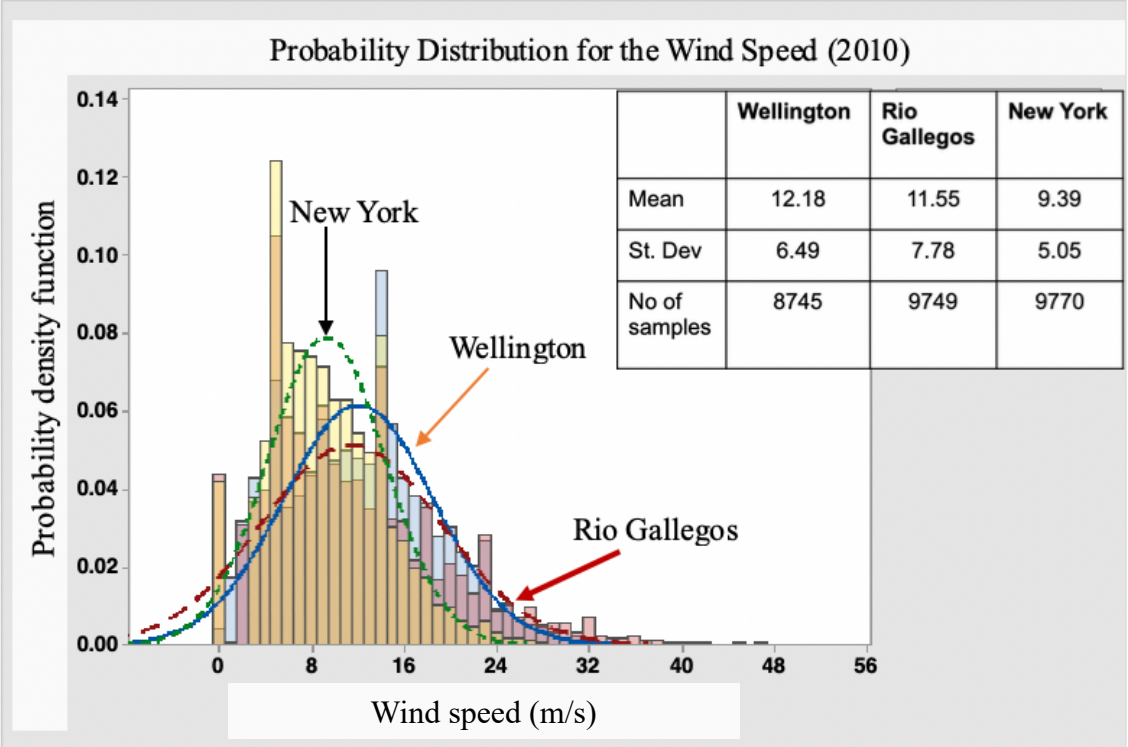

Figure 4. Histogram of wind speed data in year 2010 for the three cities studied

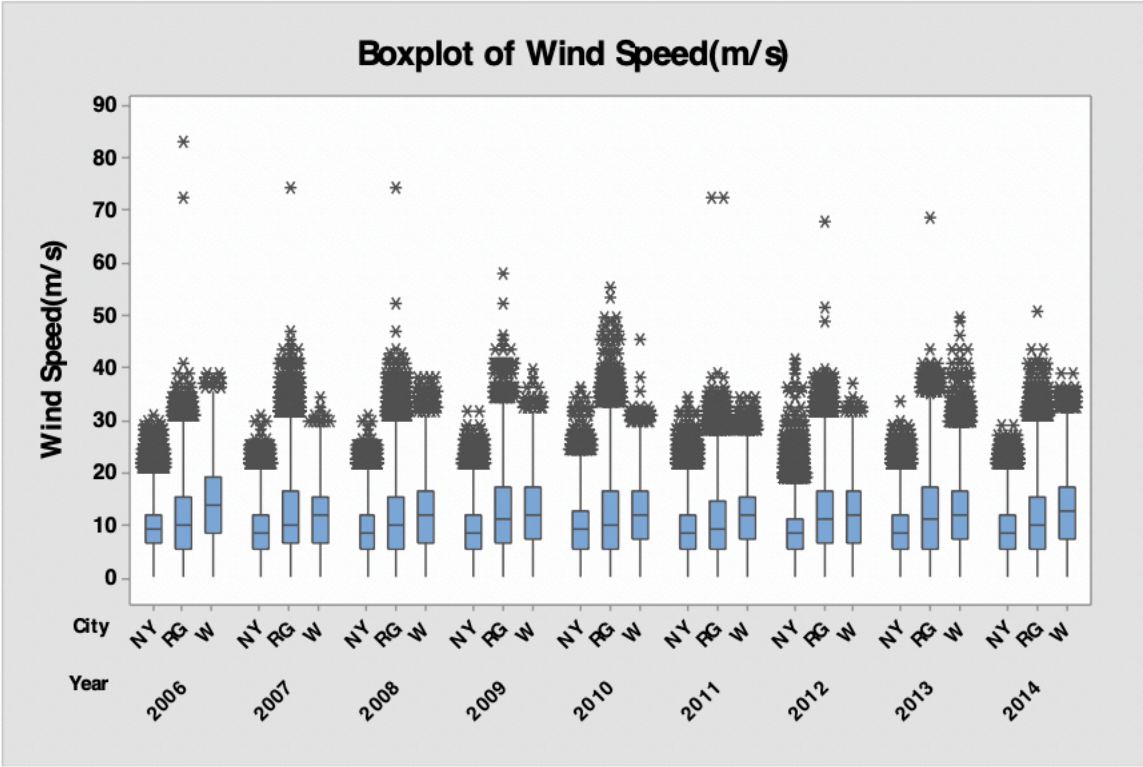

Figure 5. Boxplots of climate data collected for 9 years

The procedure to compute the empirical probability distribution of the power output of each type of WT in each node and city and its mean and variances is shown in Figure 6.

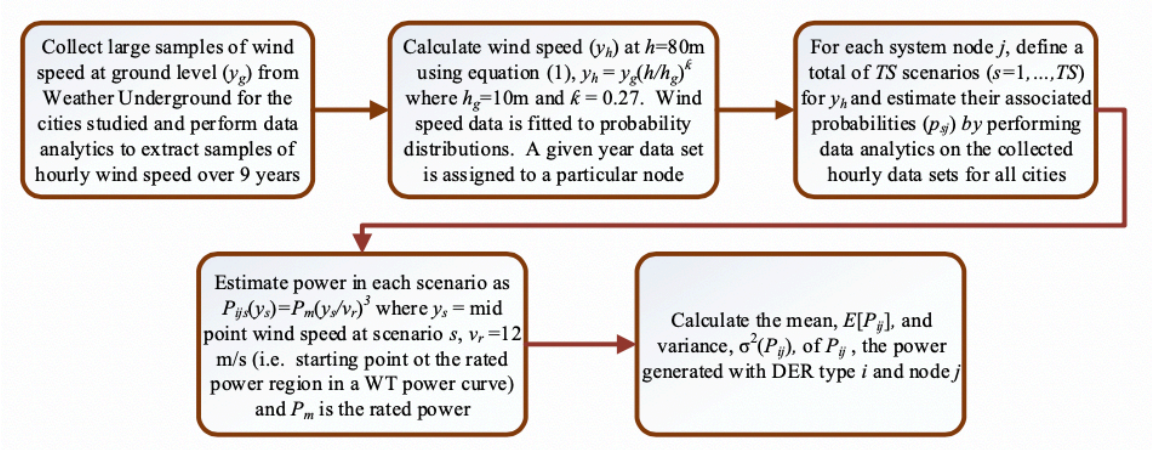

Figure 6. Procedure to compute the probability distribution for the power output

Observed wind speeds for a single year (about 9,000 observations) were used to compute the wind speed probabilities at a particular node and the power output of each type of WT using a finite number of outcomes or scenarios. The ranges to define the wind speed scenarios correspond to wind speeds that agree with those in which a WT operates (v_c = 2 m/s to v_r = 12m/s or more and v_s = 25m/s as presented in Figure 2 in Section 2.4). Table 10 lists the thirteen wind speed scenarios defined and their corresponding wind speed ranges and midpoints in m/s. Appendix D presents tables with the computed probabilities for all these thirteen scenarios in all cities. Model 3 ignored the first two scenarios since the focus of the model is to determine the best siting and sizing for the WT when the DG system is operating. Thus, scenarios 3-13 (i.e. 11 scenarios) are used in the stochastic programming model (Model 3) and the probabilities for those eleven scenarios at each node were adjusted accordingly.

Table 10. Pre-determined Wind Speed Scenarios in the Computational Study

Scenario (*s*)	**Wind Speed Range (m/s)**	**Mid-point Wind Speed at Scenario *s* (m/s) (y_s)**
1	0 - 1	0
2	1 - 2	0
3	2 - 3	2.5
4	3 - 4	3.5
5	4 - 5	4.5
6	5 - 6	5.5
7	6 - 7	6.5
8	7 - 8	7.5
9	8 - 9	8.5
10	9 - 10	9.5
11	10 - 11	10.5
12	11 - 12	11.5
13	> 12	18.5

2.8.3. System loads, maximum current at the distribution lines and other parameter values

Table 11 presents the assumed mean and variances for the load (i.e. demand for power) at each node *j* as well as the resulting total mean load and variance. The loads at each node are random variables. However, in this work, they are characterized only by their means and variances and thus there is no assumption on their underlying distributions. The right-hand side of the thermal constraints is specified by: (1) the maximum allowed current flowing towards each node I_j, given in Amperes (A) and presented also in Table 11 and (2) the voltage of the distribution lines, V_{DG}, which is assumed to be 33KV. The loss-of-load probability (α) is assumed to be 0.01 (i.e. 1%) and it corresponds to 3.65 days loss per year.

Table 11. Mean and Variance for the Loads

Node	Mean Load (MW) $E[L_j]$	Variance (MW^2) $\sigma^2(L_j)$	Maximum Load (A) I_j
1	0.00	0.000	N/A
2	7.64	0.146	500
3	7.72	0.210	250
4	4.58	0.052	450
5	4.00	0.040	210
6	7.64	0.146	500
7	7.27	0.132	250
8	6.11	0.093	450
9	5.14	0.066	210
	$E(L) = 50.10$	$\sigma^2(L) = 0.886$	N/A

2.9 Results

The models using the numerical values for the parameters given in the previous section are called “base models”. Table 12 shows the software tools used to solve each

model. In most of the models, two different commercial solvers were used to validate the results.

Table 12. Software Tools Used in each Model

Model Name	Modeling Software	Solver
1. Chance constrained non-linear	AMPL Analytic Solver Platform (ASP) software from Frontline Systems	Knitro Evolutionary Solver Algorithm
2. Deterministic linear program	AMPL	Knitro and/or CPLEX
3. Stochastic non-linear program	AMPL	Knitro
4. Simulation Optimization non-linear model	Analytic Solver Platform (ASP) software from Frontline Systems	Evolutionary Solver and the Simulation Optimization feature in ASP

Since Model 1 and Model 3 are non-linear, they were solved by performing 100 runs from different initial solutions that were randomly generated to report the best local optimal solution as the optimal solution found. The procedure followed by ASP to solve Model 4 is summarized in the flowchart in Figure 7. The Evolutionary Solver is a heuristic solution technique similar to Genetic Algorithm that explores a pool of feasible solutions and tries to improve it through iterations. Thus, Model 4 is not solved exactly while Models 1and 3 are solved by exact non-linear programming methods. Table 13 contrasts the model sizes in terms of number of rows and columns for the network topology studied.

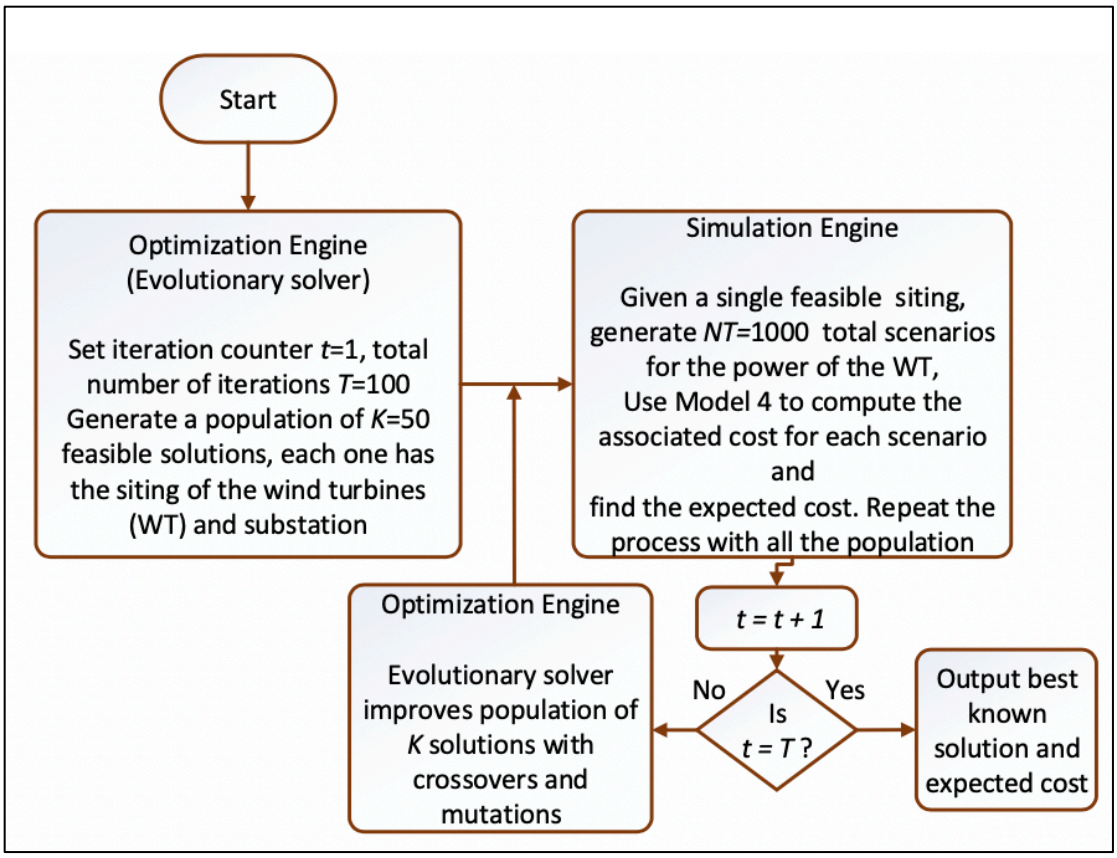

Figure 7. Simulation optimization procedure for Model 4 in Analytic Solver Platform

Table 13. Sizes for the Different Models Studied in Chapter 2

Base Model Name	Decision Variables	Constraints
1. Chance constrained non-linear	45	19
2. Deterministic linear program	45	19
3. Stochastic non-linear program	45	99
4. Simulation Optimization non-linear model	45	19

Tables 14 -16 present the results from solving the base models and assessing the expected costs of their solutions considering the stochastic wind speed scenarios. The results shown in the tables are number of turbines, total installed capacity (in MW), DER

type sited at each network node, expected total annual cost, the extra-cost incurred if not using the stochastic model (as explained in detail in section 2.9.1) and percentage of change in expected cost of each model vs. the stochastic programming model (Model 3).

Due to high-wind speeds in Wellington, medium-high wind speeds in Rio Gallegos and medium-low wind speeds in New York, the results from solving the stochastic programing base Model 3 show that for a mean total load (*E[L]*) of 50.1MW, New York requires the highest number of turbines at the highest annual cost (6 2MW, 2 3MW, $3,071,149), followed by Rio Gallegos (3 1MW, 4 2MW, $2,689,590) and Wellington (6 1MW, 1 2MW, $2,509,897).

2.9.1 Computation of models expected annual cost and value of the stochastic solution

The Value of the Stochastic solution (VSS) is often computed to numerically asses the effectiveness of a stochastic model (Birge and Louveaux 1997; Shapiro et al., 2007). Since the objective of stochastic Model 3 is cost minimization, the VSS is renamed as the cost of not using the stochastic model (CNSM). The procedure followed in this thesis to compute the CNSM consists of two steps. First, the siting solution obtained by the deterministic model (Model 2) or the chance constrained model (Model 1) is plugged into the stochastic model (Model 3) and the resulting expected annual cost of using such solutions is collected. Those costs are reported in the third to last line of Tables 14-16 for Models 1and 2. Secondly, the CNSM is computed as the difference between such resulting costs and the cost from solving the stochastic model (Model 3) and reported in the second to last line of Tables 14-16. Note that the costs reported in the third to last line of Tables 14-16 for Model 3 and 4 are the ones directly obtained from solving these models. The procedure to compute CNSM is summarized in Figure 8.

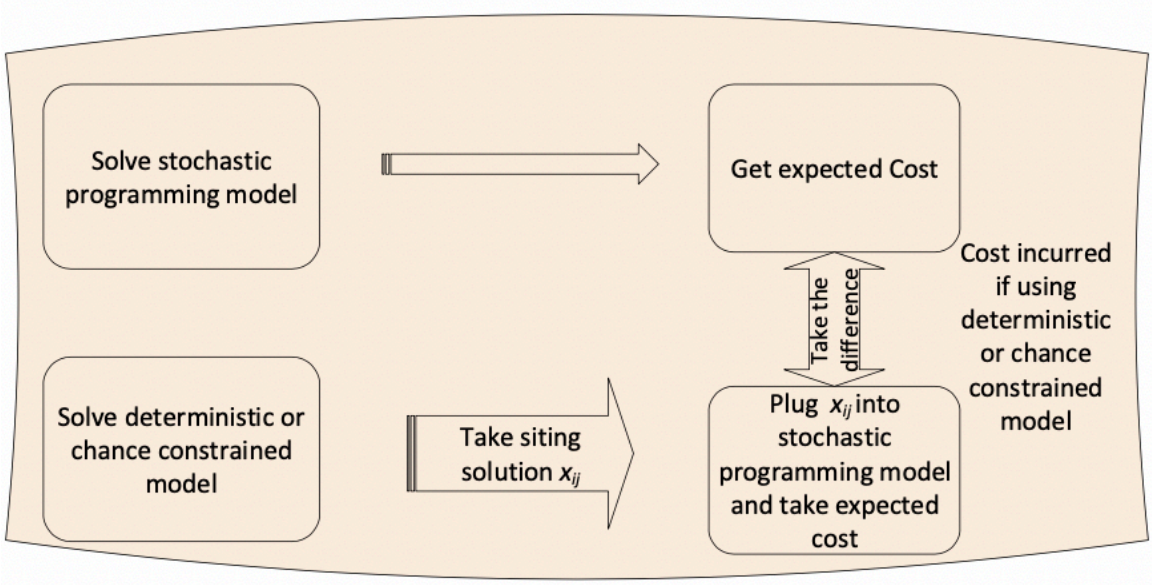

Figure 8. Steps in computing cost of not using stochastic model (CNSM)

In computing the CNSM, when the deterministic model was solved and the siting solution was plugged into the stochastic model, the stochastic model became infeasible as the loss of load probability constraint was violated. Then 3MW turbines were added one after the other till the model became feasible. The power produced by the initial plugged in solution was subtracted from the power produced by the currently found feasible solution. Such power difference was then multiplied by an assumed, relatively optimistic, price of electricity purchased from the grid ($25/MWh).

Table 14. Detailed Solution for the Base Models in Wellington

Models		Deterministic (Model 2)	Chance Constrained (Model 1)	Stochastic (Model 3)	Simulation Optimization (Model 4)
No of WT		2 turbines	7 turbines	7 turbines	7 turbines
Total Power Reported by each Model (MW)		51.93	55.12	55.39	54.03
		Installed DER capacity (MW)			
	Node	1 2 3 40 50	1 2 3 40 50	1 2 3 40 50	1 2 3 40 50
	1	0 0 0 0 1	0 0 0 0 1	0 0 0 0 1	0 0 0 0 1
	2	1 0 0 0 0	1 0 0 0 0	1 0 0 0 0	0 1 0 0 0
	3	0 0 0 0 0	1 0 0 0 0	1 0 0 0 0	1 0 0 0 0
	4	0 0 0 0 0	1 0 0 0 0	1 0 0 0 0	1 0 0 0 0
	5	0 1 0 0 0	0 1 0 0 0	1 0 0 0 0	1 0 0 0 0
	6	0 0 0 0 0	1 0 0 0 0	1 0 0 0 0	1 0 0 0 0
	7	0 0 0 0 0	1 0 0 0 0	1 0 0 0 0	0 0 0 0 0
	8	0 0 0 0 0	1 0 0 0 0	0 1 0 0 0	1 0 0 0 0
	9	0 0 0 0 0	0 0 0 0 0	0 0 0 0 0	1 0 0 0 0
Expected Total Annual Cost ($/year)		$3,379,263	$2,509,955	$2,509,897	$2,522,597
CNSM		$869,366	$58		$12.700
Percentage Increase vs. Stochastic (Model 3)		25.73%	0.00%		0.50%

Table 15. Detailed Solution for the Base Models in Rio Gallegos

Models		Deterministic (Model 2)	Chance Constrained (Model 1)	Stochastic (Model 3)	Simulation Optimization (Model 4)
No of WT		3 turbines	8 turbines	7 turbines	8 turbines
Total Power Reported by Each Model (MW)		51.62	56.33	56.87	56.63
		Installed DER capacity (MW)			
	Node	1 2 3 40 50	1 2 3 40 50	1 2 3 40 50	1 2 3 40 50
	1	0 0 0 0 1	0 0 0 0 1	0 0 0 0 1	0 0 0 0 1
	2	1 0 0 0 0	1 0 0 0 0	0 1 0 0 0	1 0 0 0 0
	3	0 0 0 0 0	1 0 0 0 0	1 0 0 0 0	1 0 0 0 0
	4	0 0 0 0 0	1 0 0 0 0	0 1 0 0 0	0 1 0 0 0
	5	0 0 0 0 0	0 1 0 0 0	1 0 0 0 0	0 1 0 0 0
	6	1 0 0 0 0	0 1 0 0 0	1 0 0 0 0	1 0 0 0 0
	7	0 0 0 0 0	1 0 0 0 0	0 1 0 0 0	1 0 0 0 0
	8	0 0 0 0 0	1 0 0 0 0	0 1 0 0 0	1 0 0 0 0
	9	1 0 0 0 0	0 1 0 0 0	0 0 0 0 0	0 1 0 0 0
Expected Total Annual Cost ($/year)		$3,665,942	$2,690,511	$2,689,590	$2,689,895
CNSM		$976,352	$921		$305
Percentage Increase vs. Stochastic (Model 3)		26.60%	0.03%		0.01%

Table 16. Detailed Solution for the Base Models in New York

Models		Deterministic (Model 2)	Chance Constrained (Model 1)	Stochastic (Model 3)	Simulation Optimization (Model 4)
No of WT		4 turbines	8 turbines	8 turbines	8 turbines
Total Power (MW)		51.75	58.03	58.41	58.23
		Installed DER capacity (MW)			
	Node	1 2 3 40 50	1 2 3 40 50	1 2 3 40 50	1 2 3 40 50
	1	0 0 0 0 1	0 0 0 0 1	0 0 0 0 1	0 0 0 0 1
	2	1 0 0 0 0	0 1 0 0 0	0 1 0 0 0	1 0 0 0 0
	3	0 0 0 0 0	0 1 0 0 0	0 1 0 0 0	1 0 0 0 0
	4	0 0 0 0 0	0 0 1 0 0	0 0 1 0 0	0 1 0 0 0
	5	0 0 0 0 0	0 1 0 0 0	0 1 0 0 0	0 1 0 0 0
	6	1 0 0 0 0	0 1 0 0 0	0 1 0 0 0	1 0 0 0 0
	7	1 0 0 0 0	0 0 1 0 0	0 0 1 0 0	1 0 0 0 0
	8	0 0 0 0 0	0 1 0 0 0	0 1 0 0 0	1 0 0 0 0
	9	1 0 0 0 0	0 1 0 0 0	0 1 0 0 0	0 1 0 0 0
Expected Total Annual Cost ($/year)		$3,782,032	$3,071,149	$3,071,149	$3,077,206
CNSM		$710,883	$0		$6.057
Percentage Increase vs. Stochastic Model (Model 3)		18.80%	0.00%		0.20%

The CNSM results in the tables show that the largest increase in cost due to not using the stochastic model occurs in Rio Gallegos ($976,352 or 26.6%) because this city has the highest variability in wind speeds as it was shown in the histogram in Figure 5 and in the boxplot in Figure 6 presented in section 2.8.2. This result corroborates the hypothesis about the value of using a stochastic model if there are highly variable wind conditions.

A further analysis on the results posted in Table 15 shows that when the load is 50.1MW in Rio Gallegos, since the chance constrained model doesn't consider high wind scenarios it does a somewhat more pessimistic plan by recommending eight turbines (5 1MW, 3 2MW). However, the stochastic model plans for seven (3 1MW, 4 2MW). However, the total amount of installed WT capacity is 11 MW in both cases. The reduction in number of turbines for the stochastic model explains the ($921/year or 0.03%) difference in model costs found.

Comparing the cost results from Model 1, Model 2 and Model 3 gotten in this section, the author in this thesis concludes that the stochastic model performs the best since it considers the uncertainties on wind speed through multiple scenarios in a single model that also has the probabilistic loss of load constraint. The system owner will have a cost saving by using the stochastic model instead of the deterministic or the chance constrained model to design the DG system especially in cities where there are strong winds and a large number of scenarios with high winds (i.e. significant variability in the winds speed towards the high side of the distribution).

2.9.2 Cost comparison for the solution of the base case using the stochastic model (Model 3) and simulation optimization model (Model 4)

Table 17 shows 95% confidence intervals (LCI, UCI) for the average cost, when solving the simulation optimization model (Model 4) 5 times in each of the cities studied using a large number of trials or scenarios (i.e. NT=1000) at each time. Shapiro (2007) mentions that the computed LCI corresponds to a 95% lower bound for the optimal objective function value of a sample average approximation problem based on a large sample of size N (i.e. in this thesis it is the number of trials or scenarios , NT; and

NT=1000). Shapiro (2007) mentions that in applications it often suffices to use small values of *M, M=5 or M=10* to compute such lower bound. He also mentions that this lower bound is also a lower bound for the optimal objective function value of the stochastic programing model. Note the closeness of the computed LCI and the resulting costs from solving the stochastic model (Model 3) in the last row of Table 17.

Table 17. Cost Comparisons between Stochastic Model (Model 3) and Simulation Optimization Model (Model 4)

	Run	Wellington	Rio Gallegos	New York
Simulation Optimization (Model 4)	1	$2,510,142	$2,689,292	$3,082,280
	2	$2,572,572	$2,690,497	$3,081,796
	3	$2,510,278	$2,689,649	$3,081,996
	4	$2,510,236	$2,690,455	$3,070,226
	5	$2,509,755	$2,689,585	$3,069,734
	Average	$2,522,597	$2,689,895	$3,077,206
	Std. Dev	$27,938	$547	$6,601
	LCI	$2,495,961	$2,689,374	$3,070,913
	UCI	$2,549,232	$2,690,417	$3,083,500
Stochastic (Model 3)		$2,509,897	$2,689,590	$3,071,149

The numbers in Table 17 allows to conclude that the costs for the stochastic and simulation optimization models are very close. Thus, the simulation optimization model has been useful in this thesis to validate the results given by the stochastic optimization model.

In the next sub-sections, sensitivity analysis is carried out to examine how changes to parameters in the stochastic model (Model 3) change its optimal total cost and the placement and sizing of the WT in the DG system.

2.9.3 Effect of load on expected annual cost for the stochastic model (Model 3)

Figure 9 shows the behavior of the expected total annual cost for Model 3 if one increases in the mean total load ranging from -6% to 6% of the base load (i.e. 50.1 MW). In other words, the mean total load is varying in the interval [47.10MW, 53.10MW]. In all cases and cities, except for those with demand increases of 4% and 6% in New York, the system meets the load by adopting WT of different capacities. This result is very satisfactory considering that in practice the load randomly fluctuates. At 53.10MW (i.e. 6% increase), Wellington and Rio Gallegos install 8 WT but the 3MW capacity used in Wellington is much less. Wellington requires (7 2MW, 1 3MW, $3,071,573) and generates total power (P) of 61.49MW while Rio Gallegos requires (1 2MW, 7 3MW, $3,323,156) and generates 64.22MW. At 51.10MW (i.e. 2% increase), New York uses all 3MW turbines and generates 61.28MW. Therefore New York is not able to accommodate additional increases in total load (i.e. the model becomes infeasible if the mean total load is increased by 4% and 6%). The results in Figure 9, give a decision maker an insight on the cities where stochastic Model 3 is feasible and more attractive to adopt. A table presenting the percentage increase in cost as total load increases is presented in Appendix E.

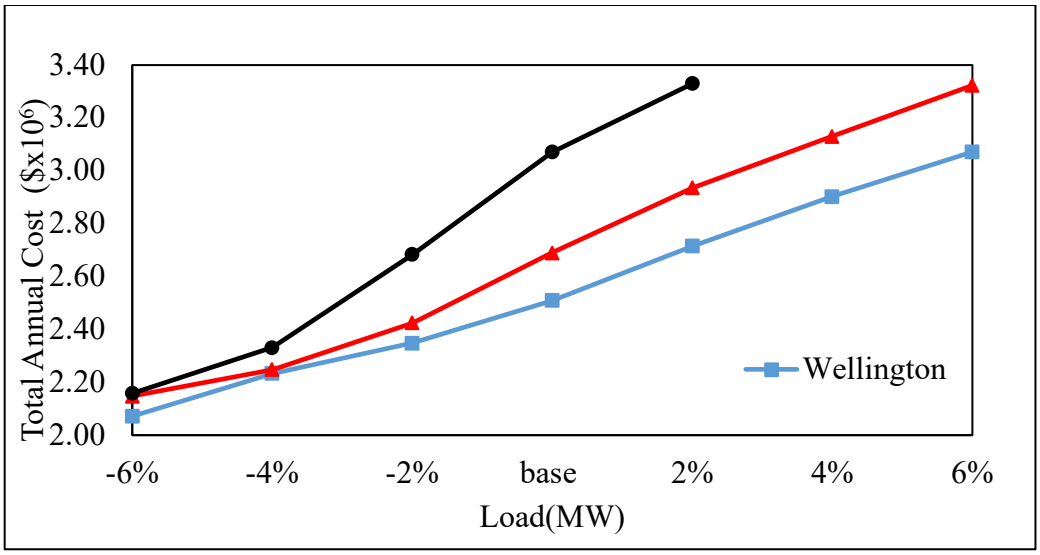

Figure 9. System cost vs total load

2.9.4 Effects of loss-of-load-probability on expected annual cost for the stochastic model (Model 3)

Figure 10 presents the sensitivity analysis for changes in expected total annual cost to variations in the loss-of-load probability (α) represented as a fraction. It shows that if α is 0.0001, which is very close to zero in Figure 10, (i.e. 0.01% or 0.0365 days with energy losses per year) the system still finds a solution for Rio Gallegos and Wellington. Rio Gallegos requires all 3MW turbines, Wellington requires (1 2MW, 7 3MW) and New York becomes infeasible at this point as it is not able to ensure that a power outage does not occur 99.999% of the time. The results in Figure 10 gives confidence to the decision maker because they show that the system designed using stochastic programming is highly reliable for the cities studied. A table also presenting the percentage change in cost while varying alpha (α) is available in Appendix E.

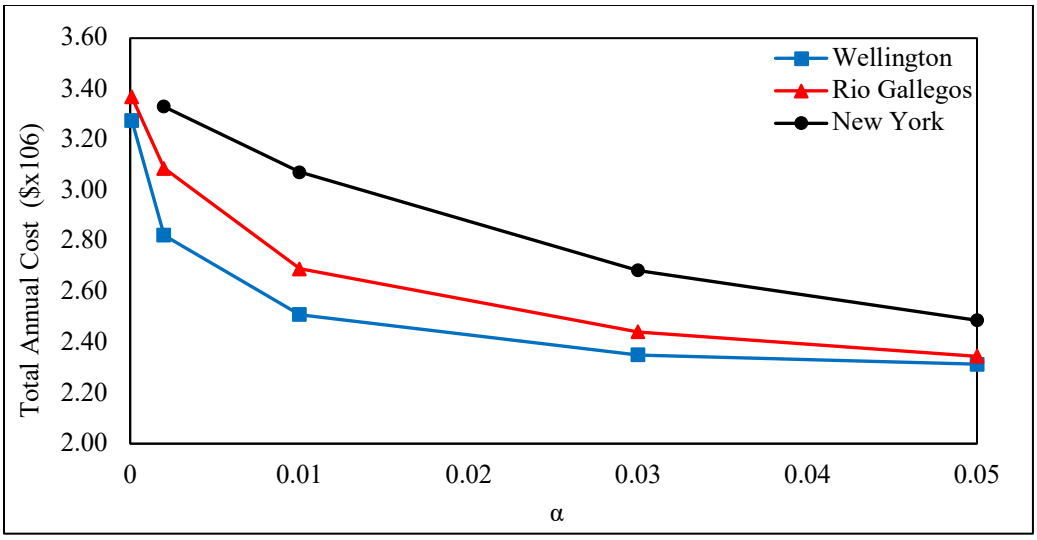

Figure 10. System cost vs of loss-of-load probability (α)

2.9.5 Effects of operating cost on expected total annual cost for the stochastic model (Model 3)

Figure 11 represents the effect of changing the operating and maintenance cost on the expected total annual cost of the system for stochastic Model 3. Here the operating cost is reduced and increased by 20% from the base O&M cost (*b*). The graph shows a linear relationship between the operating cost and the total expected annual cost of the system.

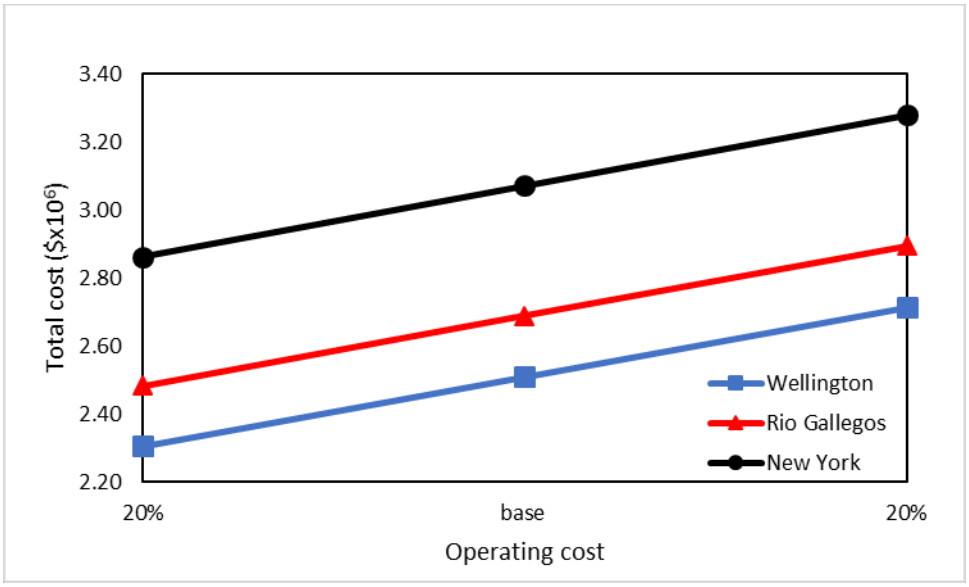

Figure 11. System cost vs of operating cost

2.9.6 Effects of equipment installation costs on total expected annual cost for the stochastic model (Model 3)

Figure 12 represents the sensitivity done on equipment installation cost for stochastic Model 3 (*a*). This cost is also reduced and increased by 20% from the base cost. The graph also shows a linear relationship between the equipment cost and the total expected annual cost.

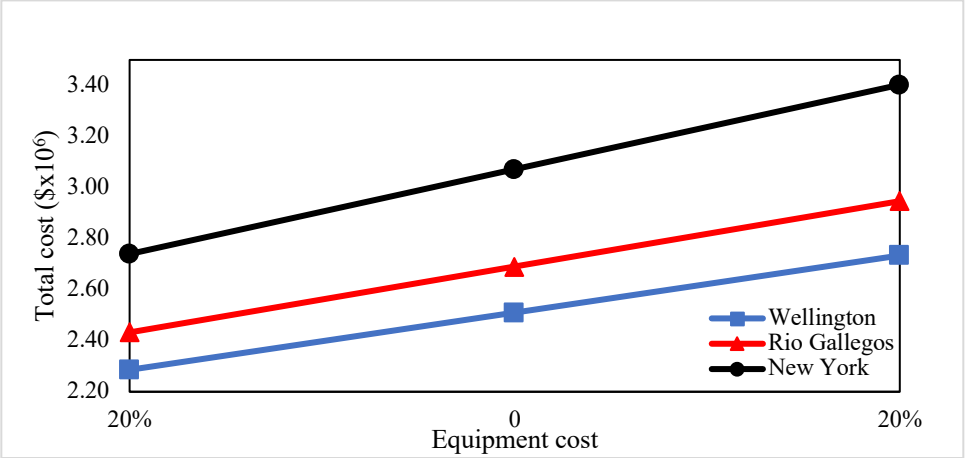

Figure 12. System cost vs of equipment cost

2.10 Practical aspects on the design of wind powered DG systems and how they impact the models proposed

The first step in the designing a wind powered DG system is to identify the location and then a decision can be taken to invest in the development. The aim of designing the DG systems is to maximize energy production, minimize capital and operating cost and minimize power shortage while taking into consideration the constraints imposed by the given site. The major factors that affect the DG system cost are the complexity of the sites and the extreme loads (e.g. a windy site with extreme loads will end up more expensive due to the investment of higher wind turbine capacity).

In identifying the suitable locations for developing wind farms, a decision must be made on whether the wind turbines are to be placed onshore or offshore. In the U.S, the offshore wind energy is a rapidly growing industry as various concerns exist with the onshore wind farms (i.e. noise pollution, aesthetic and physical blockage that could occur from buildings or hills). The first offshore wind farm was powered in December 2016 and is located in Rhode Island. The wind farm was estimated to decrease the islands electric rates by 40%. Ever since the powering of the first offshore wind farm, the US offshore wind projects have reached a total of 25,464MW across 13 states. The major drawbacks of the offshore wind farm is the cost as wind turbines are susceptible to damages due to high wind speeds that occur during storms and hurricanes.

The proposed models in this chapter apply more closely to the design of onshore wind farms. However, if including other aspects such as the distances from the turbines location to thee substation and customer nodes locations, the models could also apply to the offshore setting.

3. SITING AND SIZING OF WIND TURBINES UNDER PROSUMER MODE

This chapter is divided into 9 subsections. Section 3.1 presents the problem to be modeled and solved in this chapter. Section 3.2 gives the background information about energy prosumers. Section 3.3 presents the importance of prosumers to the grid. Section 3.4 summarizes the contributions of other authors on the topic of energy prosumers. Section 3.5 presents the methodology used. Section 3.6 describes the mathematical model. Section 3.7 shows the experimental setting used in solving the model considering customer nodes as prosumers. Section 3.8 presents the parameters used in solving the model. Section 3.9 presents the results and the sensitivity analysis carried out on the model.

3.1 Problem statement

This chapter tackles with a variant of the problem discussed in Section 2.1 of this thesis. This new problem considers decisions to be taken at the DG system design stage and a couple of additional relevant decisions that arise in the operational stage of the system.

The problem studied in this chapter considers that the DG system nodes are prosumers who not only consume energy, but also generate and trade energy with the main grid. The problem is to find the siting and sizing of the WT in this new DG system. The system consists of interconnected nodes that can be stores, factories, etc. and wind powered DER units of different capacities (i.e. 1MW, 2MW, 3MW). The DG system is connected to a substation which distributes power to the upper system nodes and whose size is also to be determined. The problem objective is to minimize the installation and operation costs of the DG system. The wind speed is assumed as a random variable that

affects the power output of the WT and consequently the total system reliability. The substation provides marginal or extra capacity sent from the main grid to absorb the power loss coming from wind uncertainty. Thus, marginal amounts of power would need to be purchased from the grid and sent to the substation to feed the system nodes. On the other hand, there will be days when the power generated by the WT exceeds the electricity load. Nodes will send back the extra renewable energy to the substation through which the renewable energy is further exported to the main grid. Nodes will receive a payment for the renewable energy returned and it is also known as feed-in-tariff. The new DG system studied in this chapter is shown in Figure 13.

In Figure 13, the grid is shown as a relevant actor of the system, the electricity loads at the nodes are denoted as L_2, …, L_9 and the bi-directional arrows at the distribution lines represent the power flowing between the substation and the nodes depending on the amount of generated wind power from the node.

In summary, the new problem objective is to find the design of minimum cost for the DG system comprised of prosumer nodes considering not only installation, maintenance and operational costs but also those costs incurred from purchasing energy from the grid and the income from selling the surplus renewable energy generated back to the grid. The optimal design for the DG system will determine the amount and capacity of the WT to install at each node of the network, the optimal capacity of the substation, the expected amount of power purchased from electric grid and sent to upper nodes to satisfy electricity loads (i.e. demands) at the nodes, and the expected amount of excess renewable power generated by the nodes that would be returned back to the main grid

through the substation. The optimal design will keep considering thermal constraints at the distribution lines and the loss-of-load probability constraint.

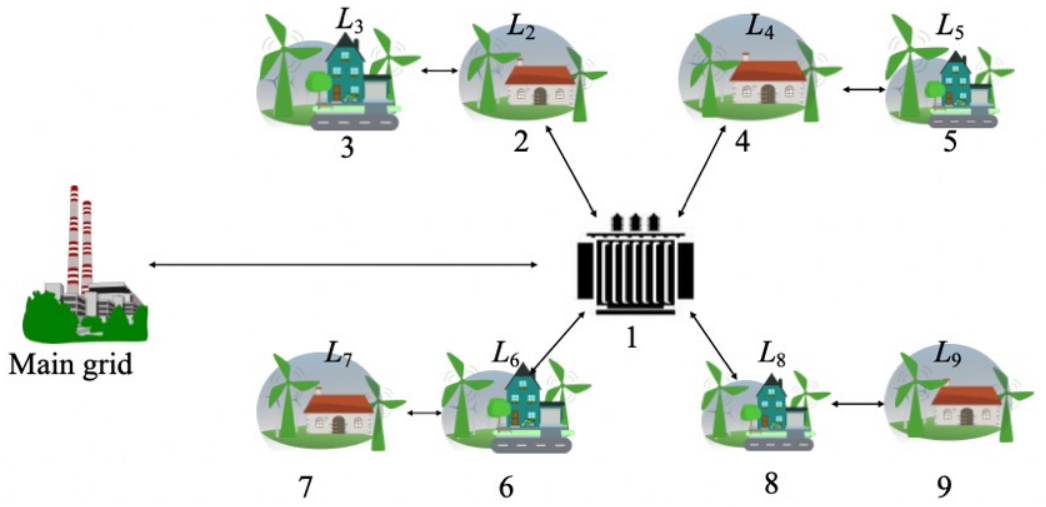

Figure 13. The DG system studied in Chapter 3

3.2 Prosumers

A prosumer can be defined as a person who consumes and produces a product. The concept of prosumer was first developed by Alvin Toffler, author of the book "The Third Wave" who argued that prosumption was already predominant in pre-industrial societies. Thus, from the beginning the economic form was neither production nor consumption, rather it was prosumption (Ritzer & Jurgenson, 2018). Ever since, the prosumer concept has been defined by various authors, in the contexts of marketing and media, mass customization and energy. In the field of energy, prosumers (i.e. producer-consumer) have been recently defined as an end-user who is able to produce and store as well as consume electricity (Zhao et al., 2015). Being a prosumer changes the role of the consumer of energy from merely being a customer to becoming an active participant in the energy grid.

3.3 Impact of prosumers to the grid

Currently, world power generation technology is rapidly changing as large and public power plants are no longer the sole source of power. Various governments have been encouraging consumers to install WT or solar PV which would increase the growth of renewable energy integration and reduce greenhouse gas emissions. The future of the electric grid would then consist of many small independent smart microgrids coupled with renewable energy generation and energy storage devices. These small microgrids would then serve as prosumers of energy.

According to Rathanayaka et al. (2011) the importance of the smart grid is its ability to achieve bi-directional energy flow between the energy users and the main grid. The impact of the presence of prosumers in the microgrid would be to increase the on-site generation of renewable energy and reduce the reliance on the central power plants through motivating energy sharing among prosumers (Cui et al. ,2019). Hussain et al. (2019) mention that prosumers have various encouraging results such as energy-cost reductions, demand-supply management, load-sharing and peak-shaving, additional services for

normal and emergency conditions, enhanced grid resilience, and increased consumer empowerment with advanced metering infrastructure.

3.4 Literature background on energy prosumers

In recent years, a significant amount of research has been done on energy prosumers as this is the future trend of smart grids. Wongwut and Nuchprayoon, (2017) proposed a mixed-integer programing model (MIP) for scheduling a prosumer where the objective was to minimize the operation cost (i.e. cost of purchasing power from the grid,

the cost of onsite generation and the cost of energy storage), given that the prosumer is able to use battery to store energy and to sell electricity under the time-of-use pricing method. The MIP model proposed by Wongwut and Nuchprayoon (2017) solves with GAMS and permits to find the size of the battery the prosumer must install and the threshold levels for charging and discharging the battery on an hourly basis. Several simulations were performed to analyze the performance of the system. One of them compare the State of Charge (SoC) when the prosumer has one, two and four sets of battery. This study seems mainly focused on scheduling the system storage devices.

Azar et al. (2019) presented two multi objective multi-period mixed integer nonlinear programming models for modeling the behavior of: (1) each independent prosumer in a residential neighborhood and (2) an aggregator or trader entity (i.e. a system operator that holds no physical connection with the grid also known as mediator, broker or coalition manager). The conflicting objectives in the prosumers model are: (1) maximizing the amount of prosumer load satisfied (i.e. the prosumers comfort level) nd charging the storage system as much as possible and (2) maximizing the prosumer's profit from selling power to the grid. The prosumers can execute only one decision (i.e. to sell or to buy energy) in each time interval. The objectives in the aggregators' model are: (1) maximizing the aggregator's profit by selecting how much energy to buy/sell from/to the prosumers and from/to the grid and (2) minimizing the grid burden by matching prosumers supply and demand. The models were solved heuristically with a nondominated sorting genetic algorithm (NSGA-III) to find the amount of power to sell or buy and the corresponding price. To simplify the communication and computational overhead, the authors modeled the negotiation of the prosumers and the aggregator as a

noncooperative game with two entities, a virtual power plant that represents the prosumers and the aggregator. The authors concluded that the proposed framework was effective and efficient and propose to extend it to include industrial and commercial prosumers.

Van der Stelt et al. (2018) compared the technical and economic feasibility of both household energy storage (HES) and community energy storage systems (CES) from the perspective of the end-consumer using as economic indicator the Levelized Cost of Energy (LCOE). In this problem, it is assumed that the feed-in pricing tariff will disappear in the future. The authors developed models that schedule the allocation of energy from the PV system, battery and grid to satisfy the demands of the households and minimize the amount of power taken from the main grid over a time horizon. The models are formulated as mixed integer linear programs with the objective of minimizing the cost of power purchased from the grid. The models presented are tested with data collected from a residential district with 39 households in the Netherlands. The authors conclude that both HES and CES are economically infeasible for households. The author of this thesis found that Van der Stelt et al. (2018) model includes constraints that bound the amount of power taken from and returned to the grid. The idea on using those constraints resembles to the one used in thermal and capacity constraints for the mathematical model in Section 3.6.

Cui et al. (2019) presented a two-stage energy sharing framework for a new prosumer microgrid comprised of PV and multiple storage units and operating under flexible load shifting. The first stage was formulated to provide a robust sharing schedule for prosumers to overcome uncertainties of market price and renewable energy while the

second stage was to ensure prosumers optimize its energy schedule at each hour according to the most current system state. Simulation studies showed the benefit of the proposed energy sharing framework and demonstrated that the models running time is small so they can be implemented in practice.

Hussain et al. (2018) proposed non-linear stochastic wind energy management model with bi-directional energy flow between a smart grid and wind energy prosumers. The model consisted of several sub-models with the objectives of maximizing smart grid revenue and prosumers energy surplus and minimizing prosumer energy costs. The sub-models tackled the uncertainties that could be faced by fluctuations on the market price and the wind profile. The models were solved heuristically with genetic algorithms. The results were compared to the ones from using particle swarm optimization through simulations that used real data. Genetic algorithms performed better than particle swarm optimization. This paper evidences the current applicability of optimization models for optimizing wind energy systems that consists of energy prosumers. To the best of our knowledge no paper has considered solving exactly a model that incorporates stochasticity of the wind generation and thermal and loss of load probability constraints on a network of prosumers

3.5 Methodology

The problem of finding the siting and sizing of WT in the DG system considering system nodes as prosumers is approached with the formulation and solution of a non-linear two-stage stochastic programming model. Stochastic programming is an approach for modeling optimization problems that include parameters that are uncertain, but assumed to lie in a given set of values at the time a decision should be made (Shapiro et

al., 2007). In a two-stage stochastic program, decisions are divided into two stages. The first stage includes decisions done before the values of the random parameter(s) are known. The second one considers a specific action or recourse to take after the stochastic parameter(s) realize. The recourse decisions look to compensate for any bad effects resulting from the first-stage decisions. Two-stage stochastic programming identifies a policy that is feasible for all (or almost all) the possible parameter realizations by optimizing the expected value of a function that assesses the simultaneous impacts of first-stage decisions and two-stage recourse actions for each scenario (Novoa et al., 2018).

In the two-stage stochastic model presented in this section, the first stage consists of the decision on the siting and sizing of the WT and the substation. The only stochastic parameter is the wind speed and its effect on the power output of the WT. The second stage is the DG system operational stage. One of the recourse actions considered to occur in the second stage of the model are the purchases of power that nodes will do from the substation to satisfy their hourly loads. The other one is the sales of power the prosumer nodes will engage with the grid when surplus renewable energy ends generated. Both recourse actions (i.e. the bi-directional flows of power between the nodes and the substation) will be considered as possible to occur under each wind speed scenario. The model looks to simultaneously minimize the annualized expected net cost of the first stage decisions and the expected cost or benefit of the second stage recourse actions.

A standard approach to solve two-stage stochastic programming problems is to assume that the random vector of model parameters has a finite number of possible realizations or scenarios with associated probabilities. Under this assumption, a two-stage

stochastic program can be formulated on its extensive form. We follow this approach; eleven different scenarios for the wind speed encountered by the WT are considered.

3.6 Mathematical model for the optimal design of a DG system powered by wind turbines in Prosumers Mode.

The DG planning problem that a system planner confronts aims to search a trade-off between the total system cost and the risk of energy losses. Such problem can be formulated as an optimization model that looks to minimize the expected system cost subject to the reliability chance-constraint on the energy losses and considering also other system constraints, such as the thermal constraints. The following subsections present the optimization model proposed to solve the DG planning problem considering the system nodes as prosumers. Such model is named as Model 5.

3.6.1 Model 5 – Two-Stage stochastic model considering nodes as prosumers:

Tables 18 - 22 present the notation for Model 5. The optimization model is presented and discussed immediately below the tables.

Table 18. Sets used in Model 5

Notation	Definition
I	Types of WT possible to install
J	Nodes in the DG system
F	Upper nodes in the DG system. Upper nodes have distribution lines that link them with other nodes different to the substation and thus they can provide power to other nodes.
E	Lower or terminal nodes in the DG network
E_f	Lower or terminal nodes emanating from upper node F
S	Wind speed scenarios. Each scenario corresponds to a vector of realizations for wind speeds at each one of the nodes in the network

Table 19. Decision Variables for Model 5

Notation	Definition
x_{ij}	Integer decision variable. Number of WT type *i* installed in node *j*
z	Capacity of the installed substation
y_{sf}^{+}	Power purchased from electric grid by upper node *f* at scenario *s*
y_{sf}^{-}	Renewable power sent from upper node *f* back to the electric grid at scenario *s*

Table 20. Power Parameters for Model 5

Notation	Definition
P_{ij}	Power generated by WT type *i* installed at node *j*. P_{ij} is a function of y_h the wind speed at WT height *h*. Function argument y_h is dropped to simplify notation
$E[P_{ij}]$	Expected value (i.e. mean) of the power generated by WT type *i* installed at node *j*.
$\sigma^2(P_{ij})$	Variance of the power output for WT type *i* at node *j*
P_{WT}	Total power generated by the WT in the DG system. *P* is a random variable. Using the central limit theorem, $P_{WT} \sim N\left(\sum_{i\in I}\sum_{j\in J} E\left[P_{ij}\right]x_{ij}, \sum_{i\in I}\sum_{j\in J}\sigma^2\left(P_{ij}\right)x_{ij}^2\right)$ Here P_{WT} is a function of P_{ij}, x_{ij} and the wind speed y_h Again the function argument y_h is dropped to simplify the notation
$E[P_{WT}]$	Expected value (i.e. mean) of the total power generated by the WT computed as: $E[P_{WT}] = \sum_{i\in I}\sum_{j\in J} E[P_{ij}]x_{ij}$
$P_i^{(c)}$	Capacity of WT type *i*
P_{ijs}	Power generated if WT type *i* is installed at node *j* under wind speed scenario *s*

Table 21. Probability Functions for Model 5

Notation	Definition
f_P	Probability density function for the system total generated power, *P*
f_L	Probability density function for the system total required load (i.e. demand), *L*

Table 22. Additional Parameters for Model 5

Notation	Definition
p_{sj}	Wind speed probability for scenario s at node j
a_i	Present cost per MW for installing WT type *i*
a_k	Present cost per MW for installing substation type *k.* We are considering only one type of substation but we preferred to keep a subscript for this parameter
$\emptyset$	Factor to convert a present worth to annuity given by: $\phi = \left(\frac{r(1+r)^h}{(1+r)^h - 1} \right)$ Where *r is* the annual interest rate and *h* is the number of years during which equipment installation cost is paid off.
b_i	Annual operation and maintenance cost per MW for WT type *i*
b_k	Annual operation and maintenance cost per MW for substation *k*
c_i	Tax incentive or subsidy per MW for installing WT type *i*
h_k	Penalty cost per MW of using the substation to send power from electric grid to the prosumer nodes
q_k	Incentive per MW, if any, for using the substation to accept power returned from prosumers nodes to the grid. This term is included in the model, but it assumed equal to zero
m_k	Purchasing cost per MW of power acquired by prosumer nodes from the electric grid
n_k	Income per MW from selling extra renewable energy produced by the nodes to the electric grid
E[L_f]	Mean load (i.e. demand) at upper node *f*
E[L_e]	Mean load (i.e. demand) at lower node *e,*
L	Total system load (i.e. demand)
E[L]	Expected value (i.e. mean) of the total system load (i.e. demand) and computed as: $E[L] = \sum_{j \in J} E[L_j]$
I_f	Maximum current flow at upper node *f*
I_e	Maximum current flow at lower node *e*
V_{DG}	Voltage at any distribution line of the DG network
α	loss-of-load probability

Minimize

$$g(x) = \sum_{i \in I} \sum_{j \in J} (a_i \phi P_i^{(c)}) x_{ij} + \sum_{i \in I} \sum_{j \in J} \sum_{s \in S} p_{sj} P_{ijs} (b_i + c_i) x_{ij} + (a_k \phi) z$$
$$+ \sum_{s \in S} \sum_{f \in F} p_{sf} (b_k \mid y_{sf}^{+} - y_{sf}^{-} \mid + h_k y_{sf}^{+} - q_k y_{sf}^{-}) + \sum_{s \in S} \sum_{f \in F} m_k p_{sf} y_{sf}^{+} - \sum_{s \in S} \sum_{f \in F} n_k p_{sf} y_{sf}^{-}$$

Subject to

$$\Pr\{(P_{WT} + P_{Sub}) > L\} \geq 1 - \alpha \tag{27}$$

$$\left| \sum_{e \in E_f} (E[L_e] - \sum_{i \in I} P_{ies} x_{ie}) + E[L_f] - \sum_{i \in I} P_{ifs} x_{if} \right| \leq V_{DG} I_f \qquad \forall f \in F, s \in S \tag{28}$$

$$\left| E[L_e] - \sum_{i \in I} P_{ies} x_{ie} \right| \leq V_{DG} I_e \qquad \forall e \in E,\ s \in S \tag{29}$$

$$\sum_{e \in E} (E[L_e] - \sum_{i \in I} P_{ies} x_{ie}) + E[L_f] - \sum_{i \in I} P_{ifs} x_{if} = y_{sf}^{+} - y_{sf}^{-} \qquad \forall f \in F, s \in S \tag{30}$$

$$\sum_{f \in F} \left| y_{sf}^{+} - y_{sf}^{-} \right| \leq z \qquad \forall s \in S \tag{31}$$

$$\sum_{i \in I} x_{i1} = 0 \tag{32}$$

$$\sum_{i \in I} x_{ij} \leq 3 \quad \text{and} \quad x_{ij} \text{ integer} \qquad \forall i \in I, j \in J \tag{33}$$

$$0 \leq z \leq M \tag{34}$$

$$y_{sf}^{+} \geq 0, y_{sf}^{-} \geq 0 \qquad \forall f \in F, s \in S \tag{35}$$

Model 5 decision variables are x_{ij}, which are integer, and y_{sf}^{+}, y_{sf}^{-} and z_k which are continuous. The objective function (26) minimizes $g(x)$, the expected cost of installing and operating the DG system. The objective function is comprised of the following six cost components: (a) annualized installation cost of the WT , (b) expected annual maintenance and operating cost (M&O) of the WT and any tax incentives associated with their adoption, (c) annualized installation cost of the substation, (d) expected annual M&O cost of the substation and penalty cost associated with the use of fossil fuels to generate power, (e) expected cost from purchasing power from the grid, and (f) expected income from selling extra renewable power generated at the nodes to the main grid. The term in (c) also considers any tax incentives resulting from the substation accepting renewable power from the nodes but they are very unlikely to happen currently.

Constraint (27) is a chance constraint to ensure that on average the power quality of service is guaranteed for a high percentage of the time. The left-side of constraint (27)

computes the probability that the total power P in the network exceeds the total load L. Here $P = P_{WT} + P_{sub}$ is the total power gotten from the WT and from the substation. Given a siting and sizing for the WT and the substation, the left-side of constraint (27) can be computed exactly by an optimization solver as detailed in Appendix F assuming the total power (P) and the total load (L) are normally distributed according to the central limit theorem (CLT). Appendix F shows some updates that were necessary to be done to formulas in Appendix A. Constraint (27) makes Model 5 a non-linear integer program and thus a non-smooth one.

Constraint (28) is the thermal constraint for those network nodes that may provide power to other nodes (i.e. upper nodes). In Model 5, this constraint ensures that the power flowing on the now considered bi-directional distribution line (DL) serving an upper node and all its lower nodes does not exceed the maximal power that the DL can bear. Constraint (28) considers that the WT installed on the nodes will mitigate some of the load. Thermal constraint (29) has a similar purpose but it is for the terminal nodes in the network (i.e. lower nodes). Equation (30) specifies that for each scenario the power flowing through the distribution lines that connect to an upper node should be equal to the power requested by the upper nodes from the substation or to the extra power sent back to the grid by the upper prosumer nodes. In other words, constraint (30) states that only one type of flow (forward or backwards) takes place at a particular upper node and scenario.

Equation (31) specifies that the total power flowing in (or out of) the upper nodes should be at most the substation capacity. Constraint (32) specifies that no WT type i should be located at node 1. In Model 5, constraint (33) permits that at most three DER

type *i* is installed in each node *j* of the DG network. This is another difference between the problem studied in this chapter and the one in chapter 2. We want to assess the impact of allowing more WT installed in each node of the DG system. Constraint (33) also indicates that the x_{ij} variables are integer. Sign constraints in (34) and (35) ensure that the decision variables *z*,, y_{sf}^{+} and y_{sf}^{-} are greater or equal to zero. The sign constraint for the substation capacity also indicates that this decision variable has an upper bound given by the parameter named *M*

3.7 Experimental setting for Model 5

3.7.1 Network topology

Model 5 is tested on the 9-node network DG system presented in Figure 14. The black arrows in the figure represent the bi-directional flow of power in the distribution lines. In the figure, L_2, …, L_9 represent the loads (i.e. demands) at the nodes. DER units can be placed in any of the nodes enumerated from 2 to 9.

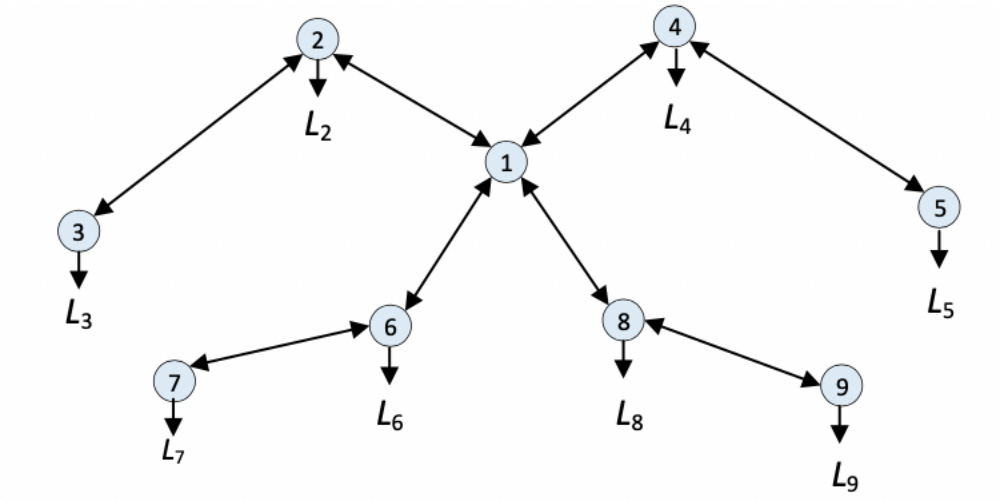

Figure 14. The DG system used for the numerical study in Chapter 3

3.8 Values for the parameters in Model 5

3.8.1 WT costs

WT with capacity 1MW, 2MW or 3MW may be installed at nodes 2 to 9. Table 23 presents the assumed WT costs.

Table 23. Costs for the WT Units Considered in Model 5

i	DER Unit	DER Capacity (MW)	Annualized Equipment Cost ($/MW) a_i	Annual Operating and Maintenance Cost ($/MW) b_i	Annual Incentive ($/MW) c_i
1	WT 1	1	1,400,000	15,000	0
2	WT 2	2	1,250,000	12,750	0
3	WT 3	3	1,100,000	10,500	0

3.8.2. Other parameter values

The experimental study is performed also in 3 cities with different wind profiles. The cities selected are the same as in Chapter 2: Wellington, Rio Gallegos and New York. Additional values for the parameters used in the objective function for Model 5 are listed in Table 24. The assumed number of hours per year used to compute these parameters is 8760.

Table 24. Parameter Values Associated with the Substation

Equipment Cost ($/MW) a_k	Annual Operating Cost ($/MW) b_k	Annual Penalty for Sending Power to Upper Nodes ($/MW) h_k	Annual Incentive for Returning Power to the Grid q_k	Annual Cost of Purchasing Power to the Substation ($/MW) m_k	Selling Price for Renewable Power Returned to the Grid ($/MW) n_k
227,500	18,750	7,500	0	438,000	219,000

The value for m_k results from if the cost of purchasing power to a substation is \$50/MWh and that there are 8760 hours per year. The value for n_k is assumed as \$25/MWh, meaning the revenue of prosumer is 50% of the utility price. Values for the remaining parameters in Model 5 are assumed to be the same as the ones mentioned in Chapter 2 in Tables 10 and 11 in Sections 2.8.2 and 2.8.3, respectively. These parameters relate to the probabilities associated with the wind speed scenarios, the loads at the nodes, the current, voltage, loss-of-load probability target value and the number of years and interest rate considered to annualize the installation costs.

3.9 Results

Model 5 is solved using the numerical values for the parameters given in the previous section. This case is named as "Base Model 5". The prosumer stochastic non-linear program is modelled in AMPL and solved using the Knitro solver. The size of Model 5 is presented in Table 25.

Table 25. Size for the Prosumer Stochastic Model

Base Model Name	Decision Variables	Constraints
The prosumer stochastic non-linear program	113	170

The result from solving Base Model 5 shows that for a mean total load of 50.1MW, all cities install (14 2MW and 24 3MW) WT units with different siting. Since the main objective of this problem is to minimize the annualized system cost, the model installs more turbines than needed in all the cities to produce extra energy that can then be sold for income. Wellington produces the largest amount of power 128.93MW with a total cost of \$6,400,876, Rio Gallegos produces a total power of 121.72MW with a total cost of \$7,994,771 while New York produces a total power of 109.36MW with the

highest cost at $12,285,994. Table 26 shows the detailed results for the base case in all cities.

Table 26. Detailed Solution of the Base Model 5 in all Cities

Cities Studied		Wellington			Rio Gallegos			New York		
No of WT		41			41			42		
Total Power Produced and Reported by each Model (MW)		80.87			77.23			69.05		
	Node	1MW	2MW	3MW	1MW	2MW	3MW	1MW	2MW	3MW
x_{ij}	1	0	0	0	0	0	0	0	0	0
	2	1	3	3	1	3	3	1	3	3
	3	0	3	3	0	3	3	0	3	3
	4	0	1	3	0	1	3	0	2	3
	5	0	0	3	0	0	3	1	0	3
	6	0	3	3	0	3	3	1	3	3
	7	0	3	3	0	3	3	0	0	3
	8	0	3	3	0	2	3	0	3	3
	9	0	0	3	0	1	3	0	1	3
Expected Total Annual Cost ($/year)		6,069,030			7,687,120			12,627,700		
Expected total power purchased from the grid		10.19			12.35			19.71		
Expected total power sold to the grid		30.68			27.30			18.52		

Figure 15 - 17 shows a pictorial of the total outputs for power purchased or sold per scenario adding over all nodes in the Base Model 5 for all cities studied.

From the figures, it is shown that Wellington and Rio Gallegos purchase power from the grid at scenarios 1-7, whereas at scenarios 8-11 the wind speeds are high so

enough power is being generated to be sold to the grid. It is shown from Figure 17 that New York is able to sell power to the grid in all scenarios. This could be as a result of the wind turbine capacity being higher than the load in some nodes.

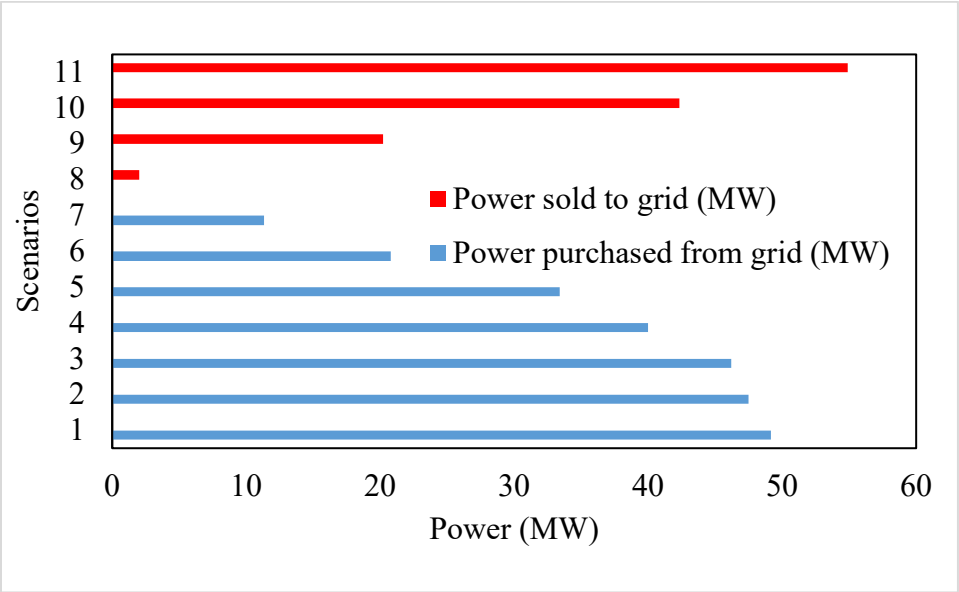

Figure 15. Power purchased and sold to the grid after solving Base Model 5 for Wellington .

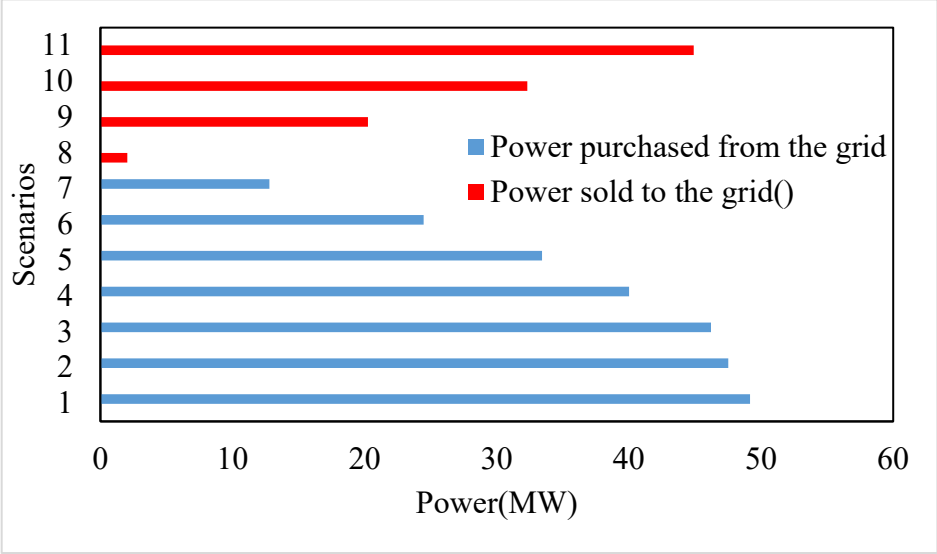

Figure 16. Power purchased and sold to the grid after solving Base Model 5 for Rio Gallegos .

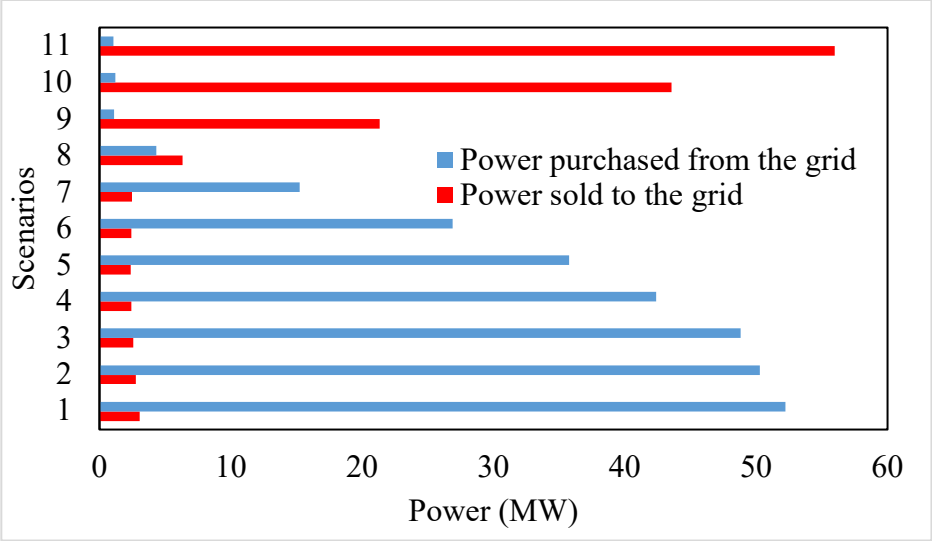

Figure 17. Power purchased and sold to the grid after solving Base Model 5 for New York .

3.9.1 Effects of varying loads on total cost

Table 27 and Figure 18 show the behavior of the total cost to changes in the mean total load ranging from -8% to 8% of the base load (i.e. total load in the range [46.10MW, 54.11MW]). In all cases and cities, the system meets the load by adopting WT of different capacities and produces extra energy that could be sold to the main grid. The sensitivity to the loads let imitate practical situations where power demands vary randomly. At 54.11MW, Wellington, Rio Gallegos and New York are still feasible to solve but generate different amount of total power. Wellington generates the largest power with 84.72MW at the lowest cost $6,937,580 while New York generates the least amount of power with 73.29MW at $13,937,100. At a 10% increase from the base load (55.11MW), the thermal constraint is violated in all cities as the current flowing in the distribution lines exceeds the maximum tolerable limits.

Table 27. Change in Cost if Varying the Mean Total Load in Model 5

% of change	Wellington ($\$x10^6$)	Rio Gallegos ($\$x10^6$)	New York ($\$x10^6$)
-8%	5.25	6.76	11.30
-6%	5.45	6.99	11.64
-4%	5.66	7.22	11.96
-2%	5.86	7.45	12.30
Base Model	6.07	7.69	12.63
2%	6.29	7.93	12.94
4%	6.50	8.17	13.28
6%	6.72	8.41	13.61
8%	6.94	8.65	13.94

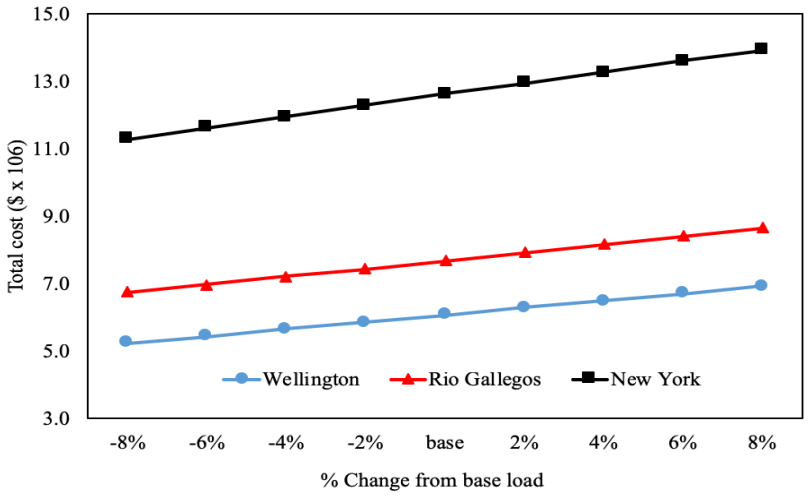

Figure 18. System cost versus varying loads

3.9.2 Behavior of power produced under the best and worst scenarios

In the Model 5 eleven wind speed scenarios were considered (speed scenarios 3 - 13). These scenarios represent all the typical wind speed scenarios that WT could encounter in the field. In Model 5, the following two extreme scenarios could occur:

The best case scenario. It happens when high wind speeds occur (i.e. speeds greater than 12 m/s but not exceeding 25 m/s). The WT produce the maximum output and the extra power generated can be sold to the grid. This is also the rated power region

phase from Figure 1. The worst case scenario occurs where there is very low wind speed (i.e. wind speeds greater than 2m/s but less than 12m/s), at this phase the WT produce reduced power. When this occurs, the loads might not be met and then the need to purchase extra power must be purchase and imported from the grid. This is also the nonlinear power production phase from Figure 1. Figure 19 shows how steep is the slope for the power purchased in the worst case scenario in Wellington when the load changes from its base value of 50.1 MW. The figure also shows that the power sold in the best scenario (line with negative slope) is not as sensitive to the changes in total load. For solving this problem, the upper bound for the capacity of the substation was assumed to be 55 MW.

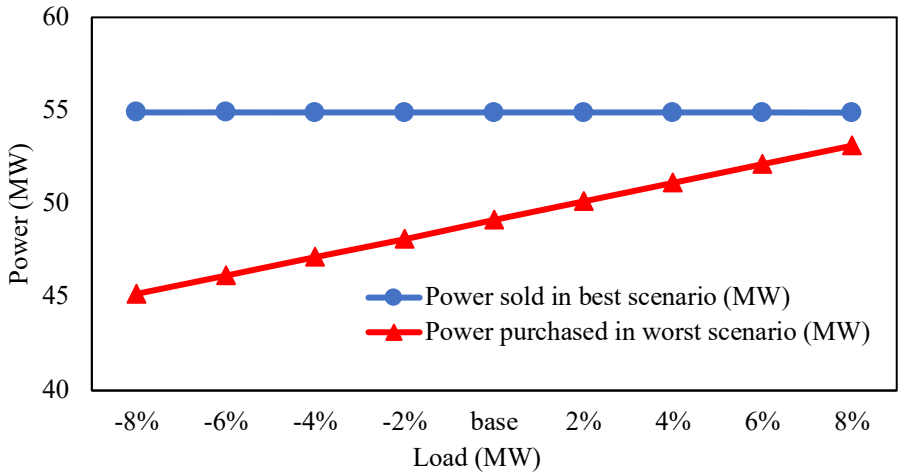

Figure 19. Behavior of power requested to or returned to the substation in the best and worst scenarios vs total load (Wellington)

3.9.3 Total cost comparison between the stochastic model (Model 3) and the stochastic model with system nodes as prosumers (Model 5)

Table 28 estimates the annual cost savings if planning the system using Model 5 instead of Model 3 presented in Chapter 2. The second and third to last columns of Table

28 (i.e. columns 5 and 6) show a direct cost comparison between stochastic model (Model 3) and stochastic model using system nodes as prosumers (Model 5). The major differences between Model 3 and Model 5 are: i) the cost of purchasing power from the grid and returning to the substation is included in Model 5 ii) the system nodes were not considered as prosumers in Model 3. To fairly compare both models, the cost of purchasing the power from the grid using the substation in Model 3 is computed and added to the total cost from solving Model 3 (see columns 2-4 in Table 28). The cost assumed was the one for purchasing electricity from the substation, $50/MWh and the number of operation hours per year assumed was 8,760 (i.e. 24*365).

The last column in Table 28 (i.e. column 7) shows the cost saving incurred if using the prosumer stochastic model (Model 5) instead of the stochastic model (Model 3) in the cities studied. The large difference in the assessed cost savings results from (1) permitting the number of WT to install in each node to be up to 3and (2) assuming system nodes as prosumers in the DG system.

Table 28. Cost Savings (in $) using Model 5 over Model 3

Cities	Objective Function Value Model 3 ($/year)	Expected Power Requested from the Sub-station in Model 3 (MW)	Cost of Purchasing the Requested Power from Grid ($/year)	Assessed Cost for Model 3 ($/year)	Objective Function Value Model 5 ($/year)	Cost Savings (Model 3 vs Model 5) ($/year)
Wellington	2,509,897	44.69	19,574,220	22,084,117	6,069,030	16,015,087
Rio Gallegos	2,689,590	43.23	18,934,740	21,624,330	7,687,120	13,937,219
New York	3,071,149	41.76	18,290,880	21,362,029	12,627,700	8,734,329

3.9.4 Total Cost Comparison between a Modified Deterministic Model (Model 6) and the Prosumer Stochastic Model (Model 5)

3.9.4.1 Modified deterministic model (Model 6)

The prosumer stochastic model (Model 5) is compared to a deterministic model similar to Model 2. This new deterministic model is called Model 6 Modified Deterministic and it is presented below. The notation for Model 6is the same presented in sections 2.6.1 and 2.6.2

Model 6

Minimize

$$g(x) = \sum_{i\in I}\sum_{j\in J} a_i \phi P_i^{(c)} x_{ij} + \sum_{i\in I}\sum_{j\in J} E[P_{ij}](b_i + c_i)x_{ij} \tag{36}$$

Subject to

$$\mu_P \geq \mu_L + z_{1-\alpha}\left(\sigma_{P(x)}^2 + \sigma_L^2\right)^{1/2} \tag{37}$$

$$\sum_{e\in E_f}(E[L_e] - \sum_{i\in I} E[P_{ie}]x_{ie}) + E[L_f] - \sum_{i\in I} E[P_{if}]x_{if} \leq V_{DG} I_f \qquad \forall f \in F \tag{38}$$

$$E[L_e] - \sum_{i\in I} E[P_{ie}]x_{ie} \leq V_{DG} I_e \qquad \forall e \in E \tag{39}$$

$$\sum_{i\in I} x_{ij} \leq 3 \qquad \forall j \in J \tag{40}$$

$$\sum_{k\in K} x_{k1} = 1 \tag{41}$$

Model 6 relaxes constraint (7) in Model 2 which ensures only one DER type *i* should be placed at a node *j*. As shown above, Model 6, constraint (40) allows at most 3 WT to be placed in each node *j*.

3.9.4.2 Computing the cost of not using prosumer stochastic model (CNPSM)

Tables 31-33 assess the annual cost incurred if not using the prosumer stochastic model (CNPSM) for planning the DG system. The last column of Tables 31-33 shows the annual extra cost incurred when using the modified deterministic model (Model 6) instead of the prosumer stochastic model (Model 5) with the total load varying between 50.1MW to 54.1MW for the cities studied. Model 6 does not consider: (1) prosumer nodes and (2) stochasticity of the wind speed and thus WT power output is replaced by the mean value; and (3) simplifies the chance constraint to a deterministic version of it.

When plugging the siting and sizing solution given by Model 6 into Model 5 the solution turned infeasible and thus it was not possible to collect the cost of adopting such deterministic solution. However, it was possible to assess the difference in power provided by the solution in Model 5 versus the one in Model 6. Such power needs to be purchased to the grid and send through the substation. The cost assumed was the one for purchasing electricity from the substation, $50/MWh, also used in Model 5. Figure 20 presents a flowchart with the computational steps to calculate the cost of not using prosumer stochastic model (CNPSM). The CNPSM was computed when the total load increases from 50.1MW to 54.1MW in all the cities studied as shown in Tables 29-31.

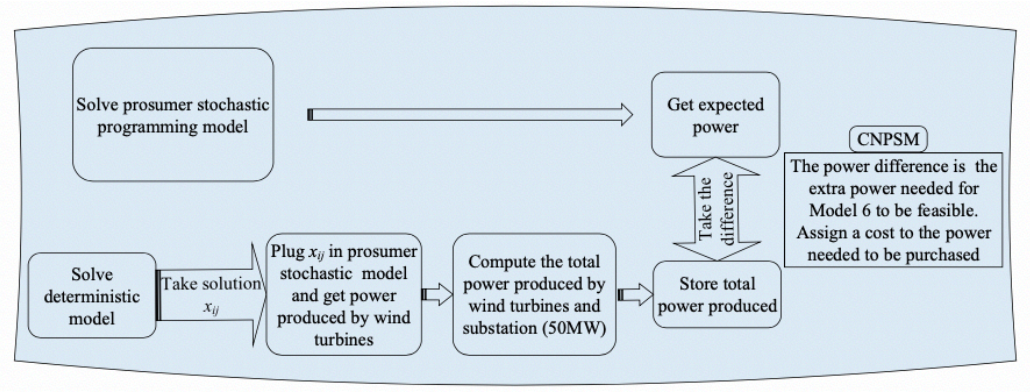

Figure 20. Steps in computing cost of not using prosumer stochastic model (CNPSM)

Table 29. Expected Annual Cost Incurred when using Model 6 instead of Model 5 in Wellington

	Modified Deterministic Model (Model 6)		Prosumer Stochastic Model (Model 5)		
Total Load (MW)	Power produced by WT (MW)	Total power produced by wind WT and substation (MW)	Power produced (MW)	Extra power to be purchased if using Model 6 (MW)	CNPSM ($/year)
50.1	1.93	51.93	80.87	28.95	12,678,392
51.1	3.25	53.25	81.96	28.71	12,574,980
52.1	4.47	54.47	82.72	28.25	12,373,500
53.1	6.42	56.42	83.65	27.23	11,926,740
54.1	7.74	57.74	84.72	26.98	11,817,240

Table 30. Expected Annual Cost Incurred when using Model 6 instead of Model 5 in Rio Gallegos

	Modified Deterministic Model (Model 6)		Prosumer Stochastic Model (Model 5)		
Total Load (MW)	Power produced by WT (MW)	Total power produced by WT and substation (MW)	Power produced (MW)	Extra power to be purchased by Model 6 (MW)	CNPSM ($/year)
50.1	1.62	51.62	77.23	25.61	11,217,925
51.1	3.45	53.45	78.28	24.83	10,875,540
52.1	4.51	54.51	79.18	24.67	10,805,460
53.1	6.78	56.78	80.12	23.34	10,222,920
54.1	9.10	59.10	83.04	23.94	10,465,720

Table 31. Expected Annual Cost Incurred when using Model 1 instead of Model 5 in New York

	Modified Deterministic Model (Model 6)		Prosumer Stochastic Model (Model 5)		
Total Load (MW)	Power produced by WT (MW)	Total power produced by WT and substation (MW)	Power produced (MW)	Extra power to be purchased by Model 6 (MW)	CNPSM ($/year)
50.1	1.75	51.75	69.05	17.30	7,575,341
51.1	3.67	53.67	70.14	16.47	7,213,860
52.1	6.18	56.18	71.19	15.01	6,574,380
53.1	8.94	58.94	72.29	13.35	5,847,300
54.1	16.40	66.40	73.29	6.89	3,017,820

The results posted in Tables 31-33, show that at every load the deterministic model always produces lesser power than the stochastic one since the deterministic model does not consider high wind scenarios and those ones have a high probability of occurrence. On the other hand, when the low wind scenarios happen, the deterministic model does a too optimistic planning for the number of WT needed and thus the system will incur in extra purchases of power.

Comparing the results gotten from Model 5 and Model 6, the prosumer stochastic model can perform the best because it considers the uncertainties on wind speeds through multiple scenarios, allows bi-directional power flow, sells extra energy produced by WT to the grid, and does not simplify the loss of load probability constraint by a streamlined deterministic counterpart. In practice, the CNPSM shows a system owner the cost saving when using the prosumer stochastic model instead of the modified deterministic model to design the DG system.

Another method to estimate the CNPSM is to assume that purchasing energy is not an available option when faced with the adoption of the sub-optimal solution from Model 6. Then, the DG system will incur in what is called loss of load. However, the author of this thesis did not adopt this method because the cost differences between the models will be even higher. Welle and Zwaan (2007) mention that with a high level of confidence the ranges for the cost of interruptions in the supply of electricity or value of loss of load (VOLL) can be in re range of $5/kWh to $25/kWh and $2/kWh to $5/kWh for developed and developing countries, respectively. Estimating VOLL is not an easy task. Methods to estimate VOLL are market behavior observations, surveys and analysis of black-outs events, among others. The VOLL vary by country and industrial sector. The authors mentioned that VOLL in the US laid between $3-12 $/kWh and that this figure is two orders of magnitude higher than the $0.05/kWh (i.e. $50/MWh) assumed to compute the results in Tables 31-33.

4. SITING AND SIZING OF WIND TURBINES AND ENERGY STORAGE DEVICES

This chapter is divided into 9 subsections. Section 4.1 presents the problem to be modeled and solved in this chapter. Section 4.2 highlights the importance of energy storage systems (ESS) to the energy grid. Section 4.3 provides a literature review on sitting and sizing of ESS. Section 4.4 presents previous contributions to the problem of sitting and sizing of ESS with WT. Section 4.5 provides the methodology used by the author in this thesis to approach the problem. Section 4.6 presents the mathematical model proposed which considers WT, ESS and prosumer nodes. Section 4.7 has the experimental setting. Section 4.8 presents the values for the parameters and Section 4.9 provides the numerical results.

4.1 Problem statement

The problem solved in this chapter is an expansion of the problem defined in Chapter 3. The new problem is to find the optimal design for a connected DG system that may simultaneously install WT units of different types, according to their capacities (i.e. 1MW, 2MW, 3MW), and Energy Storage Systems (ESS) on prosumer nodes. The ESS possible to install are batteries.

The DG system is comprised of interconnected prosumer nodes as shown in Figure 21. In the figure, the central node (node 1) represents the substation. The remaining eight nodes in the network can be small cities, companies, department stores, or farms that may host multiple WT of different capacities, as mentioned in the previous paragraph, and also ESS. The arrows in Figure 21 correspond to the bi-directional flow on the distribution lines. The challenging factor on finding the optimal design for this DG

system is that the wind speed varies hourly and it affects the power output of the WT, the charge and discharge of ESS, and consequently the total system reliability.

To tackle this problem more realistically and to go with the current research trends on designing cost-efficient wind-based DG systems that are flexible to balance the power generated and the system consumption, the system nodes are treated as prosumer nodes. Those nodes are equipped with ESS used as the first source to deliver energy needed at peak hours leaving the substation as a second choice. ESS also are the first choice to store extra renewable energy produced at the nodes when the local demand is low, while additional energy can be sold back to the grid. The optimal design for the DG system will determine the location and capacity of the WT and ESS to install at each node of the network to satisfy the electricity loads (i.e. demands) at the nodes and the thermal constraints.

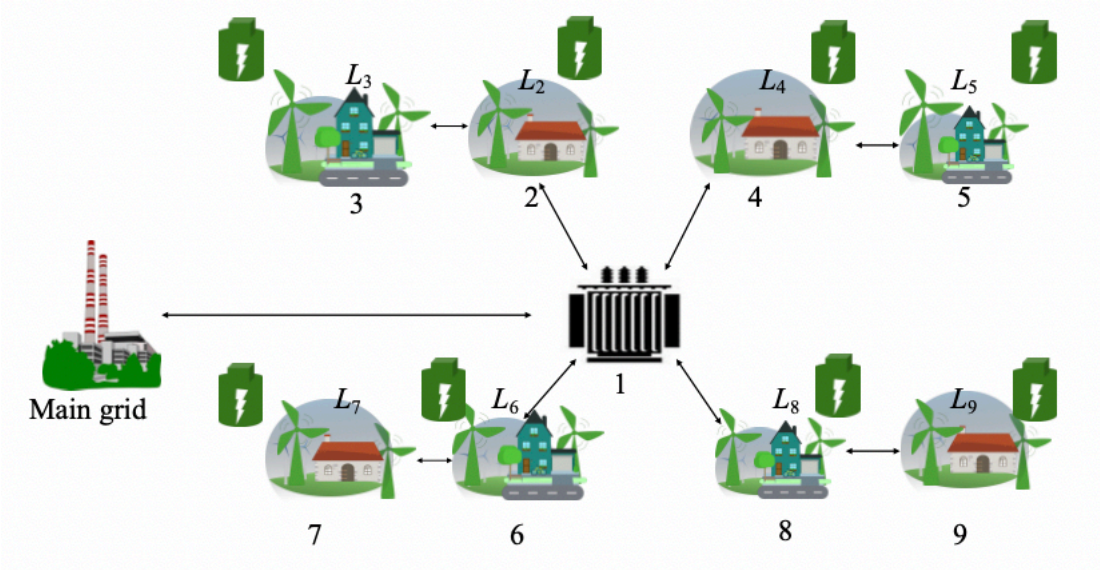

Figure 21. The DG system studied in Chapter 4

As power generation technology is rapidly changing from large and public power plants to small and private power plants, there is a need to increase the growth of

renewable energy integration. In recent years, the smart grid is incorporating prosumers to build grid independent consumers. The use of renewable energy (i.e. wind and solar) by these consumers bring various uncertainties to the energy portfolio, thereby reducing the reliability.

4.2 Importance of energy storage systems (ESS) to the grid

ESS drive the adequate integration of renewable sources of energy especially where it is more difficult to incorporate renewable energy sources to balance the power generated and system consumption in an existing grid. ESS can tackle the problems caused by wind intermittency by leveraging on technical, economical and environmental value (Miranda et al., 2016). Therefore, incorporating prosumers with various ESS now becomes important as it helps to:

i) Mitigate the uncertainties caused by renewable energy sources, by providing power when power fluctuations occur.

ii) Reduce the power flowing through the distribution lines.

iii) Enable consumers to store electricity when prices are low and to sell to the grid when prices go up.

iv) Increase the overall systems reliability.

4.3 Siting and sizing of energy storage systems (ESS)

Various studies have tackled the problem of fluctuations in wind speed faced by wind renewable energy using ESS because of ESS flexible charging and discharging capabilities. The installation of ESS at system nodes where a lot of power is being generated is desirable. Although the use of ESS in the grid can be of great benefit, an inappropriate placement and sizing of ESS results in an increase in installation, operation

and maintenance cost. These costs could eventually outweigh the intended benefits of the ESS. Capital cost and capacity to store energy are the key properties limiting the profitability of ESS applications (Xia et al., 2018).

Shu and Jirutitijareon (2012) formulated a two-stage stochastic programming model with recourse considering the day to day stochastic behavior of system load, renewable energy and electricity prices. The model was formulated to find the appropriate size of the ESS applied to a grid connected wind power plant with the objective of maximizing its expected daily profit. The ESS considered was compressed air energy storage (CAES). Due to the large size of the problem, Shu and Jirutitijareon (2012) used the sample average approximation technique to solve the two-stage stochastic programing model presented. Sensitivity analysis was used to demonstrate that ESS can increase the profit of the wind farm studied.

Xia et al. (2018) also formulated a stochastic cost-benefit model to determine the optimal size of ESS considering the intermittent wind generation. The authors first derived the marginal distributions with covariance matrix of the hourly wind generation. Then they used a hybrid solution approach to transform the stochastic problem into a deterministic one by combining the point estimates method and the parallel Branch and Bound algorithm. The results showed that installing ESS in power systems is not always appropriate especially when ESS amortized cost is high and charging and discharging rate is low.

Ye et al. (2016) focused on predicting the wind generation. They proposed a non-parametric estimation method to: (1) analyze the wind power forecast error and the cumulative wind power deviation within the scheduling period and (2) design the optimal

sizing of ESS considering wind power uncertainties and the cost-benefit optimization principle. They mentioned about the existent tradeoff if designing DG systems coupled with ESS. ESS with larger capacity will smooth better the wind power fluctuations but more cost will be paid for the energy storage devices. On the other hand, ESS with limited capacity have lower costs but are weak to smooth the wind power fluctuations. The authors confirmed the validity of their work by applying the model to a real wind farm.

Zhao et al. (2015) then proposed algorithms for both the optimal siting and sizing of ESS for operation planning of power systems with large scale wind power integration while optimizing the charge and discharge rate of ESS. Studies by Wen et al. (2015) and Miranda et al. (2016) have also presented various methodologies in the optimal integration of ESS into grids with a high wind penetration.

4.4 Siting and sizing of energy storage systems and wind turbines

Erdinc et al. (2018) presented a model to determine the optimality of different renewable energy sources (wind and solar), electric vehicle charging stations, and ESS units. The model was formulated as a deterministic second order conic programming model considering the time varying nature of DG and load consumption. Khaki et al. (2019) formulated a model coupled with ESS to mitigate wind intermittency. The model smoothed the power output injected to the grid by renewable sources. The authors used genetic algorithm to simultaneously size and place the ESS and WT in the power system. The objective was to minimize the total system loss and the costs of ESS and WT. The result of their work shows that the optimal placement and sizing of both ESS and WT helped cover the system active and reactive power requirements and improved the load

voltage profile. The authors also stated that when the cost objective was considered, it changed the result of placement and sizing significantly.

As presented in the previous subsection, there exists various literature on the optimal sizing of ESS. There is fewer literature on the optimal siting and sizing of WT and ESS simultaneously as Khaki et al. (2019) presented. To the best of our knowledge no literature was found the optimal siting and sizing of WT using ESS while considering system nodes as prosumers.

4.5 Methodology

The problem of finding the optimal siting and sizing of WT and ESS in a DG system considering system nodes as prosumers is approached with the formulation and solution of a non-linear programming model. The model is deterministic and includes thermal constraints at the upper and lower nodes which incorporate the effect of the ESS, power balance constraints and the bi-directional flow of power between prosumers and the electric grid.

4.6 Mathematical models for the optimal design of a DG system powered by wind turbines and energy storage systems considering system nodes as prosumers.

The DG planning problem faced in this chapter has a trade-off between the annualized cost of installing and maintaining ESS and the benefit from smoothing the amount of energy the system is able to supply. Such benefits include reducing the risk of energy losses and increasing the profit coming from energy sold by prosumer nodes. Such problem can be formulated as an optimization model that looks to minimize the system cost subject to various constraints. The following subsections present the optimization model. This model is named as Model 7.

4.6.1 Model 7 – Prosumer model using ESS:

Tables 34 - 37 present all Model 7 notation. The optimization model is presented and discussed immediately below the tables. Table 34 shows that the only new set in Model 7 is *T*. It represents the days in a year. Table 35 shows that in comparison to the model presented in the previous chapter, there are 3 new decision variables in the model. They are $B_j^{(c)}$, the maximum battery capacity installed at node *j* (MWh), , the amount of energy stored per day (MWh) in the battery at node *j* and , an introduced slack variable (MWh) which represents any extra amount of energy requested by lower node *j* on day *t* to another energy supplier because the substation cannot supply such energy due to capacity limitations. Some new parameters are introduced in Tables 34 and 3∞, however the notation for all model parameters is included in those tables.

Table 32. Sets for Model 7

Notation	Definition
I	Different types of WT possible to install
J	Nodes in the DG system
F	Upper nodes in the DG network. Upper nodes have distribution lines that link them with other nodes different to the substation and thus they can provide power to other nodes.
E	Lower or terminal nodes in the DG network
E_f	Lower or terminal nodes emanating from upper node F
T	Days in a year (1,2,3, …,365). The size of this set is 365 days (i.e. |T| = 365)

Table 33. Decision Variables for Model 7

Notation	Definition
x_{ij}	Binary decision variable. It becomes equal to 1 if WT type *i* is installed in node *j*, and 0 otherwise
y_{ft}^{+}	Power (MW) purchased from electric grid by upper node *f* at day *t*
y_{ft}^{-}	Power (MW) sent from upper node *f* to electric grid at day *t*
$B_j^{(c)}$	Maximum capacity of the battery (MWh) installed at node *j*
w_{jt}	Amount of energy stored at day *t* (MWh) in the battery installed at node *j*
z	Substation capacity (MW)
N_{et}^{+}	Any extra amount of energy (MWh) requested by lower node *e* in day *t* to another energy supplier if the substation cannot supply due to capacity limitations

Table 34. Power Parameters for Model 7

Notation	Definition
P_{ijt}	Power generated by WT type *i* installed at node *j* on day *t*. P_{ijt} is a function of y_h the wind speed at WT height *h* on day t. Function argument y_h is dropped to simplify notation
$P_i^{(c)}$	Capacity of WT type *i*

Table 35. Parameters for Model 7

Notation	Definition
	Number of hours of wind operation in a day (i.e. is 24 hours)
a_i	Present cost per MW for installing WT type i
a_k	Present cost per MW for installing substation k
a_b	Present cost per MWh of battery to install at node j
$Ø$	Factor to convert the present installation cost of WT or the substation to annuity. It is given by: $\phi = \left(\frac{r(1+r)^h}{(1+r)^h - 1} \right)$ Where r *is* the annual interest rate and h is the number of years during which equipment installation cost is paid off.
$Ø_b$	Factor to convert the present installation cost of the battery to annuity. It is given by the same formula in the previous line but the numerical values for interest rate, r, and number of years, h, are different as explained in the numerical experiment
b_i	Annual operation and maintenance cost per MW for WT type i
b_k	Annual operation and maintenance cost per MW for substation k
c_i	Annual tax incentive or subsidy per MW for installing WT type i
h_k	Penalty cost per MW of using the substation to send power from electric grid to the prosumer nodes
q_k	Incentive per MW, if any, for using the substation to accept power returned from prosumers nodes to the grid. This term is included in the model, but it assumed equal to zero
m_k	Purchasing cost per MW of power acquired by prosumer nodes from the electric grid
n_k	Income per MW from selling extra power produced by the nodes to the electric grid
$E[L_f]$	Mean load (i.e. demand) at upper node f
$E[L_e]$	Mean load (i.e. demand) at lower node e,
L	Total system load (i.e. demand)
$E[L]$	Expected value (i.e. mean) of the total system load (i.e. demand) and computed as: $E[L] = \sum_{j \in J} E[L_j]$
I_f	Maximum current flow at upper node f
I_e	Maximum current flow at lower node e
V_{DG}	Voltage at any distribution line of the DG network
α	loss-of-load probability
b_j	Annual operation and maintenance cost per MWh for a battery installed at node j. Units are in ($/MWh)
γ	Number of times per year the battery is maintained
o	Cost of the electricity purchased to another energy supplier because of substation capacity limitation is reached ($/MWh)
M	Maximum capacity of the substation (MW)

Model 7

Minimize

$$g(x)=\sum_{i\in I}\sum_{j\in J}(a_i\phi P_i^{(c)})x_{ij}+\sum_{i\in I}\sum_{j\in J}\sum_{t\in T}P_{ijt}\frac{(b_i+c_i)}{|T|}x_{ij}+(a_k\phi)z \tag{42}$$
$$+\sum_{t\in T}\sum_{f\in F}(\frac{h_k}{|T|}y_{ft}^{+}-\frac{q_k}{|T|}y_{ft}^{-}+\frac{b_k}{|T|}|y_{ft}^{+}-y_{ft}^{-}|)+\sum_{t\in T}\sum_{f\in F}\frac{m_k}{|T|}y_{ft}^{+}-\sum_{t\in T}\sum_{f\in F}\frac{n_k}{|T|}y_{ft}^{-}$$
$$+\sum_{j\in J}\phi_b a_b B_j^c+\sum_{j\in J}\frac{b_j}{\tau\gamma}B_j^c+\sum_{t\in T}\sum_{e\in E}oN_{et}^{+}$$

$$\left|\sum_{e\in E}(L_{et}-\sum_{i\in I}P_{iet}x_{ie}-\frac{w_{e(t-1)}}{\tau}+\frac{w_{et}}{\tau})+L_{ft}-\sum_{i\in I}P_{ift}x_{if}-\frac{w_{f(t-1)}}{\tau}+\frac{w_{ft}}{\tau}\right|\le V_{DG}I_f \quad \forall f\in F,\forall t\in T \tag{43}$$

$$\left|L_{et}-\sum_{i\in I}P_{iet}x_{ie}-\frac{w_{e(t-1)}}{\tau}+\frac{w_{et}}{\tau})\right|\le V_{DG}I_e \quad \forall e\in E,\forall t\in T \tag{44}$$

$$\sum_{e\in E_f}(L_{et}-\sum_{i\in I}P_{iet}x_{ie}-\frac{w_{e(t-1)}}{\tau}+\frac{w_{et}}{\tau})+L_{ft}-\sum_{i\in I}P_{ift}x_{if}-\frac{w_{f(t-1)}}{\tau}+\frac{w_{ft}}{\tau}= \tag{45}$$
$$y_{ft}^{+}-y_{ft}^{-} \quad \forall f\in F,\forall t\in T$$

$$\sum_{e\in E}\left(\sum_{i\in I}\tau P_{iet}x_{ie}+w_{e(t-1)}\right)+\tau y_{ft}^{+}+\sum_{i\in I}\tau P_{ift}x_{if}+w_{f(t-1)}= \tag{46}$$
$$\sum_{e\in E}(\tau L_{et}+w_{et})+\tau L_{ft}+w_{ft}+\tau y_{ft}^{-} \quad \forall f\in F,\forall t\in T$$

$$\sum_{i\in I}\tau P_{iet}x_{ie}+w_{e(t-1)}+N_{et}^{+}=\tau L_{et}+w_{et} \quad \forall e\in E,\forall t\in T \tag{47}$$

$$\sum_{f\in F}\left|y_{tf}^{+}-y_{tf}^{-}\right|\le z_k \quad \forall t\in T \tag{48}$$

$$\sum_{i\in I}x_{i1}=0 \tag{49}$$

$$0\le w_{jt}\le B_j^c \quad \forall t\in T,\forall j\in J \tag{50}$$

$$0\le x_{ij}\le 3 \quad \text{and integer} \quad \forall i\in I,j\in J \tag{51}$$

$$0\le z\le M \tag{52}$$

$$B_j^c\ge 0 \quad \forall j\in J \tag{53}$$

$$w_{jt}^{+}\ge 0,\ y_{jt}^{+}\ge 0,\ y_{jt}^{-}\ge 0 \quad \forall t\in T,\forall j\in J \tag{54}$$

$$N_{et}^{+}\ge 0 \quad \forall e\in E,\forall t\in T \tag{55}$$

The model decision variables are x_{ij}, an integer decision variable that indicates the number of WT installed at each node and $y_{ft}^{+}, y_{ft}^{-}, z, N_{et}^{+}, w_{ft}$, and $B_j^{(c)}$ continuous decision variables defined as in Table 35.

The objective function (42) minimizes $g(x)$, the annual cost of the DG system considering that it operates 365 days. The first six terms in this function are similar to the ones explained in the model in Chapter 3 on Section 3.7 but some of them consider that the costs must be converted to cost per day since there are sums over the days of the year in these terms. The seventh term is the annual cost of the ESS (i.e. batteries) adopted in the system. The eight term is the battery operating and maintenance cost and the last term is the cost of the immediate need of energy that could not be provided by the grid.

Thermal constraint (43) is for those network nodes that may provide power to other nodes (i.e. upper nodes). The constraint ensures that the total mean load (i.e. demand) on the distribution line (DL) serving an upper node and all its lower nodes does not exceed the maximal power such DL can bear after considering that the DER equipment installed on the nodes and the battery will mitigate some of the load. Thermal constraint (44) has a similar purpose but it is for the terminal nodes in the network (i.e. lower nodes).

Constraint (45) defines that in a particular day an upper node can only get power from the grid or give renewable power to it depending on value of the left-hand side of such constraint. Constraints (46) and (47) are the energy balance constraints for both the upper and lower nodes respectively. The constraints follow the pattern described in Figure 22.

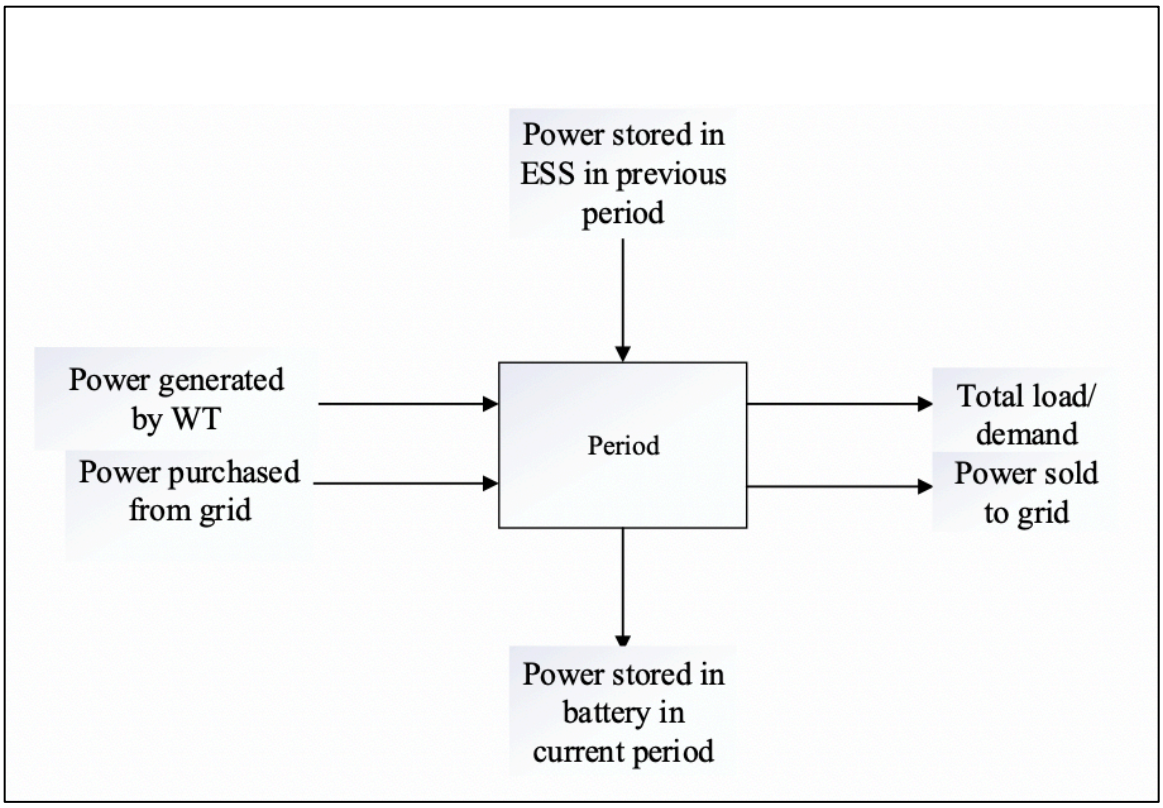

Figure 22. Power balance kept in the prosumer model using ESS

The constraint (46) ensure that the power gotten from the wind turbines, substation and batteries (what is stored in previous period) should be equal to the total load, what is sold back to the grid and what is stored in the battery (in the current period). Constraint (47) is similar to constraint (46) but includes the decision variable N_{et}^{+} to represent that any other source may be used to satisfy occasional extra power needs at lower end node *e* on day *t.*

Constraint (48) specifies that the power flowing in or out of the upper nodes should be at most the substation capacity. Constraint (49) specifies that no WT type *i* should be located at node 1. Constraint (50) limits the amount of energy stored in the batteries, so it doesn't exceed their maximum capacities. Constraint (51) specifies that at

most three WT type *i* are installed in each node *j* of the DG network and that only integer numbers are allowed for this decision variable. Constraints (52- 55) are sign constraints for the continuous decision variables. Constraint (52) also indicates that size of the substation must not exceed the parameter *M* which is the given maximum substation capacity.

4.7 Experimental setting for Model 7

Model 7 is tested on the 9-node DG system network already presented in Chapter 3, Figure 14. The major difference between Model 5 and Model 7 is the incorporation of energy storage systems to the system nodes.

4.8 Values for the parameters in Model 7

4.8.1 WT costs

WT with capacity 1MW, 2MW or 3MW may be installed at nodes 2 to 9. Table 23 in Chapter 3 has the assumed WT costs.

4.8.2. Substation parameter values

The experimental study in this chapter is performed also in 3 cities with different wind profiles. The cities selected are the same as in Chapter 2: Wellington, Rio Gallegos and New York. Some of the values for the parameters associated with the substation used in the objective function for Model 7 were listed in Table 24 in Chapter 3. In that table, the assumed number of hours per year used to compute these parameters is 8760.

4.8.3. ESS and other parameter values

Table 38 lists the values assumed for the parameters associated with the ESS and for a few more new model parameters

Table 36. ESS Parameters and other associated Parameters

Notation	Value
a_b ($/MWh)	150,000
b_j ($/MWh)	155
τ (hours/day)	24
$Ø_b$	0.05026292
o ($/MWh)	55
Γ (times/year)	30

Values for the remaining Model 7 parameters related to power for the WT, loads, probabilities associated with the wind speed scenarios, currents, voltages, loss-of-load probability and number of years and interest rate considered to annualize the installation costs are assumed equal to the ones mentioned in Chapter 2 towards the end of Section 2.8.

4.9 Results

Model 7 is solved using the numerical values for the parameters given in the previous section. For each city, the three different cases solved are shown in Table 39.

Table 37. Experimental Study in Chapter 7

Case	Battery capacity
1	Modeled as a parameter in each node of the network with a value of 100 MWh
2	Modeled as a parameter in each node with a value of 250 MWh
3	Modeled as a continuous decision variable

The prosumer stochastic non-linear program using ESS (i.e. Model 7) is modelled in AMPL and solved using the Knitro solver. The size of Model 7 if the battery capacity is assumed as a decision variable as in Case 3 is presented in Table 40

Table 38. Size of Model 7

Base Model Name	Decision Variables	Constraints
Prosumer stochastic non-linear program using ESS	7333	7666

4.9.1 Case 1 results

The result from solving Case 1 shows that for a mean total load of 50.1MW at a fixed battery capacity of 100MW, Wellington and Rio Gallegos install (14 1MW 14 2MW and 18 3MW) WT while New York installs (12 1MW 15 2MW and 19 3MW) with different siting. Wellington produces the highest total power 66.34MW with a total cost of $15,364,504, Rio Gallegos produces a total power of 60.18MW with a total cost of $17,188,122 while New York produces a total power of 55.95MW with the highest cost at $22,558,171. Table 41 shows detailed results for Case 1 in all cities.

Table 39. Detailed Solution of the Base Model 7 in all Cities under Case 1

Cities Studied		Wellington			Rio Gallegos			New York		
No of WT		46			46			46		
Total power reported by each model (MW)		66.34			60.18			55.95		
	Node	1MW	2MW	3MW	1MW	2MW	3MW	1MW	2MW	3MW
x_{ij}	1	0	0	0	0	0	0	0	0	0
	2	3	3	3	3	3	3	3	3	3
	3	0	1	2	0	1	2	0	1	2
	4	3	3	3	3	3	3	3	3	3
	5	1	0	1	1	0	1	0	1	1
	6	3	3	3	3	3	3	3	3	3
	7	1	0	2	1	0	2	0	1	2
	8	3	3	3	3	3	3	3	3	3
	9	0	1	1	0	1	1	0	0	2
Expected total annual cost ($/year)		15,364,504			17,188,122			22,558,171		
Probability of power outage		0.01			0.08			0.24		
Substation capacity (MW)		40.33			40.34			44.88		

The results presented in the last row of Table 41 show that the windier cities require less substation capacity as they are able to produce more power to meet up with the demands in every period while in New York, which has a the lowest wind, requires the highest capacity for the substation and wind turbines. It is also seen that as a result of the high wind speed in Wellington, this city has the least probability of power outage in comparison to other cities.

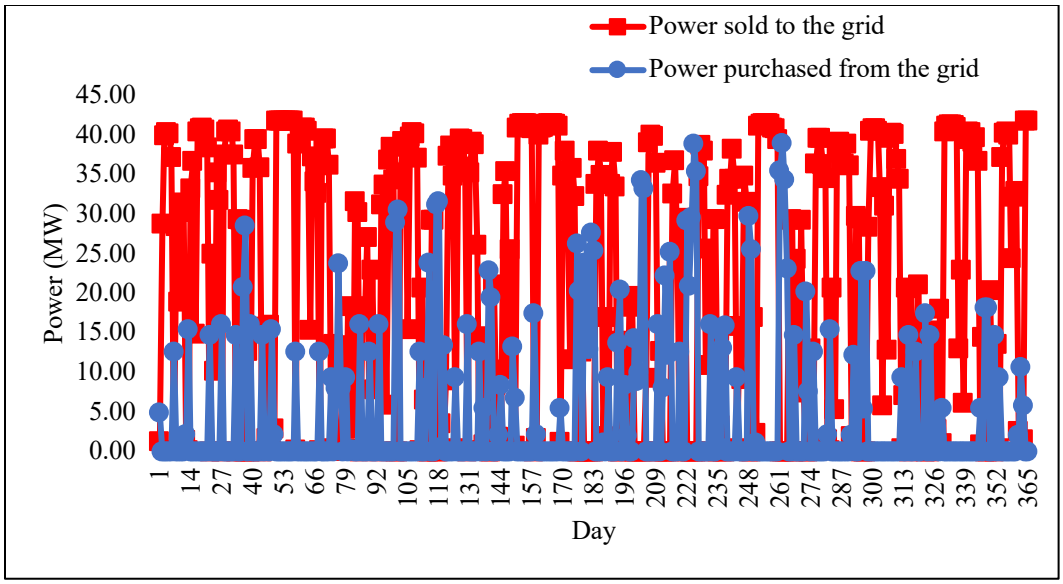

Figure 23. Behavior of total power purchased and sold to the grid in Wellington

Figure 23 shows that the total amount of power purchased from the grid is less than the total amount of power sold to the grid in Case 1 for every period in Wellington. Since the figure plots the sum of the total energy purchased and sold for all nodes it may have cases where on a same day both events occur.

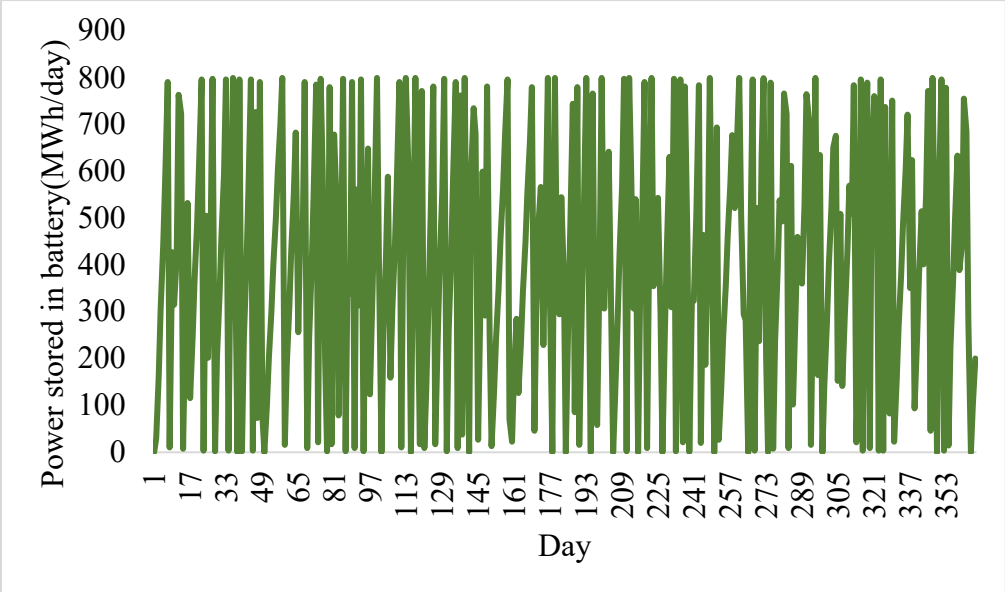

Figure 24. Behavior of total power stored in the batteries

Figure 24 presents the total amount of power stored in the batteries considering all system nodes in all days. It is expected that when a significant amount of power is generated, the surplus should be stored in the battery and sold back to the grid. For instance, in day 365 the model did not purchase power from the grid whereas it stored 200MW in the batteries and sold 46MW to the grid.

4.9.2 Case 2 results

The result from solving Case 2 shows that for a mean total load of 50.1MW at a fixed battery capacity of 250MW, Wellington installs (12 1MW 15 2MW and 19 3MW), Rio Gallegos install (13 1MW 14 2MW and 19 3MW)WT while New York installs (14 1MW 12 2MW and 22 3MW) with different siting. Wellington produces the highest total power 64.91MW with a total cost of $23,384,112, Rio Gallegos produces a total power of 57.91MW with a total cost of $25,653,433 while New York produces a total power of 53.71MW with the highest cost at $30,179,225. Table 40 shows detailed results for Case 2 in all cities. The chosen substation sizes for Case 2 end smaller than for Case 1 because of a larger battery in the nodes.

Table 40. Detailed Solution of the Base Model 7 in all Cities under Case 2

Cities Studied		Wellington			Rio Gallegos			New York		
No of WT		46			46			48		
Total power reported by each model (MW)		64.91			57.91			53.71		
	Node	1MW	2MW	3MW	1MW	2MW	3MW	1MW	2MW	3MW
x_{ij}	1	0	0	0	0	0	0	0	0	0
	2	3	3	3	3	3	3	3	3	3
	3	0	1	2	0	1	2	1	0	3
	4	3	3	3	3	3	3	3	3	3
	5	0	1	1	1	0	1	0	0	2
	6	3	3	3	3	3	3	3	3	3
	7	0	1	2	0	1	2	0	0	3
	8	3	3	3	3	3	3	3	3	3
	9	0	0	2	0	0	2	1	0	2
Expected total annual cost ($/year)		23,384,112			25,653,433			30,179,225		
Probability of power outage		0.08			0.16			0.38		
Substation capacity (MW)		38.78			36.29			44.62		

Figure 25 shows that the need to purchase power from the substation is minimal most of the time for Case 2. If comparing Figure 26 to Figure 24, it can be seen that in Case 2, more power is being stored in the batteries than in Case 1. Due to this fact, Case 2 enables the demand to be met most of the times. In Figure 26 it can also be seen that the number of days the full 250MWh battery is used is less than in Figure 24. In other words, the vertical axis in figure 26 does not reach 2,000 MWh (8 nodes*250 MWh) very often.

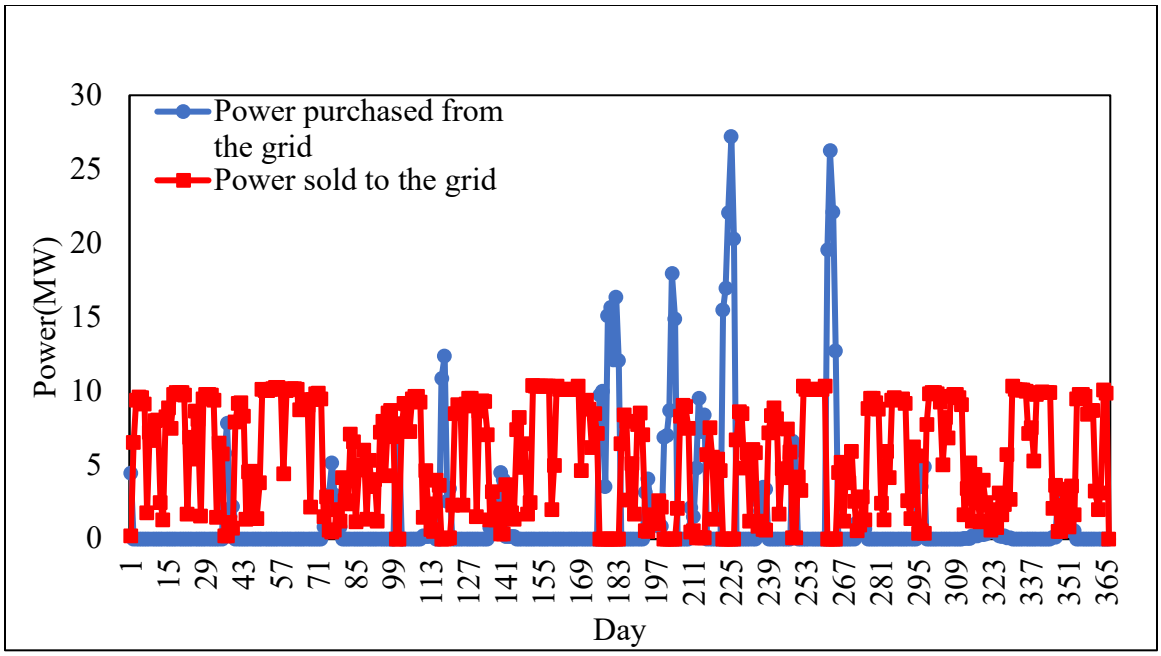

Figure 25. Behavior of total power purchased and sold to the grid in Case 2

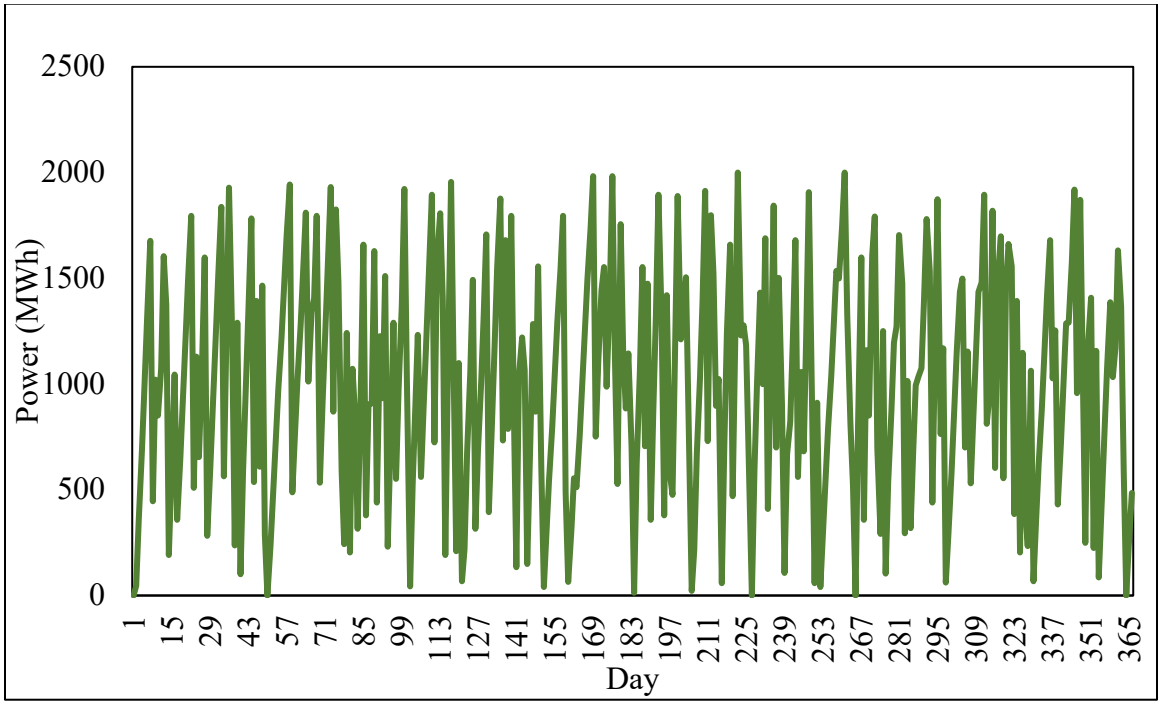

Figure 26. Behavior of total power stored in batteries in all periods (Case 2)

4.9.3 Case 3 results

The result from solving Case 3 shows that for a mean total load of 50.1MW Wellington installs (16 1MW 13 2MW and 18 3MW) and generates a total power of 72.22 MW at a cost of $10,613,423, Rio Gallegos also installs (14 1MW 14 2MW and 18 3MW)WT and generates a total power of 66.07MW at a total cost of $12,342,321 while New York installs (14 1MW 14 2MW and 18 3MW) and generates a total power of 60.42MW at a total cost of $18,386,197. Table 41 shows detailed results for Case 3 in all cities. The size of the substation chosen is larger for this case and thus the probabilities of power outage are lower than in Cases 1 and 2.

Table 41. Detailed Solution of the Base Model 7 in all Cities under Case 3

Cities Studied		Wellington			Rio Gallegos			New York		
No of WT		47			46			46		
Total power reported by each model (MW)		72.22			66.07			60.42		
	Node	1MW	2MW	3MW	1MW	2MW	3MW	1MW	2MW	3MW
x_{ij}	1	0	0	0	0	0	0	0	0	0
	2	3	3	3	3	3	3	3	3	3
	3	0	1	2	0	1	2	0	1	2
	4	3	3	3	3	3	3	3	3	3
	5	1	0	1	1	0	1	1	0	1
	6	3	3	3	3	3	3	3	3	3
	7	1	0	2	1	0	2	1	0	2
	8	3	3	3	3	3	3	3	3	3
	9	2	0	1	0	1	1	0	1	1
Expected total annual cost ($/year)		10,613,423			12,342,321			18,386,197		
Probability of power outage		0.0005			0.01			0.07		
Total battery capacity (MWh)	3	53.76			40.32			26.88		
Substation capacity (MW)		47.36			47.64			48.35		

The main objective of Model 7 is to minimize cost while satisfying the power load. From the detailed result in Table 43 it is seen that Wellington installs a slightly larger number of turbines to produce the highest power at the lowest cost and keeping the probability of power outage at the lowest value (0.0005). Rio Gallegos and New York both installed 46 wind turbines. Rio Gallegos produced more power as it is a windier city than New York. Rio Gallegos is also able to keep the probability of power outage lower than New York. From the results in the previous to last row in Table 43, it can be observed that batteries of different capacities were installed at node 3 in all cities, these differences in battery capacity result because of the power that could be generated by the turbines in each city. A city with higher wind speed is expected to generate more power, thereby able to meet the demands better and even in some days have extra power to be stored in the ESS. Figure 27 shows the total amount of power purchased from the grid, the total amount of power sold to the grid, and the power stored in the batteries for Case 3 in Wellington.

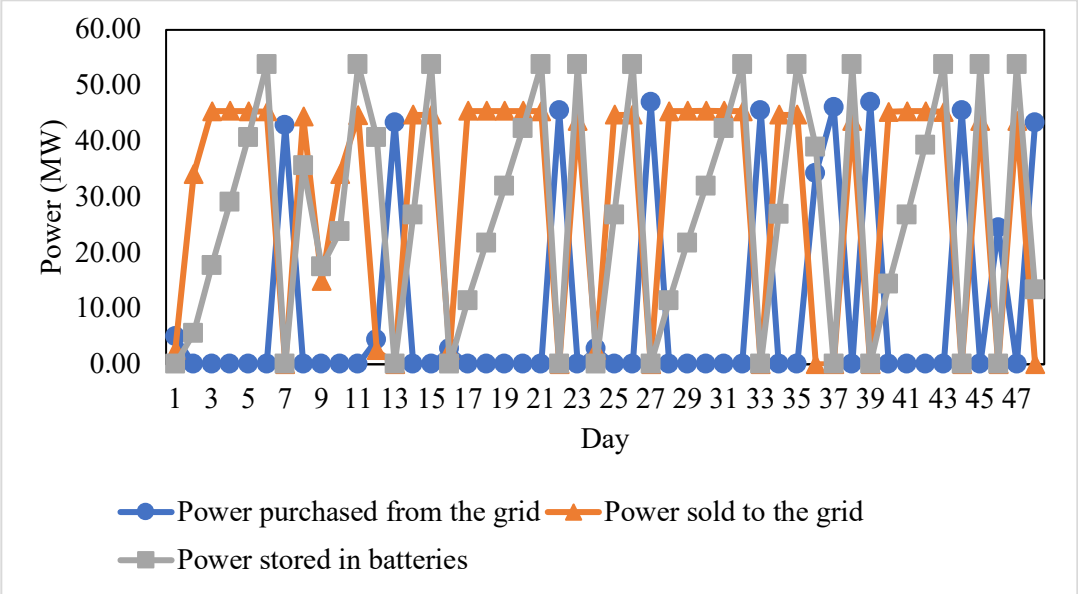

Figure 27. Total power stored in batteries, purchased and sold to the grid in first 50 days

Figure 27 displays the power purchased from the grid, the power sold to the grid and the power stored in the battery in the first 50 days for Case 3 in Wellington. It can be seen from the figure that most of the times the WT are able to generate enough power to meet the load, sell to the grid and also store in the batteries.

5. CONCLUSION

This thesis proposed and solved multiple mathematical programming models to determine the siting and type of wind DER units to install in an interconnected DG system. The main constraints considered are to keep the system loss-of-load probability below a pre-specified threshold α and satisfy the thermal constraints. The numerical experiments show that the system is feasible to adopt in all 3 cities, but it is more favorable in Wellington due to the high wind speeds as it would be able to accommodate increase in total loads. New York is the least favorable place to install wind turbines as in some scenarios when there is an increase in total load from the base case it becomes infeasible to adopt. The stochastic model (Model 3) performed the best if compared to deterministic and chance constrained modes (Models 2 and 1, respectively) as it considers the variability in WT power output by incorporating all wind speed scenarios in which the WT operate and thus modeling the wind speed variability in a closest way. The models presented in chapter 3 considers decisions to be taken at the DG system design stage and a couple of additional relevant decisions that arise in the operational stage of the system. The results gotten from the stochastic model are compared to a deterministic counterpart, the prosumer stochastic performed the best since it considers the uncertainties on wind speeds through multiple scenarios, allows bi-directional flow of power and sells extra power produced by WT to the grid, and does not simplify the loss of load probability constraint by a streamlined deterministic counterpart . The prosumer stochastic model is then extended by including ESS. Three cases were solved to access the impact of ESS on the model. The first case considered used a fixed battery capacity of 100MW in all nodes while the second case uses a battery capacity of 250MW in all nodes

whereas the third case considered the battery capacity as a variable while simultaneously finding the siting and sizing of wind turbines and ESS. Comparing the three cases, the third case gives the lowest cost since just one battery is installed at node 3 in all cities (since node 3 has the highest load). We see that in the first 2 cases installing batteries of larger capacities in all nodes is more costly and does not necessarily make the system more reliable.

Further research may consider the use of other renewable energy sources such as solar photovoltaics (PV) and model the load(demands) at the nodes as stochastic. Another future research to be considered is using the historical weather data to make forecast of the weather in an upcoming year and use these forecasts as inputs into the model. More research needs to be done on offshore wind turbines and access the cost-benefit tradeoff. The U.S currently has target to provide 20% of its energy needs by 2030 with wind energy. However, wind energy only provides about 7.6% of the energy needs as of 2019. Further research needs to be done on ways the efficiency of a wind turbine can be improved.

APPENDIX SECTION

Appendix A: Computing the left-hand Side of the loss of load chance constraint

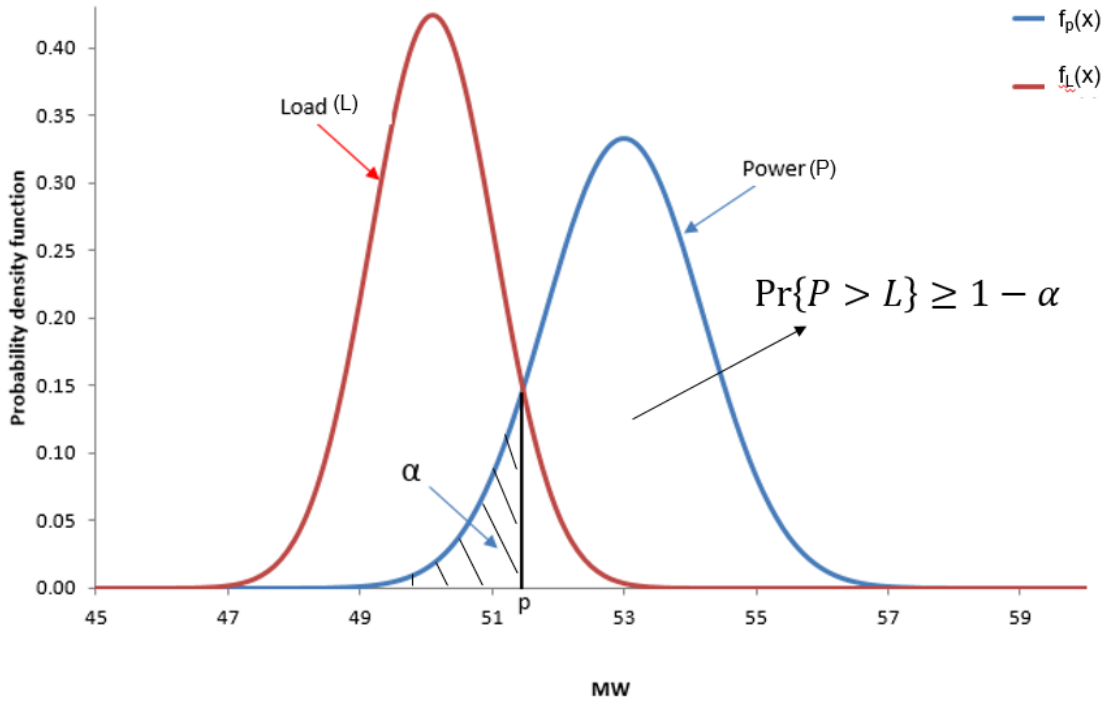

Figure 28. Figure to visualize the chance constrained problem solved by the mathematical models

By the Central limit Theorem (CLT) it is assumed that $P \sim N(E[P], \sigma_P^2)$ and $L \sim N(E[L], \sigma_L^2)$. The problem in Figure A1 can be written as

$$\int_0^{\infty} \left(\int_y^{\infty} f_P(z)\,dz \right) f_L(y)\,dy \geq 1-\alpha \qquad \text{(A1)}$$

$$\Rightarrow \Pr\{P > L\} \geq 1-\alpha \qquad \text{(A2)}$$

$$\Rightarrow \Pr\{P \leq L\} \leq \alpha \qquad \text{(A3)}$$

where the abbreviation Pr is used to represent probability.

The problem in A3 reduces to find the point p that leaves an area α to the left in the power curve, that is:

$$\Pr\left(P \le p\right) \le \alpha \tag{A4}$$

To find such point p the probability density functions of the load and the power are equated as follows:

$$f_P\left(p\right) = f_L\left(p\right) \tag{A5}$$

and it gives:

$$\frac{1}{\sqrt{2\pi\sigma_P}} e\left(\frac{-\left(p-\mu_p\right)^2}{2\sigma_P^2}\right) = \frac{1}{\sqrt{2\pi\sigma_L}} e\left(\frac{-\left(p-\mu_L\right)^2}{2\sigma_L^2}\right) \tag{A6}$$

Solving for p can be done using the well-known formula $\frac{-b \pm \sqrt{b^2-4ac}}{2a}$ to solve the resulting quadratic equation with coefficients:

$$a = \sigma_P^2 - \sigma_L^2 \tag{A7}$$

$$b = 2\left(\sigma_L^2 \mu_P - \sigma_P^2 \mu_L\right) \tag{A8}$$

$$c = \sigma_P^2 \mu_L^2 - \sigma_L^2 \mu_P^2 - 2\sigma_P^2 \sigma_L^2 \ln\left(\frac{\sigma_P}{\sigma_L}\right) \tag{A9}$$

where

$$\mu_P = E\left[P\right] = \sum_{i \in I} \sum_{j \in J} E\left[P_{ij}\right] \tag{A10}$$

$$E\left[P_{ij}\right] = \sum_{s \in S} p_{sj} P_{ijs} x_{ij} \tag{A11}$$

p_{sj} = Probability for wind speed scenario s at node j

P_{ijs} = Power output when DER type *i* is installed at node *j* and wind speed scenario is *s*

x_{ij} = Binary variable to indicate if DER type *i* is installed ad node *j*

$$\sigma_P^2 = \sum_{i \in I} \sum_{j \in J} \sum_{s \in S} p_{sj} \left(P_{ijs} x_{ij} - E[P] \right)^2 \tag{A12}$$

σ_L^2 = given variance for the total load

$\mu_L = E[L]$ = given mean for the total load

Once *p* is written as a function of the *x's*, the cumulative standard normal distribution can be used to define the left-hand side of constraint (A4) as follows:

$$\Pr(P \le p) \le \alpha \tag{A13}$$

$$\Pr\left(Z \le \frac{p - E[P]}{\sigma_P} \right) \le \alpha \;\; \Rightarrow \;\; \Pr(Z \le z) \le \alpha \Rightarrow \phi(z) \le \alpha \tag{A14}$$

Since AMPL did not have implemented in its built-in arithmetical functions the cumulative normal distribution, the author of this thesis used the very accurate approximation given in Zogheib et al. (2009):

$$\phi(z) \cong \left(1 + e^{(0.0054 - 1.610)z - 0.0674 z^3} \right)^{-1} \tag{A15}$$

Then the probabilistic constraint turns into:

$$\left(1 + e^{(0.0054 - 1.610)z - 0.0674 z^3} \right)^{-1} \le \alpha$$

Where *z* is a function of *p* which is a function of the decision variables x_{ij}

Appendix B: "Best Fits" gotten with the Arena input analyzer for the hourly samples of wind speed at the 3 cities studied

Table 42. Parameters Collected in each Distribution for Wellington

Year	Distribution Name	Multipliers	Parameters		p-Value	Squared Error
2006	Normal		13	6.95	< 0.005	0.004
2007		-0.001	12.2	28	< 0.005	0.006
2008	Normal		11.8	6.46	< 0.005	0.004
2009	Beta	-0.001 + 40 *	1.99	4.6	< 0.005	0.007
2010	Normal		12	6.42	< 0.005	0.007
2011	Normal*		15.1	1.95	< 0.005	0.574
2012	Beta	-0.001 + 46 *	2.27	6.44	< 0.005	0.008
2013	Erlang	-0.001 +	4.92	2	< 0.005	0.042
2014	Normal		12.6	6.33	< 0.005	0.008

Table 43. Parameters Collected in each Distribution for Rio Gallegos

Year	Distribution Name	Multipliers	Parameters		p-Value	Squared Error
2006	Normal		17.60	2.17	< 0.005	0.658
2007	Normal		17.80	4.39	< 0.005	0.498
2008	Beta	-0.001 + 46 *	0.19	2.04	< 0.005	0.059
2009	Beta	-0.001 + 46 *	1.56	4.38	< 0.005	0.007
2010	Gamma	-0.001 +	1.05	9.37	< 0.005	0.577
2011	Beta	-0.001 + 46 *	0.19	2.38	< 0.005	0.065
2012	Beta	-0.001 + 46 *	0.19	2.38	< 0.005	0.065
2013	Beta	-0.001 + 46 *	1.41	4.77	< 0.005	0.010
2014	Weibull	-0.001 +	15.20	1.15	< 0.005	0.017

Table 44. Parameters Collected in each Distribution for New York

Year	Distribution Name	Multipliers	Parameters		p-Value	Squared Error
2006	Beta	-0.001 + 46 *	2.74	10.00	< 0.005	0.010
2007	Beta	-0.001 + 46 *	2.75	10.20	< 0.005	0.010
2008	Beta	-0.001 + 46 *	2.75	10.20	< 0.005	0.010
2009	Beta	-0.001 + 46 *	2.52	10.40	< 0.005	0.013
2010	Normal		9.71	5.33	< 0.005	0.011
2011	Beta	-0.001 + 46 *	2.43	9.35	< 0.005	0.012
2012	Beta	-0.001 + 46 *	2.80	12.20	< 0.005	0.061
2013	Beta	-0.001 + 46 *	2.54	9.50	< 0.005	0.012
2014	Normal		10.20	4.06	< 0.005	0.142

Table 45. Parameters Collected in each Distribution Listed in Tables 31-33

Distribution	Parameters		
Normal	Mean (μ)	Standard deviation (σ)	
Weibull	Scale Parameter (β)	Shape parameter (α)	
Beta	Shape parameter (α1)	Shape parameter (α2)	
Triangular	Min	Mode	Max
Erlang	Exponential Mean	K=Erlang or shape parameter	

Appendix C: Most relevant statistics for the wind speed at the WT height (y_h)

Table 46. Statistics for Wind Speed over 9 Years for Wellington

Year	N	N*	Mean	SE Mean	StDev	Minimum	Q1	Median	Q3	Maximum
2006	8886	0	12.96	0.07	6.95	0.00	8.15	12.62	18.03	38.80
2007	8840	4	11.51	0.06	6.05	0.00	6.35	11.76	15.36	34.25
2008	8939	0	11.80	0.07	6.46	0.00	6.35	11.76	16.22	37.86
2009	8758	2	12.34	0.07	6.50	0.00	7.21	11.76	17.16	39.66
2010	8745	3	12.18	0.07	6.49	0.00	7.21	11.76	16.22	45.07
2011	8621	1	11.70	0.07	6.21	0.00	7.21	11.76	15.36	34.25
2012	8786	0	11.62	0.07	6.41	0.00	6.35	11.76	16.22	36.99
2013	10936	4	12.18	0.06	6.53	0.00	7.21	11.76	16.22	49.61
2014	17223	0	12.51	0.05	6.47	0.00	7.21	12.62	17.16	38.80

N* = number of missing values

Table 47. Statistics for Wind Speed over 9 Years for Rio Gallegos

Year	N	N*	Mean	SE Mean	StDev	Minimum	Q1	Median	Q3	Maximum
2006	9588	7	11.01	0.07	7.08	0.00	5.41	9.95	15.36	83.00
2007	9541	2	11.56	0.08	7.46	0.00	6.35	9.95	16.22	73.99
2008	9120	5	11.06	0.08	7.63	0.00	5.41	9.95	15.36	73.99
2009	9238	0	12.15	0.08	7.50	0.00	6.35	10.82	17.16	57.84
2010	9749	1	11.56	0.08	7.78	0.00	5.41	9.95	16.22	55.02
2011	9952	4	10.15	0.07	6.85	0.00	5.41	9.01	14.42	72.18
2012	10055	0	11.87	0.07	7.21	0.00	6.35	10.82	16.22	67.64
2013	10349	0	11.85	0.13	13.28	0.00	5.41	10.82	17.16	783.68
2014	11767	0	10.65	0.07	7.98	0.00	5.41	9.95	15.36	211.07

N* = number of missing values

Table 48. Statistics for Wind Speed over 9 Years for New York

Year	N	N*	Mean	SE Mean	StDev	Minimum	Q1	Median	Q3	Maximum
2006	9567	0	9.30	0.05	4.80	0.00	6.35	9.01	11.76	30.64
2007	9732	1	9.01	0.05	4.63	0.00	5.41	8.15	11.76	30.64
2008	9732	1	9.01	0.05	4.63	0.00	5.41	8.15	11.76	30.64
2009	9965	0	8.62	0.05	4.80	0.00	5.41	8.15	11.76	31.59
2010	9770	0	9.39	0.05	5.05	0.00	5.41	9.01	12.62	36.05
2011	10200	7	8.60	0.05	4.94	0.00	5.41	8.15	10.82	34.25
2012	9930	4	8.45	0.05	4.86	0.00	5.41	8.15	10.82	41.46
2013	9831	0	8.95	0.05	4.66	0.00	5.41	8.15	11.76	33.39
2014	9797	2	8.89	0.05	4.79	0.00	5.41	8.15	11.76	28.84

N* = number of missing values

Appendix D: Estimated probability for the wind speed at scenario s and node *j* (p_{sj})

Table 49. Estimated Probability for the Wind Speed at Scenario *s* and Node *j* in Wellington

	Year and node number (*j*)								
	2006	2007	2008	2009	2010	2011	2012	2013	2014
Scenario (*s*)	1	2	3	4	5	6	7	8	9
1	0.02	0.02	0.02	0.01	0.02	0.02	0.02	0.02	0.01
2	0.03	0.03	0.03	0.03	0.03	0.03	0.04	0.03	0.03
3	0.04	0.04	0.05	0.04	0.04	0.04	0.05	0.04	0.04
4	0.03	0.03	0.04	0.03	0.03	0.03	0.04	0.03	0.04
5	0.03	0.04	0.04	0.04	0.03	0.03	0.04	0.03	0.04
6	0.03	0.04	0.04	0.04	0.04	0.04	0.04	0.04	0.04
7	0.03	0.04	0.04	0.04	0.03	0.04	0.04	0.04	0.04
8	0.04	0.04	0.04	0.04	0.04	0.04	0.04	0.04	0.04
9	0.04	0.04	0.04	0.04	0.04	0.04	0.04	0.05	0.04
10	0.09	0.10	0.10	0.11	0.10	0.12	0.10	0.10	0.09
11	0.05	0.06	0.05	0.04	0.05	0.06	0.05	0.05	0.04
12	0.05	0.06	0.05	0.05	0.05	0.05	0.05	0.05	0.04
13	0.53	0.45	0.48	0.50	0.49	0.45	0.46	0.49	0.52
Total	1.00	1.00	1.00	1.00	1.00	1.00	1.00	1.00	1.00

Table 50. Estimated Probability for the Wind Speed at Scenario *s* and Node *j* in Rio Gallegos

	Year and node number (*j*)								
	2006	2007	2008	2009	2010	2011	2012	2013	2014
Scenario (*s*)	1	2	3	4	5	6	7	8	9
1	0.05	0.04	0.05	0.04	0.04	0.09	0.03	0.08	0.14
2	0.03	0.03	0.03	0.02	0.03	0.02	0.02	0.02	0.01
3	0.04	0.03	0.05	0.03	0.04	0.03	0.04	0.02	0.02
4	0.05	0.04	0.05	0.04	0.04	0.04	0.04	0.04	0.03
5	0.05	0.05	0.06	0.05	0.05	0.05	0.04	0.04	0.04
6	0.06	0.04	0.06	0.04	0.05	0.06	0.05	0.05	0.05
7	0.05	0.05	0.05	0.05	0.06	0.06	0.05	0.05	0.05
8	0.05	0.06	0.06	0.05	0.05	0.07	0.06	0.05	0.06
9	0.05	0.05	0.04	0.04	0.04	0.06	0.05	0.05	0.04
10	0.11	0.11	0.09	0.10	0.11	0.10	0.11	0.09	0.09
11	0.05	0.05	0.04	0.05	0.04	0.04	0.04	0.04	0.04
12	0.04	0.04	0.03	0.04	0.04	0.05	0.05	0.04	0.04
13	0.38	0.40	0.39	0.45	0.40	0.33	0.43	0.43	0.38
Total	1.00	1.00	1.00	1.00	1.00	1.00	1.00	1.00	1.00

Table 51. Estimated Probability for the Wind Speed at Scenario *s* and Node *j* in New York

	Year and node number (*j*)								
	2006	2007	2008	2009	2010	2011	2012	2013	2014
Scenario (*s*)	1	2	3	4	5	6	7	8	9
1	0.03	0.04	0.04	0.05	0.04	0.05	0.05	0.04	0.04
2	0.00	0.00	0.00	0.00	0.00	0.00	0.00	0.00	0.00
3	0.03	0.03	0.03	0.04	0.04	0.05	0.05	0.04	0.05
4	0.05	0.05	0.05	0.06	0.05	0.06	0.06	0.05	0.06
5	0.06	0.06	0.06	0.07	0.06	0.07	0.07	0.06	0.07
6	0.08	0.08	0.08	0.08	0.07	0.08	0.08	0.08	0.08
7	0.09	0.08	0.08	0.09	0.08	0.08	0.09	0.08	0.07
8	0.08	0.09	0.09	0.08	0.08	0.08	0.08	0.08	0.08
9	0.08	0.09	0.09	0.09	0.07	0.08	0.08	0.08	0.08
10	0.14	0.15	0.15	0.14	0.13	0.14	0.14	0.15	0.13
11	0.06	0.06	0.06	0.05	0.06	0.06	0.05	0.06	0.06
12	0.06	0.05	0.05	0.05	0.05	0.05	0.05	0.06	0.05
13	0.24	0.23	0.23	0.21	0.27	0.20	0.19	0.23	0.23
Total	1.00	1.00	1.00	1.00	1.00	1.00	1.00	1.00	1.00

Appendix E: Values used in computing sensitivities in all cities

Table 52. Percentages of Change in Expected Total Annual Cost if the System Mean Total Load varies from the Base (50.1 MW) for Model 3

	% of Change in Mean Total Load						
City	-6%	-4%	-2%	base	2%	4%	6%
Wellington	2,071,553	2,232,838	2,348,400	2,509,897	2,715,425	2,902,534	3,071,573
% change vs base cost	-7.2%	-4.9%	-6.4%		8.2%	6.9%	5.8%
Rio Gallegos	2,148,009	2,248,374	2,424,130	2,689,590	2,935,894	3,129,997	3,323,156
% change vs. base cost	-4.5%	-7.3%	-9.9%		9.2%	6.6%	6.2%
New York	2,158,119	2,331,117	2,683,767	3,071,149	3,329,628	3,329,629	Infeasible
% change vs. base case	-7.4%	-13.1%	-12.6%		8.4%	0.0%	N/A

Table 53. Percentages of Change in Expected Total Annual Costs to Variations on the Loss of Load Probability for Stochastic Model 3

	α				
City	0.0001	0.005	0.01 (base case)	0.02	0.05
Wellington	$3,274,924	$2,822,022	$2,509,897	$2,349,686	$2,313,654
% change vs. base case	16.0%	12.4%		-6.4%	-1.5%
Rio Gallegos	$3,367,266	$3,086,607	$2,689,590	$2,441,393	$2,344,558
% change vs. base case	9.1%	14.8%		-9.2%	-4.0%
New York		$3,329,628	$3,071,149	$2,683,507	$2,486,730
% change vs. base case		8.4%		-12.6%	-7.3%

Appendix F: Computing the left-hand side of the loss of load chance constraint in Model 5

$$\int_0^{\infty}\left(\int_y^{\infty} f_P(z)\,dz\right) f_L(y)\,dy \geq 1-\alpha \tag{F1}$$

$$\Rightarrow \Pr\{P_{WT}+P_{sub} > L\} \geq 1-\alpha \tag{F2}$$

$$\Rightarrow \Pr\{P_{WT}+P_{sub} \leq L\} \leq \alpha \tag{F3}$$

$$\Rightarrow \Pr\{P \leq L\} \leq \alpha \tag{F4}$$

where the abbreviation Pr in the formulas above is used to represent probability, P_{WT} represents the total power generated by the WT, P_{sub} is the total power generated by the substation and P the total power generated by the WT and the substation. By the Central limit Theorem (CLT) it is assumed that:

$$P_{WT} \sim N(E[P_{WT}], \sigma^2_{P_{WT}}) \tag{F5}$$

and then

$$P = P_{WT} + P_{sub} \sim N(E[P_{WT}] + \sum_{s\in S}\sum_{f\in F} p_{sf} y^{+}_{sf}, \sigma^2_{P_{WT}}) \tag{F6}$$

where:

$$E[P] = E[P_{WT}] + \sum_{s\in S}\sum_{f\in F} p_{sf} y^{+}_{sf} = \sum_{i\in I}\sum_{j\in J} E\left[P_{ij}\right] + \sum_{s\in S}\sum_{f\in F} p_{sf} y^{+}_{sf} \tag{F7}$$

$E[P_{ij}]$ = Mean power output when WT type i is installed at node j

p_{sf} = probability for wind speed scenario s at upper node f

$\sum_{f\in F} y^{+}_{sf}$ = power sent by the substation to upper nodes under scenario s

$$\sigma^2_{P_{WT}} = \sum_{i\in I}\sum_{j\in J}\sum_{s\in S} p_{sj}\left(P_{ijs}x_{ij} - E\left[P_{WT}\right]\right)^2 \tag{F8}$$

p_{sj} = probability for wind speed scenario s at node j

P_{ijs} = power output when WT type i is installed at node j and wind speed scenario is s

x_{ij} = binary decision variable that indicates if WT type i is installed at node j

From the computational experiments done with Models in Chapter 2, the author in this thesis found that it is reasonable to assume that the variance for P_{sub} is zero and then P_{sub} mainly behaves as a constant defined by $E[P_{sub}] = \sum_{s\in S}\sum_{f\in F} p_{sf}y^+_{sf}$. Using a graph similar to the one in Appendix A, the reader can see that the problem in F4 above reduces to find the point p that leaves an area α to the left in the total power curve, that is:

$$\Pr\left(P \le p\right) \le \alpha \tag{F9}$$

To find such point p the probability density functions of the total load and the total power are equated as follows:

$$f_P\left(p\right) = f_L\left(p\right) \tag{F10}$$

and it gives:

$$\frac{1}{\sqrt{2\pi\sigma_P}}e\left(\frac{-\left(p-\mu_p\right)^2}{2\sigma_P^2}\right) = \frac{1}{\sqrt{2\pi\sigma_L}}e\left(\frac{-\left(p-\mu_L\right)^2}{2\sigma_L^2}\right) \tag{F11}$$

Finding the expression to solve for p can be done using the well-known formula $\frac{-b\pm\sqrt{b^2-4ac}}{2a}$ to solve the resulting quadratic equation with coefficients:

$$a = \sigma_P^2 - \sigma_L^2 \tag{F12}$$

$$b = 2\left(\sigma_L^2 \mu_P - \sigma_P^2 \mu_L\right) \tag{F13}$$

$$c = \sigma_P^2 \mu_L^2 - \sigma_L^2 \mu_P^2 - 2\sigma_P^2 \sigma_L^2 \ln\left(\frac{\sigma_P}{\sigma_L}\right) \tag{F14}$$

where all formulas to compute the terms above have been previously defined except the ones below:

σ_L^2 = given variance of the total load

$\mu_L = E[L]$ = given mean of the total load

Once the formula to solve for *p* is written as a function of the x_{ij} and $\sum_{f \in F} y_{sf}^{+}$, the cumulative standard normal distribution can be used to compute the left-hand side of $\Pr(P \le p) \le \alpha$ as follows:

$$\Pr\left(Z \le \frac{p - E[P]}{\sigma_P}\right) \le \alpha \;\Rightarrow\; \Pr(Z \le z) \le \alpha \Rightarrow \phi(z) \le \alpha \tag{F15}$$

Since AMPL did not have implemented in its built-in arithmetical functions the cumulative normal distribution, the author in this thesis used the very accurate approximation given in Zogheib et al. (2009):

$$\phi(z) \cong \left(1 + e^{(0.0054 - 1.610)z - 0.0674z^3}\right)^{-1} \tag{F16}$$

Then the probabilistic constraint turns into:

$$\left(1 + e^{(0.0054 - 1.610)z - 0.0674z^3}\right)^{-1} \le \alpha$$

Where *z* is a function of *p* which is a function of the decision variables x_{ij} and $\sum_{f \in F} y_{sf}^{+}$

Appendix G: Glossary

Energy storage system

An energy storage system (ESS) is a device used for storing electric energy when needed and releasing it when required.(Chemicals, 2013).

Feed-in Tariffs (FITs)

A payment that renewable energy producers receive from the electricity grid, system or market operators when they supply energy to the electric grid. The tariff varies by type and size of the renewable technology and geographic region among others. (https://www.gov.uk/feed-in-tariffs)

Life-cycle

A series of stages through which something (such as an equipment, manufactured product or equipment) passes during its lifetime/existence.

Loss of load

A Loss of Load Expectation (LOLE) or Loss of Load Probability (LOLP), analysis is typically performed on a system to determine the amount of capacity that needs to be installed to meet the desired reliability target, commonly expressed as an expected value, or LOLE of 0.1 days/year (NERC, 2011).

Radial distribution system

A radial system has only one power source for a group of customers. A power failure, short-circuit, or a downed power line would interrupt power in the entire line which must be fixed before power can be restored (WPPI energy,2013).

Strategic Planning

Organizational management activity that is used to set priorities, focus energy and resources, strengthen operations, ensure that employees and other stakeholders are working toward common goals (Kagendo, 2015).

Thermal constraints

A thermal operating constraint (specified in real power, or megawatts) is often placed on troublesome transmission lines to control the permissible power transfer across the lines. This limit establishes an upper bound on a particular lines transfer capability(Argonne national laboratory, 2007).

Transmission lines

Transmission lines carry electric energy from one point to another in an electric power system. They can carry alternating current or direct current. The main characteristics that distinguish transmission lines from distribution lines are that they are operated at relatively high voltages, they transmit large quantities of power and they transmit the power over large distances (United states department of labor, 2007).

Distribution lines

Distribution lines also carry electric energy from one point to another in an electric power system, but distribution lines operate at a much lower voltage to transmission lines (United states department of labor, 2007).

Lines

The lines going into a substation are called lines whereas the bus is the common connection point for all the incoming lines and sources. When developing a

model, buses could be seen as nodes and Lines as branches (Engineering forums,2012).

Load bus

This is also called the P-Q bus. In a load bus, the active and reactive power is injected into the network. Magnitude and phase angle of the voltage are to be computed. The active power P and reactive power Q are specified, and the load bus voltage can be permitted within a tolerable value (Engineering forums,2012).

Time of use (TOU)

Customers are billed differently according to the time of day they use the energy. Residential customers face a higher cost of energy at night hours that during day hours because the utility company charges higher prices during the hours people demand higher amounts of energy. It obligates customers to adapt their patterns of use of energy in a way that is favorable to them.

REFERENCES

Abdul kadir, A.F., Mohamed, A., Shareef, H., Che Wanik, M.Z., 2013. Optimal placement and sizing of distributed generations in distribution systems for minimizing losses and THDv using evolutionary programming. *Turkish J. Electr. Eng. Comput.* Sci. 21, 2269–2282. https://doi.org/10.3906/elk-1205-35

Alarcon-Rodriguez, A., Ault, G., Galloway, S., 2010. Multi-objective planning of distributed energy resources: A review of the state-of-the-art. Renew. Sustain. *Energy Rev*. 14, 1353–1366. https://doi.org/10.1016/j.rser.2010.01.006

Azar, A.G., Nazaripouya, H., Khaki, B., Chu, C.C., Gadh, R., Jacobsen, R.H., 2019. A Non-Cooperative Framework for Coordinating a Neighborhood of Distributed Prosumers. *IEEE Trans. Ind. Informatics* 15, 2523–2534. https://doi.org/10.1109/TII.2018.2867748

Bañuelos-ruedas, F., Camacho, C.Á., n.d. Methodologies Used in the Extrapolation of Wind Speed Data at Different Heights and Its Impact in the Wind Energy Resource Assessment in a Region.

Begovic, M., Pregelj, A., Rohatgi, A., 2001. Impact of Renewable Distributed Generation on Power Systems, in: 34th Hawaii International Conference on System Sciences. pp. 1–10.

Blackadar, A.K., Tennekes, H., 1968. Asymptotic Similarity in Neutral Barotropic Planetary Boundary Layers. J. Atmos. Sci. https://doi.org/10.1175/1520-0469(1968)025<1015:ASINBP>2.0.CO;2

Cetinay, H., Kuipers, F.A., Guven, A.N., 2017. Optimal siting and sizing of wind farms. Renew. Energy 101, 51–58. https://doi.org/https://doi.org/10.1016/j.renene.2016.08.008

Cui, S., Wang, Y.W., Xiao, J.W., Liu, N., 2019. A Two-Stage Robust Energy Sharing Management for Prosumer Microgrid. IEEE Trans. Ind. Informatics 15, 2741–2752. https://doi.org/10.1109/TII.2018.2867878

El-Fergany, A., 2015. Optimal allocation of multi-type distributed generators using backtracking search optimization algorithm. Int. J. Electr. Power Energy Syst. 64, 1197–1205. https://doi.org/10.1016/j.ijepes.2014.09.020

El-Khattam, W., Bhattacharya, K., Hegazy, Y., Salama, M.M.A., 2004. Optimal investment planning for distributed generation in a competitive electricity market. IEEE Trans. Power Syst. 19, 1674–1684. https://doi.org/10.1109/TPWRS.2004.831699

Erdinc, O., Tascikaraoglu, A., Paterakis, N.G., Dursun, I., Sinim, M.C., Catalao, J.P.S., 2018. Comprehensive Optimization Model for Sizing and Siting of DG Units, EV Charging Stations, and Energy Storage Systems. IEEE Trans. Smart Grid 9, 3871–3882. https://doi.org/10.1109/TSG.2017.2777738

Hadian, A., Haghifam, M.R., Zohrevand, J., Akhavan-Rezai, E., 2009. Probabilistic approach for renewable DG placement in distribution systems with uncertain and time varying loads. 2009 IEEE Power Energy Soc. Gen. Meet. PES '09 1–8. https://doi.org/10.1109/PES.2009.5275458

Haghifam, M.R., Omidvar, M., 2006. Wind farm modeling in reliability assessment of power system. 2006 9th Int. Conf. Probabilistic Methods Appl. to Power Syst. PMAPS. https://doi.org/10.1109/PMAPS.2006.360414

Heier, G., 2005. Effective finiteness theorems for maps between canonically polarized compact complex manifolds. Math. Nachrichten 278, 133–140. https://doi.org/10.1002/mana.200310230

Hussain, I., Ali, S.M., Khan, B., Ullah, Z., Mehmood, C.A., Jawad, M., Farid, U., Haider, A., 2019. Stochastic Wind Energy Management Model within smart grid framework: A joint Bi-directional Service Level Agreement (SLA) between smart grid and Wind Energy District Prosumers. Renew. Energy 134, 1017–1033. https://doi.org/10.1016/j.renene.2018.11.085

Karki, R., Member, Senior, Hu, P., Member, Student, Billinton, R., Fellow, L., 2006. A Simplified Wind Power Generation Model for Reliability Evaluation. IEEE Trans. Energy Convers. 21, 533–540. https://doi.org/10.1109/TEC.2006.874233

Khaki, B., Das, P., Member, S., n.d. Sizing and Placement of Battery Energy Storage Systems and Wind Turbines by Minimizing Costs and System Losses.

Kwon, S., Ntaimo, L., Gautam, N., 2017. Optimal Day-Ahead Power Procurement with Renewable Energy and Demand Response. IEEE Trans. Power Syst. 32, 3924–3933. https://doi.org/10.1109/TPWRS.2016.2643624

Lopes, J.A.P., Hatziargyriou, N., Mutale, J., Djapic, P., Jenkins, N., 2007. Integrating distributed generation into electric power systems: A review of drivers, challenges and opportunities. Electr. Power Syst. Res. 77, 1189–1203. https://doi.org/10.1016/j.epsr.2006.08.016

Miranda, R., Soria, R., Schaeffer, R., Szklo, A., Saporta, L., 2017. Contributions to the analysis of "Integrating large scale wind power into the electricity grid in the Northeast of Brazil" [Energy 100 (2016) 401–415]. Energy 118, 1198–1209. https://doi.org/10.1016/j.energy.2016.10.138

Mohandas, N., Balamurugan, R., Lakshminarasimman, L., 2015. Optimal location and sizing of real power DG units to improve the voltage stability in the distribution system using ABC algorithm united with chaos. Int. J. Electr. Power Energy Syst. 66, 41–52. https://doi.org/10.1016/j.ijepes.2014.10.033

Nguyen, N.T.A., Le, D., Bovo, C., Berizzi, A., 2017. Optimal siting and sizing of Energy Storage Systems for Wind Integration. IREP'2017 - 10th Bulk Power Syst. Dyn. Control Symp. 2017 Porto 1–7.

Novoa, C., Jin, T., 2011. Reliability centered planning for distributed generation considering wind power volatility. Electr. Power Syst. Res. 81, 1654–1661. https://doi.org/10.1016/j.epsr.2011.04.004

Novoa, C. M., Siddique, K., Guirguis, M. S., & Tahsini, A. (2018). A Game-Theoretic Two-Stage Stochastic Programing Model to Protect CPS against Attacks. In *IEEE 16th International Conference on Industrial Informatics (INDIN)* (pp. 15–22).

Omu, A., Choudhary, R., Boies, A., 2013. Distributed energy resource system optimisation using mixed integer linear programming. Energy Policy 61, 249–266. https://doi.org/10.1016/j.enpol.2013.05.009

Rathnayaka, A.J.D., Potdar, V.M., Hussain, O., Dillon, T., 2011. Identifying prosumer's energy sharing behaviours for forming optimal prosumer-communities. Proc. - 2011 Int. Conf. Cloud Serv. Comput. CSC 2011 199–206. https://doi.org/10.1109/CSC.2011.6138520

Ren, H., Gao, W., 2010. A MILP model for integrated plan and evaluation of distributed energy systems. Appl. Energy 87, 1001–1014. https://doi.org/10.1016/j.apenergy.2009.09.023

Ritzer, G., Jurgenson, N., 2010. Production, Consumption, Prosumption: The nature of capitalism in the age of the digital "prosumer." J. Consum. Cult. 10, 13–36. https://doi.org/10.1177/1469540509354673

Shapiro, A., Philpott, A., 2007. A Tutorial on Stochastic Programming 1–35. https://www-m9.ma.tum.de/foswiki/pub/SS2014/StochPro/TutorialSP.pdf

Shu, Z., Jirutitijaroen, P., 2014. Optimal operation strategy of energy storage system for grid-connected wind power plants. IEEE Trans. Sustain. Energy 5, 190–199. https://doi.org/10.1109/TSTE.2013.2278406

Spahić, E., Underbrink, A., Buchert, V., Hanson, J., Jeromin, I., Balzer, G., 2009. Reliability model of large offshore wind farms. 2009 IEEE Bucharest PowerTech Innov. Ideas Towar. Electr. Grid Futur. 1–6. https://doi.org/10.1109/PTC.2009.5281878

van der Stelt, S., AlSkaif, T., van Sark, W., 2018. Techno-economic analysis of household and community energy storage for residential prosumers with smart appliances. Appl. Energy 209, 266–276. https://doi.org/10.1016/j.apenergy.2017.10.096

Wen, S., Lan, H., Fu, Q., Yu, D.C., Zhang, L., 2015. Economic allocation for energy storage system considering wind power distribution. IEEE Trans. Power Syst. 30, 644–652. https://doi.org/10.1109/TPWRS.2014.2337936

Wongwut, K., Nuchprayoon, S., 2018. Optimum hourly operation of a prosumer with battery energy storage system under time-of-use pricing. Asia-Pacific Power Energy Eng. Conf. APPEEC 2017-Novem, 1–6. https://doi.org/10.1109/APPEEC.2017.8308997

Xia, S., Chan, K.W., Luo, X., Bu, S., Ding, Z., Zhou, B., 2018. Optimal sizing of energy storage system and its cost-benefit analysis for power grid planning with intermittent wind generation. Renew. Energy 122, 472–486. https://doi.org/10.1016/j.renene.2018.02.010

Ye, R.L., Guo, Z.Z., Liu, R.Y., Liu, J.N., 2016. An optimal sizing method for energy storage system in wind farms based on the analysis of wind power forecast error. IOP Conf. Ser. Mater. Sci. Eng. 161. https://doi.org/10.1088/1757-899X/161/1/012085

Zhao, H., Wu, Q., Huang, S., Guo, Q., Sun, H., Xue, Y., 2015. Optimal siting and sizing of Energy Storage System for power systems with large-scale wind power integration. 2015 IEEE Eindhoven PowerTech, PowerTech 2015 1–6. https://doi.org/10.1109/PTC.2015.7232615